**The University of Nottingham**

# Genetic Dissection of Root Adaptive Responses to Water Stress

**DALIA MOHAMMAD MELEBARI**

**Thesis submitted for a degree of Doctor of Philosophy**

**December 2022**

## ABSTRACT

Land plants have evolved root adaptive responses which facilitate water exploration by sensing soil moisture availability, then modifying traits such as the orientation and velocity of primary root growth, as well as the frequency and patterning of root branching. Exploiting such plant root traits conferring resilience to water stress provides a novel way to close the yield gap but requires new knowledge about these adaptive processes and their underlying molecular mechanisms.

This PhD thesis addressed the molecular mechanisms underpinning two water stress adaptive root responses, namely hydrotropism (Chapters 3 & 4) and xerobranching (Chapter 5; Mehra et al, 2022). Hydrotropism orients root growth towards the best available soil moisture source. In contrast, the xerobranching response prevents the initiation of lateral roots when roots lose contact with moist soil. Despite their obvious developmental differences, I have demonstrated root adaptive responses are regulated by the same abiotic stress hormone, abscisic acid (ABA; Chapter 3-5; Mehra et al, 2022). This observation raises important questions about whether ABA regulates both root water stress adaptive responses using identical, related or distinct molecular mechanisms and/or components?

My thesis studies have focused on revealing how ABA is transported during these root adaptive responses. Following a root hydrotropic stimulus, ABA must move from its phloem source to target cortex (response) cells. To address whether specialised transporters are involved, an amiRNA transportome library was screened to discover novel genes that regulate ABA mobilisation in *Arabidopsis* roots (Chapter 3). Putative ABA transporters were identified such as ATP binding cassette family (ABCG); a MATE transporter family member *DTX1;* and a glucosinolate influx transporter *GTR1* (Chapter 4).

This PhD study also revealed that ABA is a key regulator of the root adaptive response xerobranching (Chapter 5; Mehra et al, 2022). This represents an ABA-dependent root adaptive response to loss of contact with moist soil, that is conserved in eudicot and monocot species, which inhibits lateral root development after a xerobranching stimulus. ABA functions as a phloem-derived stress hormone disrupting intercellular communication between inner and outer cell layers via plasmodesmata. The closure of these intercellular pores prevents lateral root branching by impeding the inward passage of the hormone signal auxin.

# ACKNOWLEDGEMENT

Dedicated to my parents... you are my strength and my idol.

I would like to thank God for giving me the power, ability, and opportunity to finish this research project. This Challenging journey would not have been possible without the support of a number of respected people who assisted and supported me. I owe my heartfelt gratitude and thanks to all of them.

First and foremost, I am incredibly grateful to my supervisor Prof. Malcolm Bennett for his invaluable advice, continuous support, patience during my PhD study and care during the pandemic period. His immense knowledge, insightful opinion, and abundant experience have motivated me in my academic research. I am proud to be a member of his group.

I would like to express my gratitude to Dr. Poonam Mehra for her mentorship, and support and for giving me valuable ideas at the right time. I would also like to thank my assessor Dr. Ranjan Swarup for his advice, especially in the first year. I also had the great pleasure of working with Dr. Daniela Dietrich and Prof. Eilon Shani. My Special thanks to my friends in Malcolm's group, you are my supportive friends. Also, many thanks to the root group members for their valuable research discussions and advice.

I would also like to extend my deepest gratitude to my family, especially to my sisters and brother, I felt your support despite the distance, and I share my success with you. Getting through my PhD required more than academic support, and I have many people to thank for listening, being around in hard and happy times, and having to tolerate me over the past five years. I cannot begin to express my gratitude and

appreciation for their friendship. I am extremely grateful to my friends Afaf, Doha, Khulud, Nora and Shiah for their help, support, and many good suggestions provided me during myPhD study. I also wish to thank all my friends in Nottingham for their kindness and support.

I also thank the Saudi Ministry of Education in particular, Um-Alqura University for the financial support providing me during my PhD study.

# ABBREVIATIONS

| | |
|---|---|
| ABA | Abscisic Acid |
| AmiRNA | Artificial microRNA |
| cDNA | Complementary Deoxyribonucleic Acid |
| Col-0 | Columbia-0 |
| Col.0 | Columbia (Arabidopsis Wild-Type) |
| dNTPs | Deoxyribonucleotide Triphosphate |
| DR5 | Direct Repeat5 |
| DS | Downstream |
| DZ | Differentiation Zone |
| GFP | Green Fluorescence Protein |
| GTR | Glucosinolate Transporter |
| IAA | Auxin (Indole-3-Acetic Acid) |
| LR | Lateral Root |
| MCT | Micro Centrifuge Tube |
| MIZ | MIZU–KUSSEI1 |
| mRNA | Micro RNA |
| NASC | Nottingham Arabidopsis Stock Centre |
| NPF | Nitrate Peptide Transporter Family |
| PD | Plasmodesmata |
| PIN | PIN-FORMED |
| PR | Primary Root |
| CT | Computed Tomography |
| RAM | Root Apical Meristem |
| RNAseq | RNA Sequencing Technology |
| SCR | SCARECROW |
| SHR | SHORTROOT |
| T-DNA | Transferred-Deoxyribonucleic Acid |
| TAIR 10 | The Arabidopsis Information Resource |
| TF | Transcription Factor |
| TM | Target Mimic |

# Table of Contents

## TABLE OF FIGURES

## LIST OF TABLES

# CHAPTER 1: GENERAL INTRODUCTION

Plants are amongst the most important life forms on earth. All terrestrial ecosystems rely on plant-derived products, which are the main resource of food for animals and humans, whilst providing many products, services, and habitats for them (Corlett 2016). In this era of climate change, much current research focuses on identifying the processes that regulate abiotic stress tolerance mechanisms in plants. The new knowledge resulting promises to contribute to global food security by facilitating the development of crops better adapted to future climatic circumstances.

## 1.1 The Impact of Climate Change:

The demands on agriculture are increasing due to a growing global population combined with the increasing impact of climate change (Jägermeyr et al., 2021). Recent environmental changes have emerged due to increased industrial activity and the consumption of biofuels which is known as climate change (Ahuja et al., 2010). As shown in (Figure 1.1), climate change has caused an increase in global temperature and extreme weather events such as drought (Hertel et al., 2010).

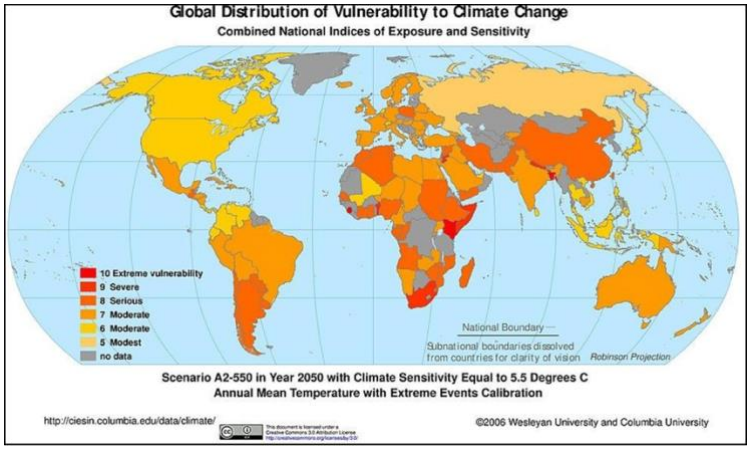


**Figure 1.1** Predicted scenarios in the year 2050 with climate change by 5.5°C (Sedac.ciesin.columbia.edu, 2019).

As a result of changes in precipitation (Raza et al., 2019) and temperature brought about by climate change, natural and agricultural systems must rapidly adapt or perish (Chen and Gong, 2021). Combined with intensive farming practices, environmental changes have a deleterious effect on soil quality. The majority of global crop yield loss is attributable to soil deterioration and other abiotic stressors, which have devastating effects on plant development (Teh and Koh, 2016) such as desertification (Huang et al., 2020) and salinization (Harper et al., 2021).

Plant growth and development is closely linked to environmental conditions(Saito et al. 2015). Water is arguably the most important limiting factor for plant growth in different ecosystems (Voesenek and Bailey-Serres, 2015). Plants have developed a range of mechanisms to adapt to water scarcity (Cattivelli et al., 2008). For example, plants modify their stomatal properties, photosynthesis efficiency, and leaf elongation (Seo and Park, 2009). The FAO global drought map (2007-2022) in (Figure 1.2) depicts the frequency of drought occurrences that affected agriculture-stressed (drought) cropland in each region. Severe droughts occur practically yearly in places like southern Africa, India, and Australia.

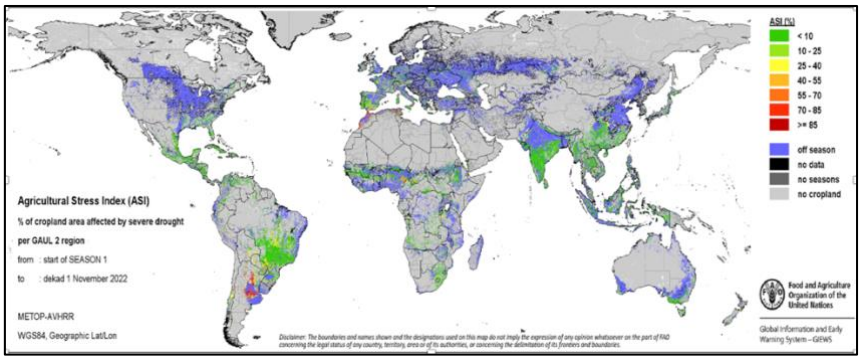


**Figure 1.2** FAO data in 2022 shows regions of the world where water stress is likely to occur (drought). The indexes are based on historical data, a worldwide crop mask, and remote sensing data of vegetation and land surface temperature. The maps show agricultural zones with probable drought and unique vegetation development.

https://www.fao.org/giews/earthobservation/asis/data/nrt/ASI/ot2231h_aC1_s1_g2.png

Many crop improvement programmes now concentrate on improving drought and heat tolerance (Davies et al., 2015). Several root responses have been identified that could help plants obtain water more effectively under drought conditions such as increasing their root growth angle to forage for water in deeper soil profiles ( Lynch, 2013). Root angle is controlled, in part, by the acclimative response hydrotropism (Dietrich et al., 2017), enabling plants to sense gradients of water availability and grow towards the best source. Droughts are predicted to become increasingly more severe as a result of changes in rainfall patterns and rising temperatures caused by global climate change (Lobell and Gourdji, 2012; Moritz and Agudo, 2013). Furthermore, freshwater sources needed for crop irrigation are depleting at an alarmingly rapid rate (Cotterman, 2017). More drought-tolerant crops are needed to avert yield losses. Therefore, since root traits determine how much water can be taken up, a better understanding of how roots are able to forage for this resource in the soil is crucial for crop breeders. However, we must first understand the processes which roots use to detect and react to the availability of soil water resources. Gene-directed breeding can only significantly advance soil exploration to maximise water and nutrient uptake through leveraging a new understanding of the underpinning mechanisms.

Climate change has already started to alter many plants species distribution, with its impact predicted to increase as insufficient efforts are being made to slow $CO_2$ emissions (Lobell and Gourdji, 2012). In response to extreme climate events, rapid and large-scale changes in ecosystem structure and function can result in forest (Gitlin et al., 2005) and woodland mortality (Allen and Breshears, 1998; Condit et al., 1995). According to The Intergovernmental Panel on Climate Change perceptions about climate change effects on agriculture such as decreased yield as a result of high temperature stress, crop losses and soil erosion caused by drought (IPCC, 2009).

Future climate change scenarios predict shortages in food production particularly in tropical regions (Cerri et al., 2007). However, many other parts of the world will be affected by global warming through increased abiotic stresses on crop production. For example, (Lobell and Gourdji, 2012) reported global maize and wheat production will decrease by 3.8% and 5.5%, respectively, compared to the climate-free trend.

## 1.2 Root Anatomy, Architecture and Adaptation

The roots are often described as the hidden half of plants but provide vital functions. For example, the nutrients and water necessary for a plant's growth and development are initially foraged by roots, whilst roots also provide the aerial parts of the plant with anchorage (Kramer and Boyer, 1995). Due to its simple cellular organisation and architecture, *Arabidopsis thaliana* has been widely used as a model for examining root development and adaptive responses.

The majority of plants, as sessile organisms, are remarkably adept at adapting their root systems architecture (RSA) to their immediate surroundings. Plant roots are able to respond to numerous abiotic stimuli thanks to their developmental plasticity (Morris et al., 2017; Lavenus et al., 2013). As it is shown in (Figure 1.3) different plant species exhibit different root patterns. Many dicotyledonous plants such as *Arabidopsis thaliana* have a primary embryonic root that branches repeatedly to form lateral roots (Péret et al., 2009). Cereals contain embryonic and seminal roots (Hochholdinger and Tuberosa, 2009). Researchers have identified a number of root responses that could help plants obtain water more effectively under drought conditions such as increasing their growth angle and enabling roots to forage for water in deeper soil profiles (Lynch, 2013). Root angle is controlled by the adaptive response hydrotropism (Dietrich et al.,

2017), enabling plants to sense gradients of water availability and grow towards the best source.

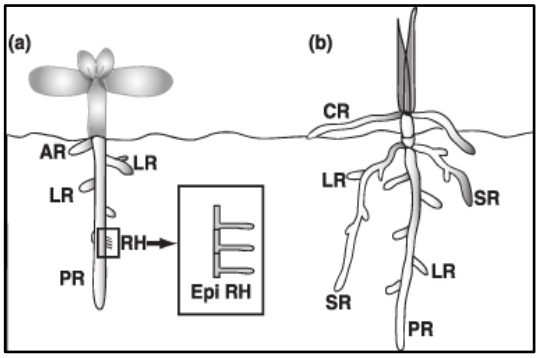


**Figure 1. 3** Root systems architecture (RSA) (a) A typical dicot (e.g. *Arabidopsis*) seedling root system, with a primary root (PR) emerging from the embryo, lateral roots (LR) branching out from the PR throughout the seedling development, and root hairs (RH) originating from PR epidermal (Epi) cells. LRs will branch into secondary and tertiary LRs. At the shoot-root junction, adventitious roots (AR) form. (b) A typical cereal (e.g. *Rice, Maize*) seedling root system consists of a primary root (PR) originating from the embryo, seminal roots (SR) close to the top of the primary root, and crown roots (CR) from the stem. Together, PR, SR, and CR branch higher orders to produce LR (Nibau et al. 2008)

The primary root (PR) develops from the seed and grows downwards with gravity after germination. Multiple levels of development zones build the longitudinal organisation within the root. This occurs through repeated cellular divisions and subsequent cell elongation within four distinct growth zone (Figure 1.4), the root apical meristematic (RAM) zone where cells divide; the transition zone (TZ) where cells cease dividing and start to elongate; the elongation zone (EZ) where root cells undergo rapid expansion; and differentiation zone (DZ) where cells develop specialised functions and structures (e.g. root hairs, Casparian strip) and from where lateral roots initiate and emerge (Benfey, Scheres 2002). These zones have been clearly defined, and everything starts at the apical meristem, which is located at the root tip (Péret et al. 2009). The root cap (RC) is the apical meristem surrounding the root tip. As it continuously presses downward into the soil, this protective layer made up of lateral and columella root caps is constantly being renewed (Eapen et al. 1991). The stem cell

niche is located immediately after the RC, in the core of the root apical meristem. The quiescent centre (QC) is encircled by the initials vascular, cortex/endodermal, epidermal/lateral root cap, and columella (Clark et al., 2014). The QC is made up of four mitotically dormant core cells that encourage adjacent cells to divide constantly (Smith, de Smet 2012).

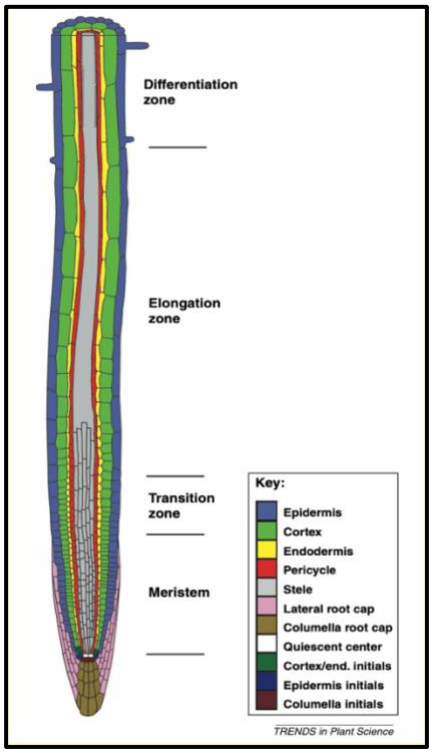


**Figure 1.4** Primary root anatomy of the model plant *Arabidopsis thaliana.* The apex of the *Arabidopsis* root is composed of four separate zones of growth activities. These zones are, in order, the meristem zone of active cell division, the transition zone (TZ) where cells stop dividing and increase slowly in length, the elongation zone (EZ) where cells undergo rapid expansion, and the differentiation zone (DZ) where cells cease elongation and form differentiated structures such as root hairs and Casparian strip (Ubeda-Tomás et al. 2012)

In the presence of an auxin gradient, these initials are known to cause radial patterning of the concentric cell layers (Verstraeten et al., 2014). The cell layers of the epidermis, cortex, endodermis, pericycle, and stele make form the radial organisation of the PR. There is still time for these cell layers to mature and develop their specialised functions (Péret et al., 2009).

The basal meristem is the first developmental zone to move out from the root apical meristem (RAM) as a result of constant cellular division (De Smet et al. 2007). In this region, cells expand, and division levels slow down. Differentiating epidermal cells mark the boundary between the meristematic and elongation zones (Smith, de Smet 2012). Once root hairs begin to form, this marks the beginning of the maturation zone, from which lateral roots (LR) develop (Smith and de Smet, 2012).

The first Lateral Root (LR) is initiated at a set distance from the root tip (Verstraeten et al., 2014). The earliest cellular divisions that give rise to the emerging LR differ greatly from those that give rise to the PR (Benfey and Scheres, 2002.; Péret et al., 2009). Over many studies, eight distinct phases of development have been identified as crucial to LR formation (reviewed in Lavenus et al., 2013). It all starts in the pericycle layer of the primary root, where PIN3, GATA23, and ACR4 are involved (Chen et al., 2015). All of them are characteristics of LR beginning (Figure 1.5). The pericycle layer, as well as the protoxylem, phloem, xylem, their relative poles, and cambium, make up the stele. A subset of pericycle cells proximal to the xylem pole undergo cyclic pre-initiation (Péret et al., 2009; Lavenus et al., 2013). This supports the diverse character of the pericycle layer in the start of LR (Parizot et al., 2008). The xylem pole pericycle cells are then primed to become founder cells at pre-branch locations in the basal meristem (De Smet et al., 2007; Lavenus et al., 2013).

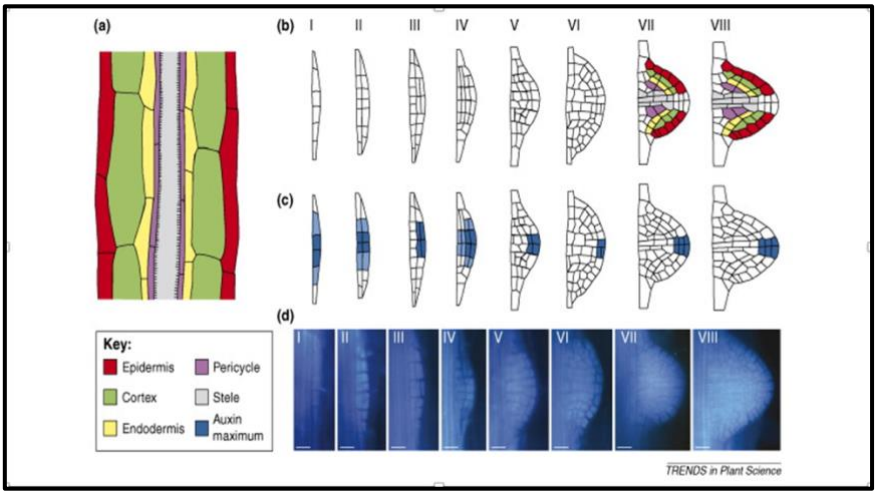


**Figure 1.05** Schematic of Arabidopsis thaliana LR development. (A) LRP come from the founder cells in the pericycle of the PR. The PR's shape is made up of different layers. (B) The process of forming an LRP goes through eight stages. (C) and the maximum levels of auxin signalling are seen with the DR5::GUS reporter line (blue gradient). (D) The LR figure of development came from roots that had been stained with aniline blue(Péret et al. 2009).

## 1.3 Plant Hormone Biology

Hormones play a key role regulating how plants develop and react to their environment. Plants control hormone production, transport, perception and signalling in a variety of ways. For example, hormone distribution within a plant is precisely managed by specialised carriers. Hormones can move within cells, cell-to-cell and across large distances (Figure 1.6) (Anfang and Shani, 2021). Plants also transport peptides to various areas of the plant, in addition to hormones (Takahashi et al., 2019). In recent years, many transporters have been identified for the majority of plant hormones. This section focuses on the key hormones ABA and auxin which regulate plant root adaptations to water stress (Anfang and Shani 2021).

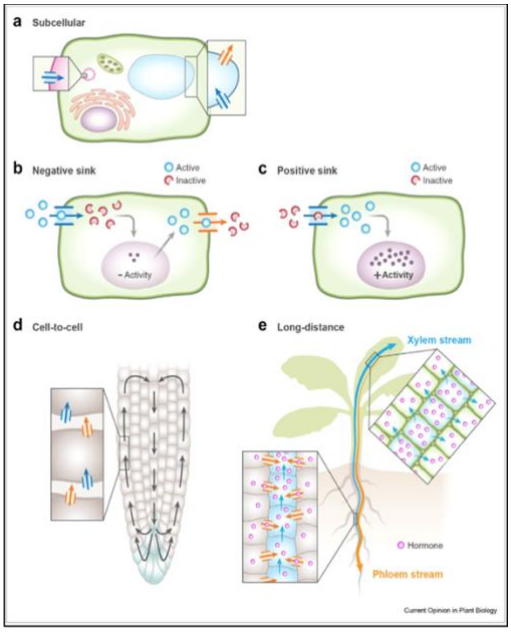


**Figure 1.6** Overview of plant hormone transport related regulatory mechanisms. Hormones are small molecules that play important roles in the regulation of plant growth and development. (a) Subcellular transport involves a hormone moving into or out of organelles within cells. (b) Negative sink: reduced hormone activity can occur in several ways. 1. hormones may be transported into cell but become inactivated by conjugation and degradation. 2. Hormones can be exported from cells, reducing its activity. (c) Positive sink: by increasing the uptake of hormones into cells. (d) Cell to cell: Inter-cellular hormone movement can take place via polar localised hormone influx (ions movement into cells) and efflux (ions movement out of cells) carriers. (e) Long distance: hormones are transported from root to shoot or vice versa via the vasculature. This mode of transportation comprises the loading and unloading hormones via xylem and phloem (Anfang and Shani, 2021)

### 1.3.1 Abscisic Acid (ABA)

Abscisic acid (ABA) is a 15-carbon ring sesquiterpenoid ($C_{15}H_{20}O_4$) (Figure 1.7) that is present in a wide range of organisms from cyanobacteria to sponges to algae to lichens to mosses to mammals (Wasilewska et al., 2008; Mehrotra et al., 2014). ABA was discovered in the 1960s and has since proven to be a very important plant growth regulator.

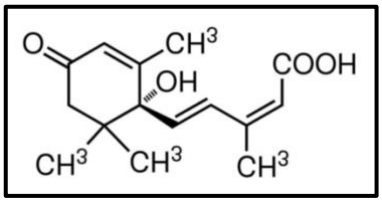


**Figure 0.7** The chemical structure of Abscisic acid (ABA)

ABA regulates a large number of plant processes relating to abiotic stress tolerance including germination, seed dormancy, drought tolerance, stomatal closure, improving root hydraulic behaviour and regulating gene expression (Boursiac et al., 2013; Davies & Zhang, 1991; Kuromori et al., 2014). Drought causes plants to increase levels of ABA (Zhu, 2002). ABA was originally assumed to be produced only in roots then transferred to shoots to control stomatal closure. ABA is now known to be also produced in shoots (Kuromori et al., 2014, 2018), mainly in the vasculature (Seo and Koshiba, 2002). ABA can control stomatal closure even when synthesised in phloem, suggesting ABA is transported to different areas of the plant to regulate various responses (Kuromori et al., 2014; Merilo et al., 2018). The increase in ratio of root to shoot growth at low water potential is observed in the presence of ABA, but this difference is not observed in the absence of ABA (Saab et al., 1990). (Spollen et al. 2000) reported ABA accumulation maintains primary root elongation in maize at low water potential by restricting ethylene production which inhibits root elongation.

Knowledge of ABA as a key regulator of abiotic stress responses was used to develop crops with increased tolerance under stress conditions. In various crop plants, molecular manipulation of ABA synthesis or signalling has been performed to improve stress tolerance in tomato (Gonzalez-Guzman et al., 2014; Orellana et al., 2010; Thompson et al., 2000), rice (Kim et al., 2014; Lu et al., 2009; Tang et al., 2012; Tian et al., 2015), wheat (Sivamani et al. 2000), canola(Wang et al. 2009) and tobacco (Luo et al. 2016; Zhijin et al. 2009).

#### 1.3.1.1 ABA Signalling

To understand how ABA is perceived and signals in plants, scientists have studied the components of ABA signalling in *Arabidopsis thaliana*(Raghavendra et al., 2010). ABA binds to receptor proteins called Regulatory Component of ABA Receptors are members RCAR/PYR/PYLs which belong to the START-domain superfamily (Nishimura et al., 2010; Cutler et al., 2010). RCAR/PYR/PYLs proteins are found in the cytoplasm and nucleus of plant cells. ABA binding to RCAR/PYR/PYLs leads to inactivation of type 2C protein phosphatases ($PP2C_s$), such as ABSCISIC ACID INSENSITIVE 1(ABI1) and its close homolog (ABI2) (Nishimura et al., 2010; Cutler et al., 2010). All 14 members of the RCAR family of proteins can bind to ABA and interact with PP2Cs, with the exception of RCAR7/PYL13, which are positive regulators of ABA signalling (Nishimura et al., 2010).

Arabidopsis encode 80 different PP2Cs, and six of the nine clade A PP2C genes function as negative regulators of ABA signalling (Nishimura et al., 2010). As co-receptors, these phosphatases and RCAR/PYR1/PYLs create a high affinity binding site for ABA. PP2Cs are positive regulators of ABA signalling, and their inactivation prevents PP2C-mediated dephosphorylation of Sucrose nonfermenting kinase-1-related protein kinase 2s (SnRK2s). Activated SnRK2s phosphorylate ABA-responsive element Binding Factors (ABFs) which encode transcription factors that bind to ABA-Responsive Elements (ABREs) found in the promoter regions of genes induced by ABA (Busk and Pagès, 1998; Lumba et al., 2014).

As shown in (Figure 1.8), the ABA signalling complex/ABA signalosome is a system made up of three parts. The first part is RCAR/PYR/PYLs, which are proteins that help

regulate the response to stress. The second part is PP2Cs, which are proteins that help control the activity of other proteins. The third part is SnRK2s, which are proteins that help control the activity of other proteins in a way that prevents them from becoming too active. All of these parts work together in a double negative regulatory system, meaning that they work together to keep the activity of the proteins in balance (Mehrotra et al., 2014). In the absence of ABA, PP2Cs dephosphorylate SnRK2s, which inhibit kinase activity and, as a result, prevent the expression of downstream genes (Fernando and Schroeder, 2016).

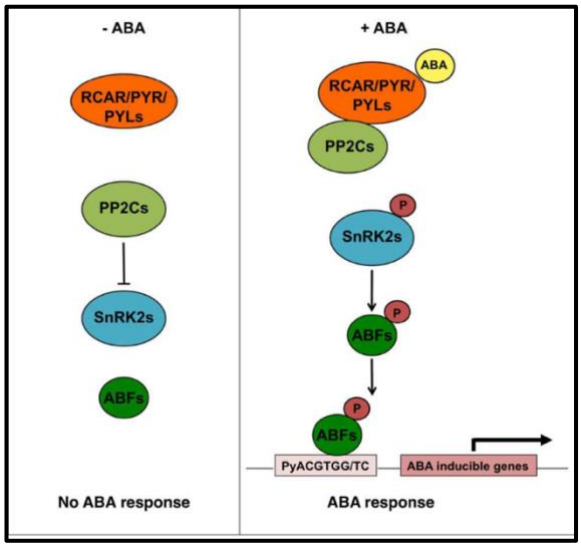


**Figure 1. 8** Schematic of the primary ABA signalling pathway in the absence (-ABA) and presence (+ABA) of this hormone signal (Fernando and Schroeder, 2016).

Several studies have shown that the core components of ABA signalling are essential for it to work properly. (Fujita et al., 2009) found that when the *snrk2.2/2.3/2.6* triple null mutant was used, ABA signalling was completely blocked, and the expression of ABF genes was reduced. Additionally, the phosphorylation of other bZip transcription factors, such as ABI5 which promotes dormancy, was also reduced.

#### 1.3.1.2 ABA Biosynthesis

ABA (abscisic acid) is a plant hormone that is important in many physiological processes, including stress response and growth and development. ABA is synthesised by a complicated route comprising numerous enzymatic activities. Isopentenyl pyrophosphate (IPP) synthesis is a precursor for ABA biosynthesis that is produced from the mevalonic acid (MVA) or 2-C-methyl-D-erythritol 4-phosphate (MEP) pathways. Both processes contribute to the creation of IPP (Verslues and Bray 2006). Zeaxanthin, a carotenoid pigment, is the precursor for ABA production. It is made from geranylgeranyl pyrophosphate (GGPP), which is made from IPP. Several enzymatic stages are involved in the conversion of GGPP to zeaxanthin, which **is** catalysed by enzymes such as phytoene synthase, phytoene desaturase, and ζ-carotene desaturase (Finkelstein, 2013). Violaxanthin, a carotenoid pigment, is broken enzymatically to form xanthoxin. A particular enzyme termed 9-cis-epoxycarotenoid dioxygenase (NCED) catalyses this process (Verslues and Bray, 2006). Five genes in Arabidopsis encode the 9-cis-epoxycarotenoid dioxygenases (NCEDs), which are important enzymes in the regulation of ABA production. NCED3 has been demonstrated to play an important role in the regulation of ABA synthesis in response to water deficiency, whereas NCED6 and NCED9 are required for ABA biosynthesis in the embryo and endosperm, which causes dormancy (Hu et al., 2021)**.** The action of abscisic aldehyde oxidase (AAO) converts xanthoxin further into abscisic aldehyde. This enzyme catalyses the oxidation of xanthoxin, resulting in abscisic aldehyde production(Verslues and Bray, 2006). The final stage in ABA biosynthesis is the conversion of abscisic aldehyde to abscisic acid. This step is catalysed by abscisic aldehyde oxidase or short-chain alcohol dehydrogenase/reductase (ABA2). Abscisic acid is the biologically active form of ABA (Verslues and Bray, 2006) (Figure 1.9).

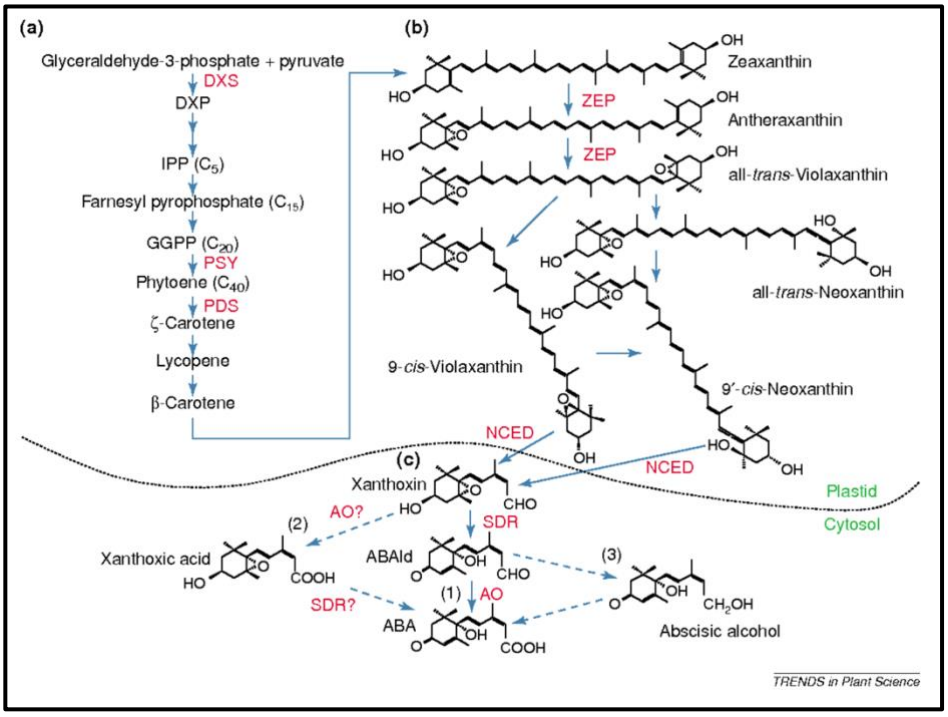


**Figure 1.9** The ABA biosynthetic pathway in plants. (a) In plastids, IPP is synthesized via DXP from glyceraldehyde-3phosphate and pyruvate. Carotenoids are synthesized from a C5 compound, IPP. (b) Epoxycarotenoid and plastid cleavage. This ABA synthesis route begins with two-step epoxidation of zeaxanthin to generate all-transviolaxanthin. NCED oxidises 9-cis epoxycarotenoid isomers such violaxanthin and neoxanthin to generate xanthoxin. The enzyme(s) that convert all-trans-violaxanthin to 9-cis or 9′-cisneoxanthin is unknown. (c) Cytosolic reactions for ABA production. Three paths are suggested. (1)Arabidopsis AO, which catalyses ABAld oxidation, suggests that plants use it. ABA2 transforms xanthoxin to ABAld in Arabidopsis. Xanthoxic acid's second route. (2) AO oxidises xanthoxin to xanthoxic acid, which SDR converts to ABA in this process. Pathway. (3) Through abscisic alcohol appears to be a shunt mechanism but is significant in ABAld mutants. Figure shows text-mentioned enzymes (red) and chemical names (black) (Seo and Koshiba, 2002).

### 1.3.1.3 ABA Transporters

Several ABA transporter genes have been discovered, providing insight into the molecular mechanics of ABA delivery. ABCG25 and ABCG40 transporters from the ATP binding cassette (ABC) family have been identified as ABA transporters in Arabidopsis. ABCG25 exports ABA from the vasculature, while ABCG40 imports ABA into guard cells (Kang et al. 2010a; Kuromori et al., 2010). This indicates that ABA is actively transported from the vasculature to guard cells. ABCG25 and

ABCG31 export ABA from the endosperm, while ABCG30 and ABCG40 import ABA into the embryo (Park et al., 2017; Kang et al., 2015). AIT1-4 (also known as NPF4.6, 4.5, 4.1, and 4.2, respectively) was discovered as a type of ABA transporter that regulates the stomatal aperture in inflorescence stems and acts as an ABA influx facilitator at the site of ABA biosynthesis (Kanno et al., 2012). According to (Zhang et al., 2014), DTX50 a member of DTX/MATE family in *Arabidopsis* played a role in ABA-mediated growth inhibition and responses to drought.

ABA transporters have also been identified in other plant species. SlAIT1.1, for example, was discovered to be an ABA importer in tomato (*Solanum lycopersicum*) and to activate downstream of the DELLA gibberellin suppressor response to induce stomatal closure (Shohat et al., 2020). MtABCG20 is an ABA exporter found in *Medicago truncatula* roots and seeds (Pawela et al., 2019). Furthermore, DG1 is a MATE family exporter engaged in the long-distance transport of leaf-derived ABA to govern seed development, whereas OsPM1 is an importer implicated in stomatal closure and drought responses (Qin et al., 2021; Yao et al., 2018). Furthermore, UDP-glucosyltransferases conjugate ABA with glucose to produce ABA-glucosyl ester (ABA-GE), a nonactive form of ABA (Xu et al., 2012). ABCC1 and ABCC2 have been found on the plant tonoplast membrane and have been shown to have ABA-GE import activity in a heterologous yeast system (Burla et al., 2013).

No ABA transporters have been described to regulate hydrotropism, to date. Dietrich et al., (2017) demonstrated that hydrotropism requires ABA. Responses to ABA in the cortex of the root elongation zone play an important role during hydrotropism, but whether and how ABA is mobilized to this tissue from its phloem site of synthesis

remains unclear (Fig. 1.9). To name a few, The SnRK2 kinases have had the most extensive study done on them relating to the role of ABA signalling in hydrotropism (Mustilli et al., 2002). Demonstrating that all three family members, *SnRK2.2, SnRK2.3, and SnRK2.6*, play a role in ABA signalling (Kaneyasu et al., 2007). The hydrotropism of the *snkr2.2 snrk2.3* double mutant decreases significantly. Cortex-specific expression of *SnRK2.2* in a double mutant context demonstrated that it is sufficient to rescue the response (Dietrich, 2017).

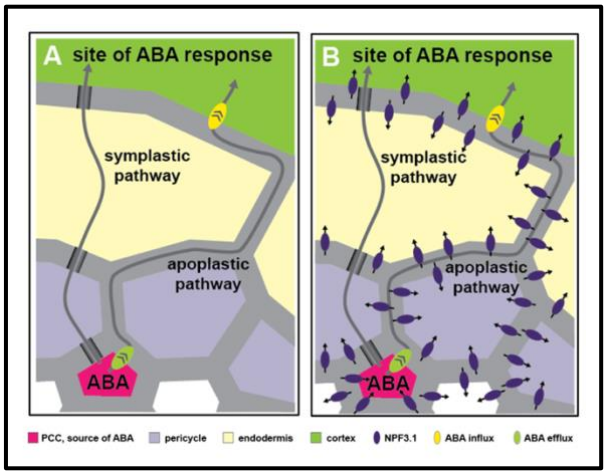


**Figure 1. 10** Hydrotropism and ABA transport mechanism. (A) In the early elongation zone (no Casparian strip) scenarios for radial ABA transport, ABA can move from its Phloem Companion Cell (PCC) source to surrounding cells either symplastically or apoplectically. Apoplastic ABA movement implies the activity of an efflux transporter in the source tissue and an influx transporter in the responding tissue. (B) Perturbation of radial ABA transport: Overexpression of an ABA influx transporter should lead to a strong increase in influx capacity in all root cells. This affects only the apoplastic pathway, as ABA entering the apoplast would be transported back into the cytoplasm of the cortex cell. (Dietrich et al., 2017)

### 1.3.2 Auxin

Auxin was the first plant hormone discovered, and it is also a critical regulator in coordinating plant growth and organ development, as well as regulating plant response to environmental changes. There are four different types of auxins found naturally in plants, and they are all referred to by their chemical formulas: indole-3-acetic acid (IAA), 4-chloroindole-3-acetic acid (4-cl-IAA), indole-3-butyric acid (IBA), and 2-phenylacetic acid a (PAA) (Lavy and Estelle, 2016).The most abundant auxin in plants is indole-3-acetic acid. Due to its importance, auxin has been extensively researched, and the production, primary signalling pathway, and polar transporters have been identified (Figure 1.11) (Anfang and Shani, 2021; Geldner et al., 2003; Webb and Hall,1995).

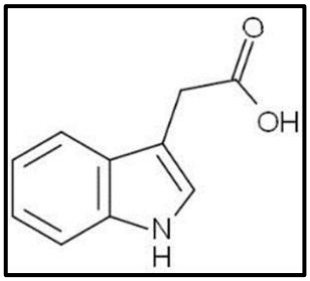


**Figure 1.11** The Chemical structure of Auxin (IAA). Auxin (pKa = 4.75, IAA)is a cyclic molecule composed of a side-carrying ring covalently bonded to a carboxyl group (Vanneste and Friml, 2009; Webb and Hall, 1995).

Auxin controls the majority of the growth and patterning processes in a plant across its entire lifetime (Vanneste & Friml, 2009). Auxin regulates a wide variety of cellular and developmental processes, including cell division, embryonic and post-embryonic patterning (Abualia et al., 2018; Paciorek and Friml, 2006), vascular differentiation, cell elongation (Teale et al., 2006), the commencement of roots and lateral roots, and tropic responses (in reaction to factors like light and gravity) (Teale et al., 2006; Ubeda-Tomás et al., 2012).

#### 1.3.2.1 Auxin Synthesis Pathway

Plants produce auxins primarily at the tips of their shoots and in their youngest leaves (Friml et al., 2002). IAA can also be synthesised in roots (Zhao, 2012). Auxin production occurs primarily via two pathways in bacteria and plants; these are the TRP-dependent and TRP-independent processes, respectively. Figure 1.12 depicts the TRP-dependent pathway, which contains four distinct auxin production routes: indole-3-pyruvic acid (IPyA), indole-3-acetamide (lAM), tryptamine (TAM), and indole-3-acetaldoxime (IAOx) (Mashiguchi et al., 2011; Mano and Nemoto, 2012; Larrieu, 2011). Key enzymes include TRYPTOPHAN AMINOTRANSFERASE OF ARABIDOPSIS (TAA), responsible for biosynthesis of Indole-3-Pyruvic Acid (IPA) from L-tryptophan (L-TRP), and YUCCA FLAVIN MONOOXYGENASE-LIKE proteins (YUC), which catalyse the conversion of IPA to IAA in Arabidopsis (Casanova-Sáez et al., 2021; Swarup et al., 2001).

Auxin is transported from its synthesis sites to target tissues. Two transport routes are used to mobilise auxin between synthesis and target plant tissues. First, auxin can be transported over long distances from its biosynthetic sources (e.g., young shoots) to sink tissues (e.g., roots) via the phloem (Swarup et al., 2001; Marchant et al., 2002). Auxin influx and efflux carriers mediate cell-to-cell movement within organs over short distances (Abel and Theologis, 2010; Vanneste and Friml, 2009).

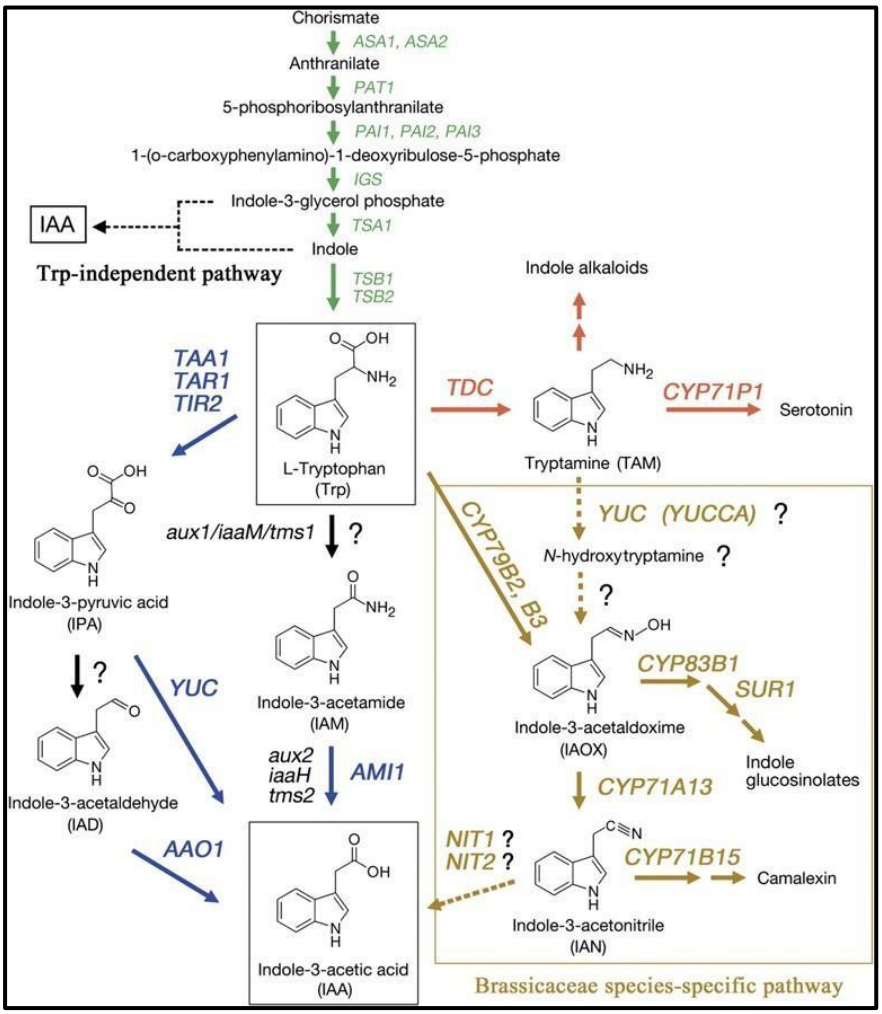


**Figure 1.12** Auxin synthesis pathway. Synthetic route for tryptophan in chloroplasts (green arrows). The known genes and enzymes in the Tryptophan-dependent IAA synthesis pathway (blue arrows). Indole alkaloid and serotonin biosynthesis pathways (red arrows). Brassicaceae species-specific route (yellow arrows). Unknown genes and enzymes (black arrows). (This figure is adapted from (Mano and Nemoto, 2012).

Several families of auxin influx and efflux transporters have been discovered and characterised. This includes PIN efflux proteins which promote polar cell-to-cell IAA transport. Eight PIN proteins in Arabidopsis have been identified (Benková et al., 2003). It is the polarised plasma-membrane location of PIN1-4 and 7 that dictates the direction of auxin transport. PIN proteins PIN5, 6, and 8 function maintaining intracellular auxin homeostasis, which are endoplasmic reticulum- and plasma membrane-localized, respectively (Mravec et al., 2009).

The AUX/LAX family consists of four functional auxin influx carriers that mediate auxin-related developmental programmes in distinct organs and tissues. In order to control root gravitropism and root hair formation, AUX1, the most extensively researched member of the family, transfers auxin from the root tip to the shoot. Recent studies in Arabidopsis and rice (Giri et al., 2018)demonstrated that AUX1 stimulates root hair elongation in response to phosphate restriction.

ABCB1 (also known as PGP1), 4, 14, 19 (also known as MDR1), and 21 are all members of the ABCB family and are essential for polar auxin distribution (Zazímalová et al., 2010; Noh et al., 2001). Additional members of the auxin exporter family, ABCB6 and 20, have been implicated in controlling shoot growth (Zhang et al., 2018). (Chen et al., 2020) recently showed that ABCB15-18 and 22 allow IAA to travel redundantly from the lateral root cap, shoot-wards via the epidermis, to regulate lateral root initiation. Auxins are also transported via a number of NPF proteins. In addition to transporting nitrate and IAA (Krouk et al., 2010), NRT1.1 (also known as NPF6.1 or CHL1) mediates nitrogen uptake from the rhizosphere.

The NITRATE TRANSPORTER 1/PEPTIDE TRANSPORTER FAMILY (NPF) are transporters of indole-3-butyric acid (IBA), an IAA precursor, have recently been discovered. TOB1 (also known as NPF5.12) is the first which faciitates IBA sequestration into the vacuole. NPF7.3 is the second factor, and it transports IBA into the root cap cells of the columella to control gravitropic responses (Watanabe et al., 2020). These two NPF IBA transporters are joined by three others: PXA1 (also known as ABCD1) (Zolman et al. 2001), ABCG36(Strader & Bartel, 2009), and

ABCG37(Růžička et al., 2010). Regulating molecules involved in IBA absorption and long-distance transport efflux are not well understood (Damodaran et al., 2019).

### 1.3.2.2 The Role of Auxin in Hydrotropism

Different plant species have different auxin needs throughout the hydrotropic response (Table 1.1). The hydrotropic response is unaffected in *aux1* and *pin2* mutants, which have defects in their gravitropic auxin transport (Takahashi et al., 2002). Hydrotropism is also not inhibited by the auxin transport inhibitors 2,3,5-triiodobenzoic acid (TIBA), 1-naphthylphthalamic acid (NPA), or 3-chloro- 4-hydroxyphenyl acetic acid (CHPAA); in fact, treatment with TIBA or NPA results in an earlier increase in root tip angle in hydrotropism assays, even though final angles remain the same (Kaneyasu et al., 2007; Shkolnik and Fromm, 2016). Moreover, the expression of the auxin reporters DII-Venus and DR5 does not change at any point in the hydrotropism response (Shkolnik and Fromm, 2016).

**Table 1.1** Species-specific variations in hydrotropism in plants (ND not determined) (Dietrich, 2018)

| Plant species | Gravitropism masks hydrotropism | Root cap needed for hydrotropism | Auxin transporters inhibitor blocks hydrotropism | Auxin responses inhibitor blocks hydrotropism | Auxin biosynthesis inhibitor blocks hydrotropism | Hydrotropism genes |
|---|---|---|---|---|---|---|
| Pea | Yes | ND | Yes/No | Only at 100 μ M (PCIB) | ND | ND |
| Cucumber | Yes | No | Yes | Yes (PCIB) | ND | *IAA1,PIN 5* |
| *Arabidopsis thaliana* | No | No | No | Yes (PCIB) No (auxinole, PEO, IAA) | ND | MIZ1,MIZ2 PTR/PYL, PP2CA, SnRK2.2, ABA.1, PLDζ2 |
| Rice | No | No | Yes | Yes (PCIB) | Yes | ND |
| *Lotus japonicus* | No | ND | No | No (PCIB) | Yes | ND |

Although hydrotropism does not require auxin transport, it does appear to require an auxin response machinery. The effects of auxin response inhibitors appear contradictory. The addition of auxinole or α-(phenylethyl-2-oxo)-indole acetic acid (PEO-IAA) sped up the reaction, while $\rho$-chlorophenoxyisobutylacetic acid (PCIB) caused the response to slow down (Shkolnik and Fromm, 2016). Different mechanisms of action and inhibitor specificities may explain these differences. Auxinole and PEO-IAA bind to the auxin receptor TIR1, but PCIB method of action is unknown (Oono et al., 2003; Hayashi et al., 2012) . PCIB cannot reverse exogenous IAA effects on root development, while auxinole and PEO-IAA can(Oono et al., 2003; Hayashi et al., 2012). The particular inhibitors auxinole and PEO-IAA imply that auxin inhibits hydrotropism in *Arabidopsis thaliana*, although this needs confirmation from auxin response mutants.

The role of auxin in hydrotropism has been studied in four additional plant species, including cucumber, rice, birdsfoot trefoil, and pea. Experiments with peas need the use of the totally a gravitropic *ageotropum* mutant, while those with cucumber seedlings require either microgravity, clinorotation, or the removal of the root tip to reveal the hydrotropism response (Morohashi et al., 2017).

Briefly, auxin role in hydrotropism differs greatly amongst plant species. Hydrotropism is independent of gravitropism in some species (such as rice) but still requires auxin. This may be because different plant species have different water requirements for a successful life cycle. The integration of gravitropic and hydrotropic signals determines the growth direction of the root tip, so knowing the role of auxin in hydrotropism is crucial (Dietrich, 2018).

## 1.4 Root, Soil and Water

Water stresses like drought and waterlogging have a significant negative impact on plant development. Drought inhibits root growth and development (Comas et al., 2013; Gupta et al., 2020), and poor root water uptake stresses xylem tissue. Without xylem acclimation, embolism can cause hydraulic failure (Sevanto, 2014; Levionnois et al., 2020; Li et al., 2021). Drought stress decreases nutrient mobility and diffusion, affecting nutrient intake (Rouphael et al., 2012; He and Dijkstra, 2014), alters soil microbial populations and activity (Naylor and Coleman-Derr, 2018; Nguyen et al., 2018) and lowers root penetration ability (Correa et al., 2019).

Clay, peat, loam, and sandy soil types have varied structural compositions that impact water availability to roots (Morris et al., 2017). For example, pore size influences soil moisture gradients (Bao et al., 2014). Roots have developed a number of adaptive responses to maximise water uptake (Figure 1.13 ). For example, roots often grow towards deeper soil layers where water is more available and away from dry topsoil layers where heat stress is greatest (Comas et al., 2013; Gandullo et al., 2021). By increasing root angle, rice becomes more drought resilient (Uga et al., 2013). Drought stress also causes fewer axial/lateral roots and a deeper rooting architecture (Lynch, 2013). (Zhan et al., 2015; Dinneny, 2019). Another component that influences RSA and drought tolerance is positive hydrotropism (next section), where roots grow towards available water (Dietrich et al., 2017; Dinneny, 2019).

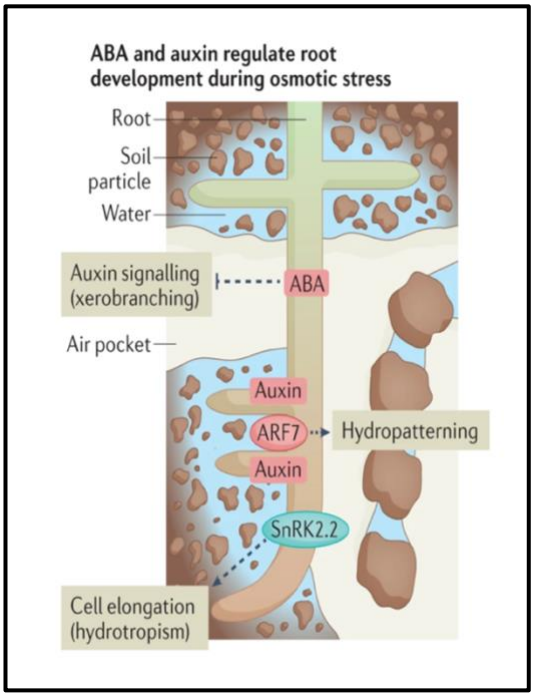


**Figure 0.13 Root adaptive responses to water stress.** Primary roots show hydrotropism which requires SnRK2.2 activation in elongation zone cortical cells. ABA inhibits auxin signalling to limit lateral root growth (xerobranching) when roots encounter air gaps. In asymmetrically watered locations, roots produce lateral roots on the water-contacting side, a process called hydropatterning. ARF7 enhances lateral root initiation in hydropatterning (Waadt et al., 2022)

### 1.4.1 Hydrotropism: Growing Towards Moisture

Water is becoming an increasingly precious resource on our planet, with agriculture using up over 70% of all freshwater worldwide (Davies and Bennett, 2015). Current approaches for improving water usage efficiency in crops through changes in root system architecture focus on constitutive traits such as steeper root angle to tap water resources in lower soil horizons (Gao et al., 2015; Henri, 2010; Uga et al., 2013). However, integrating plastic/adaptive root traits like enhanced hydrotropic response could deliver real value for improving water foraging and stress resilience. To do so requires knowledge of the key regulatory genes and processes.

The term tropism is used to describe the regulation of plant growth direction in response to directional environmental signals such as gravity, light (Galvan-Ampudia et al., 2013; Monshausen and Gilroy, 2009) and moisture (Su et al., 2017). Hydrotropism refers to root growth towards soil moisture to avoid drought (Moriwaki et al. 2013; Dietrich 2018). Historical accounts of hydrotropism can be found (Bonnet, 1754; Knight, 1811), and in the 19th century, researchers conducted elegant studies to determine the root tip is required for perception of the water gradient (Sachs, 1872; Darwin and Darwin, 1880; Wiesner, 1881; Molisch, 1883). Hydrotropism has received increasing attention in recent years (reviewed in Cassab et al., 2013; Monshausen and Gilroy, 2009; Moriwaki et al., 2013; Shkolnik and Fromm, 2016). Hydrotropic response has been demonstrated for the following species: pea (*Pisum sativum*), cucumber (*Cucumis sativus*), wheat (*Triticum aestivum*), maize (*Zea mays*), rice (*Oryza sativa*), birdsfoot trefoil (*Lotus japonicus*), sitka spruce (Picea sitchensis), and *Arabidopsis thaliana* (Coutts et al., 1993; Dietrich et al, 2017; Jaffe et al., 1985; Mizuno et al., 2002; Nakajima et al., 2017; Takahashi et al., 2002).

#### 1.4.1.1 Selected Phytohormones Regulate Hydrotropism

The phytohormone auxin is crucial for many tropisms and may also be involved in hydrotropism. However, the hydrotropic response is unaffected in *aux1* and *pin2* mutants of *Arabidopsis thaliana*, which have defects in their ability to transport auxin during a gravitropic response (Takahashi et al., 2002).In contrast, genetic evidence clearly supports a role for the phytohormone ABA during hydrotropism (Takahashi et al., 2002; Dietrich et al, 2017). Mutants defective either in ABA synthesis (Takahashi et al., 2002) or signalling (Dietrich et al., 2017) exhibited

strong hydrotropic defects. Tissue specific rescue experiments in *Arabidopsis* revealed that ABA is required to target root cortical cells in the elongation zone to trigger a hydrotropic response (Dietrich et al., 2017). The authors found that a hydrotropic response still occurs after meristem and cap removal by laser ablation. Hence, in contrast to gravitropism, the elongation zone alone is able to perceive a water potential gradient and guide a hydrotropic growth response using ABA signalling (Dietrich et al., 2017).

#### 1.4.1.2 Hydrotropism Genes

Only two genes involved in hydrotropism in Arabidopsis have been identified using classical forward genetic screening. The hydrotropism-affected semi-dominant mutants with *no hydrotropic response 1* (*nhr1*) and *altered hydrotropic response 1* (*ahr1*) have been identified (Eapen et al., 2003; Saucedo et al., 2012). However, the defective genes in either mutant have not yet been isolated (Dietrich, 2018). Hydrotropism also requires a novel gene called MIZU–KUSSEI1(MIZ1) (Kobayashi et al., 2007), which is upregulated by ABA (Moriwaki et al., 2013). The ABA signalling kinase SnRK2.2 and MIZ1 were both identified to play a role in cortical cells of the elongation zone (Dietrich et al., 2017).

Another hydrotropic defect mutant *miz2* encodes a weak *GNOM* allele (Miyazawa and Takahashi, 2009). GNOM is a GDP/GTP exchange factor for small G proteins of the ARF class (ARF-GEF) that regulate intracellular vesicle trafficking, the best-known activity of which is polar targeting of PIN proteins to the plasma membrane (Geldner et al., 2003). *miz2* has no effect on auxin response or PIN localisation (Miyazawa, Ito, et al., 2009). The G951E mutation of *miz2* is located downstream

of the Sec7 domain and affects an amino acid that is conserved in GNOM homologues from other plant species (Miyazawa and Takahashi, et al. 2009). BFA, a recognised ARF-GEF inhibitor, mimics the phenotype of *miz2*. Furthermore, BFA cannot inhibit the hydrotropic response of the BFA-resistant $GN^{M696L}$ allele, whereas the weak $gnom^{B/E}$ allele is hydrotropic (Miyazawa and Takahashi, et al. 2009).

A phospholipase D mutant that is modestly deficient in hydrotropism provides additional evidence for the relevance of vesicle trafficking in hydrotropism (Taniguchi et al., 2010). In addition, another Arabidopsis phospholipase Dζ2 mutant, *pldζ2*, displayed considerably delayed or disrupted root hydrotropic response, and the inhibitory impact of ABA on gravitropism was eliminated in *pldζ2* mutant roots. Furthermore, both dryness and the presence of exogenous ABA can promote the expression of *PLDζ2* in the root cap. These findings suggest that ABA signalling in the root cap can promote root hydrotropism while suppressing gravitropism (Taniguchi et al. 2010). However, tissue-specific rescue of ABA response in just cortical (but not lateral root cap) tissues of the *snrk2.2,2.3* mutant could restore hydrotropism (Dietrich et al, 2017), does not support the importance of the root cap ( see Table 1.1 in P21).

### 1.4.2 Hydropatterning: Root Branching Toward Water

Lateral roots (LRs) exhibit a strong bias in their positioning when exposed to asymmetric water availability (Bao et al, 2014). For example, when roots are in contact with moist soil growing down a macropore. This bias in lateral root branching is referred to as hydropatterning (Fig 1.14). This adaptive response to water was observed in situ using X-ray micro CT images (Fig 1.14 A) (Bao et al., 2014; Morris et al., 2017). Resource savings and enhanced water uptake are two putative benefits of this root adaptation(Bao et al., 2014).

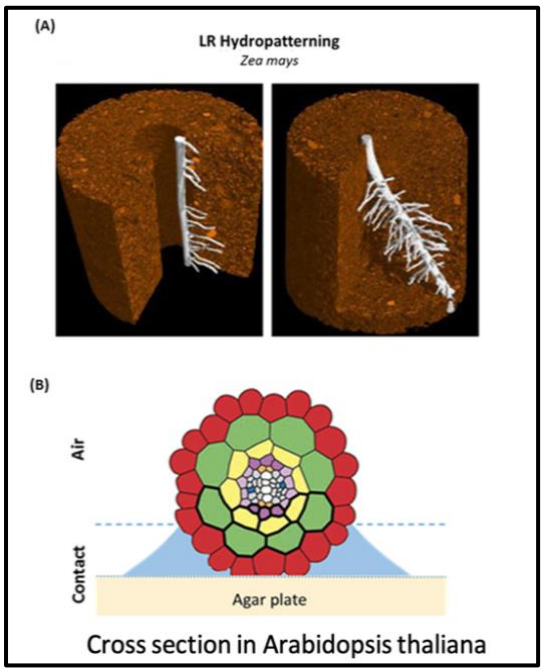


**Figure 0.14** Schematic diagram depicting LR hydropatterning. (A) *Zea mays* roots propagating down soil columns can be clearly shown by micro-CT imaging to exhibit LR hydropatterning responses. In order to place their LRs in contact with moisture, roots are positioned to grow down an artificial air pore (left). On the other hand, LRs form a random pattern when roots are grown properly in soil (right) (Bao et al., 2014). (B) A diagrammatic cross section of *Arabidopsis thaliana* root showing the meniscus that forms as the plant is growing on an agar plate and indicating the air/contact divide (Bao et al., 2014).

LR hydropatterning is not exclusive to monocot roots; dicot roots also exhibit this behaviour, suggesting that it is a well-conserved adaptive response in higher plants

(Bao et al. 2014). Plant roots that grow vertically on the surface of an agar plate also undergo this adaptive response. The creation of a meniscus causes opposite sides of the root to be in direct touch with liquid or exposed to air (Fig 1.14 B) (Bao et al., 2014). A differential auxin response gradient is triggered in response to asymmetric moisture distribution (Bao et al. 2014).

In fact, auxin production, transport, and signalling appear crucial in controlling LR hydropatterning(Bao et al., 2014). Auxin is known to play an important function in the early stages of LR formation. Auxin has been extensively documented to enhance xylem pole pericycle founder cell specification (De Smet et al., 2007; Lavenus et al., 2013; Péret et al., 2009). In *Arabidopsis* founder cells from only one of the two xylem poles is chosen to form a LR. (Bao et al., 2014)observed using early LR markers that hydropatterning regulated founder cell specification. Moisture variation across the PR is thought to influence xylem pole selection towards the contact side. As a result, LRs initiate mostly on the contact side of the PR, as opposed to the air side (Bao et al., 2014).

ABA mutants extremely resistant to ABA treatment, like *pyr/pyl 112458*, exhibit a typical LR hydropatterning response (Bao et al., 2014). Therefore, hydropatterning is not mediated by ABA signalling. Instead, auxin biosynthesis (*wei8-1*) and auxin transport (*pin2/3/7*) mutations led to an increase in the fraction of lateral roots that exited toward the air rather than just the agar, which suggests that this hormone modulates root hydropatterning (Bao et al., 2014) Recent research established the relevance of auxin response during hydropatterning by demonstrating that transcription factor AUXIN RESPONSE FACTOR 7 (ARF7) knock-out mutants could no longer orient their lateral roots towards water (Orosa-Puente et al., 2018).

ARF7 is a key regulator of auxin-dependent LR initiation and represents a target for regulation by the SUMOylation machinery (Orosa-Puente et al., 2018). The addition of SUMO to ARF7 triggers the recruitment of auxin response repressor proteins and suppresses lateral root initiation. Hydropatterning is blocked in mutants disrupting the SUMO machinery or ARF7 variants lacking SUMOylation sites. Hence, hydropatterning represents an auxin (not ABA) dependent adaptive response that relies on post-translational modification of the key lateral root regulator ARF7.

### 1.4.3 Xerobranching: Root Branch Inhibition to water deficit

Plants have evolved other root adaptive systems (in addition to hydrotropism and hydropatterning) to locate and respond to local water availability. The xerobranching response prevents the initiation of lateral roots when roots lose contact with moist soil. For instance, branching of barley and maize roots whilst growing through an air-filled gap is completely inhibited, but resumes once contacting soil moisture (Orman-Ligeza et al., 2018). This adaptive reaction, known as Xerobranching (Figure 1.15), was originally observed in aeroponically grown maize and barley roots exposed to a temporary water deficit (Babé et al., 2012).

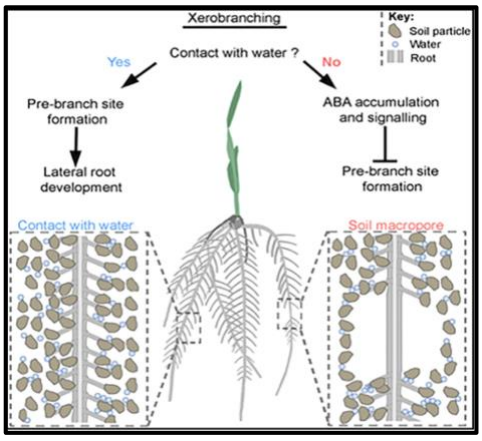


**Figure 1. 15** Schematic of root responses to water availability and shortage. The accumulation of ABA causes xerobranching formation (Orman-Ligeza et al., 2018).

Anatomical studies revealed that barley roots exposed to a Xerobranching water deficit resulted in the initial stage of lateral root initiation being blocked (Babé et al., 2012). This observation suggested that xerobranching regulates a very early developmental stage close to the root tip (Babé et al., 2012).In the study of (Orman-Ligeza et al., 2018), X-ray microscale computed tomography (MicroCT) was used (Figure 1.16 ) to non-invasively image maize and barley roots growing across a large macropore. Seedling roots first grew through 4 cm of moist soil, then into a 2 cm air space, and then back into 4 cm of moist soil. MicroCT imaging revealed that LR branching was extremely responsive to water availability. (Orman-Ligeza et al., 2018) observed LR branching along roots developing within the soil, which is totally suppressed in root segments growing through the air-filled macropore, then is re-activated when roots re-enter the moist soil (Figures 1.16 A and 1.16 B). However, when the air space was filled with water, maize roots continued to create LRs as if they were in moist soil (see air versus water-filled spaces).

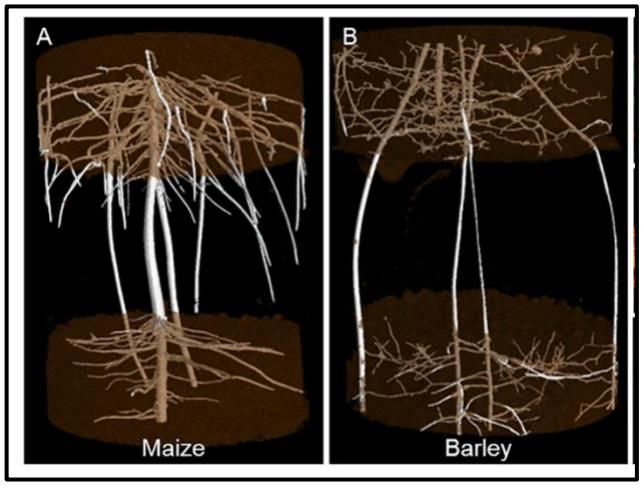


**Figure 0.16** Xerobranching Response Observed in Maize and Barley Grown in Soil. X-ray CT images of 16-day-old (A) maize (B73) (n = 5) and (B) barley (B83) (n = 3) plants growing through a 2-cm air gap (Orman-Ligeza et al. 2018)

A similar repression of LR initiation was found when barley roots were treated with ABA using aeroponics (Orman-Ligeza et al., 2018). When compared to plants that were kept hydrated, levels of ABA were found to be much higher in root tips subjected to water deficit (Orman-Ligeza et al., 2018).

The PYR/PYL/RCAR family of ABA receptors is responsible for the regulation of plant ABA response(Dietrich, 2018). When treated with ABA, *Arabidopsis* mutants lacking several members of the PYR/PYL gene cluster displayed reduced LR suppression (Orman-Ligeza et al., 2018). The DR5-Luciferase reporter was used to examine changes in the lateral root related auxin response following an ABA treatment, which revealed that the number of pre-branch sites formed was reduced. Based on their findings, the authors hypothesised that ABA build up in the water deficit zone inhibits auxin response or accumulation, hence suppressing the establishment of lateral root pre-branch sites which blocks organ initiation.

## 1.5 ARTIFICIAL microRNA (amiRNA)

MicroRNAs (miRNAs) are small, single-stranded, non-coding RNA molecules found in plants, animals, and some viruses that contain 21 to 23 nucleotides (Hauser et al. 2013; Schwab et al. 2006). They function in RNA silencing and post-transcriptional regulation of gene expression through base-pairing to complementary sequences in mRNA molecules, which ultimately results in gene silencing via translational repression and mRNA degradation (Lambert et al., 2019). MiRNAs act a critical function in the regulation of gene expression in all organisms; miRNAs are widely distributed tiny regulatory RNA genes in plants that target both messenger RNA (mRNA) degradation and protein translation inhibition based on sequence similarity between the miRNA and its targeted mRNA (Lambert et al. 2019). Plant microRNAs have a limited target set with high sequence complementarity (Schwab et al. 2006). MiRNAs are in control of RNA silencing as well as post-transcriptional gene expression regulation (Li et al., 2018).

Artificial microRNAs (amiRNAs) are a type of non-coding RNA molecule that is developed to target individuals or groups of natural genes in plants. They are comparable to natural miRNAs in that they have an unpredictable number of target mismatches (Schwab et al., 2006). AmiRNAs are a recently developed technique for small RNA-based gene silencing in plants. They have been found to successfully alter gene expression in monocot crops and to efficiently activate gene silencing in rice (Ossowski et al., 2008). Schwab et al., (2006) employed artificial miRNAs (amiRNAs) to see if the narrow action spectrum of natural plant miRNAs is due to intrinsic plant miRNA machinery qualities or if it is also owing to prior selection against natural miRNAs with broader specificity. AmiRNAs were created to target specific genes or

sets of endogenous genes, they are single-stranded 21mer RNAs that are not found naturally in plants and are synthesised from endogenous miRNA precursors. Their sequences are tailored in accordance with plant miRNA target selection determinants so that the 21mer selectively silences its chosen target gene(s). Short-hairpin RNAs generated by miRNA precursors can be used to express amiRNAs can exactly cause gene silence and give viral resistance (Ossowski et al., 2008).

Large gene families including genes with relatively similar or even identical sequences are widespread in many organisms, but plants, especially *Arabidopsis thaliana*, are statistically more abundant. (Arabidopsis Genome Initiative, 2000). Genetic redundancy can involve partially overlapping roles of gene family members (Briggs et al., 2006; Kafri et al., 2009; Tautuz, 2000) and is closely related to cellular network mechanistic robustness (Wagner, 2005). Functional overlap and partial or complete redundancy between different family members are thought to be the causes of the lack of observable phenotypes in single-gene deletion mutants, while higher-order mutants exhibit increasing severity of phenotypes (Arabidopsis Genome Initiative, 2000; Bouché and Bouchez, 2001; Cutler and McCourt, 2005; Kwak et al., 2003; Park et al., 2009). Traditional forward genetic screens using various mutagens are restricted in their ability to identify functionally overlapping genes.

Lloyd and Meinke ,(2012) found 591 (partially) redundant genes in *Arabidopsis*. These studies highlight the need for new techniques to screen functionally redundant genes. Different overexpression and RNA interference–based techniques (Abbott et al., 2002; Ott et al., 2005; Wagner, 2005) have been used to address functional overlap. Overexpression can create difficult-to-interpret neomorphic and pleiotropic traits.

RNA interference (Abbott et al., 2002; Ott et al., 2005) may have off-target effects since one double-stranded RNA generates several small RNAs with potentially unwanted targets (Jackson et al., 2003; Wickham, 2009). AmiRNA precursors can be created to target a specific collection of possibly redundant genes, and then processed to provide one mature amiRNA (Schwab et al., 2006).

### 1.5.1 Different Methods for Generating AmiRNA Libraries

AmiRNAs can be produced in plants using a variety of ways, including cloning with designed pre-miR319a as a backbone (Zhang et al., 2019), genetic alteration of miRNA genes (Yu and Pilot, 2014), exploitation of endogenous miRNA precursors (Ossowski et al., 2008), and transgenic expression(Jover-Gil et al., 2014). These approaches have been used to effectively silence genes in plants and to build amiRNA libraries for functional genomics research.

#### 1.5.1.1 *Arabidopsis thaliana* AmiRNA

The First library created by Dr. Hannon at Cold Spring Harbour Laboratories (CSHL). It is a collection of artificial microRNAs (amiRNAs) for Arabidopsis thaliana (Schwab et al., 2006 ; Ossowki et al., 2008).

#### 1.5.1.2 Hauser Library

Hauser et al. created the first genome-scale amiRNA library for *Arabidopsis thaliana* by synthesising 22,000 amiRNA constructs that putatively silence 18,117 *Arabidopsis* genes 96% of the amiRNAs co-silencing 2-5 closely related genes in different combinations (Hauser et al., 2013). Genome-scale amiRNA library is divided into ten sub-libraries, each of which has 22,000 distinct amiRNA designs that are thought to silence a significant number of *Arabidopsis* genes (Hauser et al., 2019). The method

for creating a genome-scale amiRNA library includes synthesising a large number of amiRNA constructs that are thought to silence a large number of genes in the target organism. The amiRNA constructs are designed to inactivate a group of two to six paralogs encoding transcription factors at the same time, allowing for the identification of functionally redundant genes.

#### 1.5.1.3 PHANTOM Library

The PHANTOM amiRNA library is a comprehensive computational design of genome-wide family-specific artificial microRNAs (amiRNAs) that may be used to produce amiRNA libraries. The library was produced by performing a computational design of genome-wide family-specific amiRNAs using high-performance computing features (Hauser et al., 2013). The amiRNA designs can be found online at http://phantomdb.ucsd.edu/. The PHANTOM amiRNA library is made up of a computationally developed library of 22,000 amiRNAs that were synthesised into ten sub-libraries of 1505 to 4082 amiRNAs, each targeting a different functional protein class (Hauser et al. 2013). The PHANTOM amiRNA library is a valuable tool for exploring *Arabidopsis thaliana's* functionally redundant gene space and finding novel morphological and abscisic acid-insensitive seed germination mutants (Hauser et al., 2013).

#### 1.5.1.4. A Genome-Wide Design of an AMiRNA Library

A Genome-Wide Design of an AmiRNA Library includes the compilation of gene family definitions, the computational design of genome-wide family-specific amiRNAs, the synthesis of amiRNA constructs, and the development of the amiRNA library (Hauser et al., 2019).

#### 1.5.1.5. Transportome-specific amiRNA library

A transportome library was used in this thesis. (Zhang et al. 2018) analysed transport pathways in plants using a method called "transportome-scale artificial microRNA (amiRNA)". 3,000 amiRNA lines were generated, which target members of different transporter gene family clades. Following the screening of these lines, 95 reproducible shoot phenotypes were identified, 80 of which had not been previously linked to the targeted genes. Given its auxin-related shoot characteristics, one of these lines (amiR1334) was selected for study. Two genes, ABCB6 and ABCB20, were found to be redundantly required for transportation of auxin in the shoot by expression analysis and transport experiments.

In library design, the genome-wide design of an amiRNA library entails the assembling of gene family definitions, whereas the PHANTOM amiRNA library employs pre-existing gene family definitions. The Genome-Wide Design of an AmiRNA Library method can be used to build an amiRNA library that targets all genes in the genome, whereas the PHANTOM amiRNA library is a pre-designed library that targets certain functional protein classes. (Hauser et al., 2013). In method, the Genome-Wide Design of an AmiRNA Library can be used to examine a target organism's functionally redundant gene space, whereas the PHANTOM amiRNA library is a technique for co-silencing genes (Zhang et al., 2018).The computational design of genome-wide family-specific amiRNAs is involved in Genome-Wide Design of an AmiRNA Library, whereas the PHANTOM amiRNA library is a thorough computational design of genome-wide family-specific amiRNAs that may be used to build amiRNA libraries (Hauser et al., 2013). AmiRNAs were designed using the freely accessible Web microRNA designer (WMD; Ossowski et al., 2008). The WMD3 tool for miRNA creation is a user-friendly web-based software application for designing amiRNAs for

a variety of species, including plants. It produces all feasible amiRNA sequences and designs 21mer amiRNA sequences for target gene silencing. It can also create numerous amiRNAs for multiplex gene silencing (Mickiewicz et al., 2016). Designing gene-wide amiRNAs needed 90,000 h of CPU time on a high-performance cluster. In the same study (Ossowski et al., 2008), amiRNAs were designed using 12 family definitions. This produced amiRNAs with varying coverage based on family size, sequence diversity, and off-target locations. In the second step, an iterative technique was employed to cover 75% of family members with amiRNAs (Figure 17.1 A). Families were subclustered using a Dirichlet process clustering technique (Brown, 2008). In cases where first- and second-round amiRNAs did not exceed 75% coverage, researchers used the Markov chain clustering technique (Enright et al., 2002) groupings with smaller subclusters. amiRNAs were created against these subclusters. 2,002,149 amiRNAs targeting 18,117 genes in 58,232 target classes were developed. One or more amiRNAs target a class of genes (Figure 1.17 B). All amiRNAs target 18,117 of 22,020 two-gene families. Thus, computationally produced amiRNAs match 80% of protein-coding loci in examined family definitions. Lack of nucleotide sequence conservation within a targeted gene family or similar sequences in non-targeted genes (possible off-targets) prevented complete coverage of all gene family members (Hauser et al., 2013) .

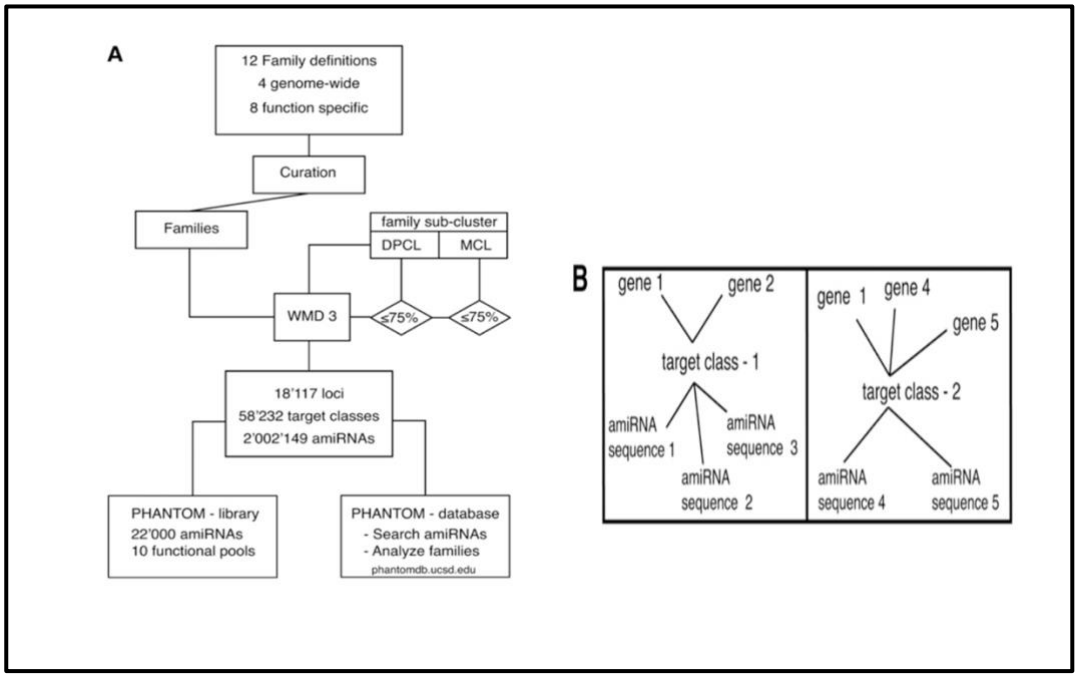


**Figure 1. 1** Design of a Genome-Wide AmiRNA Collection for Targeting Gene Families. (A) Schematic of the computational iterative design of family-targeting amiRNAs. amiRNAs were designed using full families and subclusters to increase the number of targets per family. amiRNAs were compiled into a Web-accessible database. 22,000 amiRNAs were synthesised. (B) Schematic showing target classes, amiRNAs, and targeted genes. Two target classes target two or three genes (targets). The target class is a set of amiRNA-targeted genes.(Hauser et al. 2013)

As a result of multi-targeted gene silencing, the authors aim to develop resources that will be used to illuminate hitherto unknown pathways in hormone signalling and small molecule transport. In this thesis, the aim was to use the amiRNA resources to characterise novel ABA transporters regulating hydrotropism.

## 1.6 THESIS AIMS AND OBJECTIVES

The thesis aims to discover novel ABA regulated molecular mechanisms that control root adaptive responses to water stress. This project had two main objectives.

1. Identifying novel ABA transporters regulating hydrotropism in *Arabidopsis* roots using an amiRNA transportome-based approach (detailed in Chapter 3). This required optimisation of a high throughput hydrotropism mutant screen, identification of promising amiRNAllines and performing an initial characterisation of genes targeted by amiRNA (Chapter 3), followed by the detailed characterization of one novel ABA transporter candidate GTR1 (Chapter 4).
2. Characterising the role of ABA during the water stress adaptive response Xerobranching (Chapter 5; published in Mehra *et al*, 2022, *Science*).

# 2 CHAPTER2: MATERIALS AND METHODS

## 2.1 PLANT MATERIALS

### 2.1.1 Arabidopsis thaliana

**Table 2.1** *Arabidopsis thaliana* seeds used in this study.

| Line name | Source |
|---|---|
| *Col-0* | Daniela Dietrich (The University of Nottingham 2018) |
| *miz1* | Daniela Dietrich (The University of Nottingham 2018) |
| *snrk2.2/2.3* | Daniela Dietrich (The University of Nottingham 2018) |
| Library of amiRNA lines | Elon Shani (2018, Tel Aviv University) |
| *gtr1* (SALK_090694.2) N923939 | Nottingham Arabidopsis Stock Centre (NASC, 2020) |
| *dtx1 (*SALK_081560) N581560 | Nottingham Arabidopsis Stock Centre (NASC, 2020) |
| *aba2-1* | Nottingham Arabidopsis Stock Centre (NASC, 2020) |

### 2.1.2 Plasmid Materials

pGreenBarT binary vector was choosen as the backbone for the constructs because of its size (7035 bps) and because it confers spectinomycin resistance, which differs from the commonly used kanamycin resistance in most pDONR entry clones as previously described. The pGreenBarT destination vector was designed for multisite gateway cloning. As a result, pGreenBarT contains the ccdB and CmR genes flanked by attR4 and attR3 recombination sites that react simultaneously with three different entry clones (generally pDONR P4-P1R containing the promoter fragment, pDONR 221 containing the gene of interest, and pDONR P2R-P3 encodes a protein tag) to create a construct that drives marked promoter specific (Zhang et al. 2020) gene

expression. Cloning was carried out using MULTISITE GATEWAY CLONING kit as manufacturer's protocol (Thermo Scientific, USA) .

### 2.1.3 Seed Sterilization and Growth Conditions

Seeds were surface sterilized by washing with 700 µl of 50% Sodium hypochlorite (v/v) for 5 minutes followed by two washes with 700 µl of 0.0001%Triton, then three washes with 1000 µl of sterile distilled water. Sterilized seeds were sunk in 1000 µl of distilled water and stored for 48 hours at 4 °C before sowing to synchronise germination. Thereafter, sterilized seeds were plated on plastic square Petri dishes containing 70 ml of half-strength of MS salt (2.2 g/L) (Murashige and Skoog media, Sigma) solidified with 1% bacto agar at pH 5.6 – 5.8. Micropore tape was used to seal all plates which were incubated vertically in growth chamber for germination under long-day conditions at a continuous temperature of 21°C and 16 hours photoperiod (120 µmol $m^{-2}$ $s^{-1}$). Seeds were left to germinate for 7-10 days, depending on the experiment design. For seed bulking, seedlings were transferred to 9 cm plastic pots filled with Levington M3 compost and kept in a growth room (16 h light l8 h dark, 22 C° day / 18 ° night). Seeds were harvested when siliques were dried. All seeds were kept in paper bags at room temperature.

## 2.2 PLANT PHYNOTYPE ASSAES AND ANALYSIS

### 2.2.1 Different Root Phenotype Assays

#### 2.2.1.1 Root-Lift Assay

After 5 days of incubation at 21°C, all Petri dishes containing grown seedlings were set up over another petri-dish containing 75 ml of calcium chloride ($CaCl_2$.6H2O) (4 M) (as shown in Figure 2.1). Petri dishes were supported by adaptors and parafilm. After two days of incubating horizontally, images were taken of roots to observe root lifting/movement.

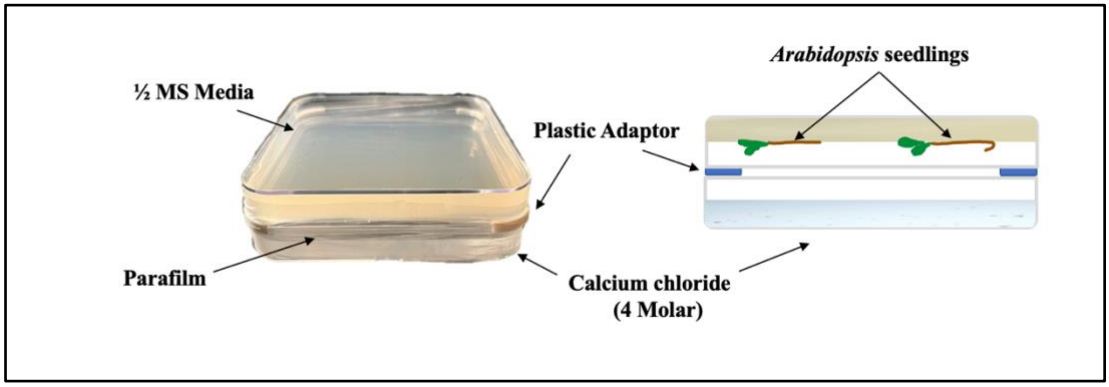


**Figure 2.1** The inverted plate method used in the assay**.** The upper plate contains *Arabidopsis* seedlings grown on half-strength of MS which was set up over $CaCl_2$.6H2O.

#### 2.2.1.2 Split–Agar Plate Assay

Split agar plates were prepared one day before seedlings transfer by using half-strength MS salt media to fill the upper half of square Petri dishes; the lower half of Petri dishes were filled with half-strength MS salts and 0.4 M Sorbitol (Figure 2.2). Therefore, a water potential gradient was created between the two parts. *Arabidopsis sp.* seedlings were transferred from normal half-strength salt plates to split plates using a guide template to arrange root tips above the edge of two media types.

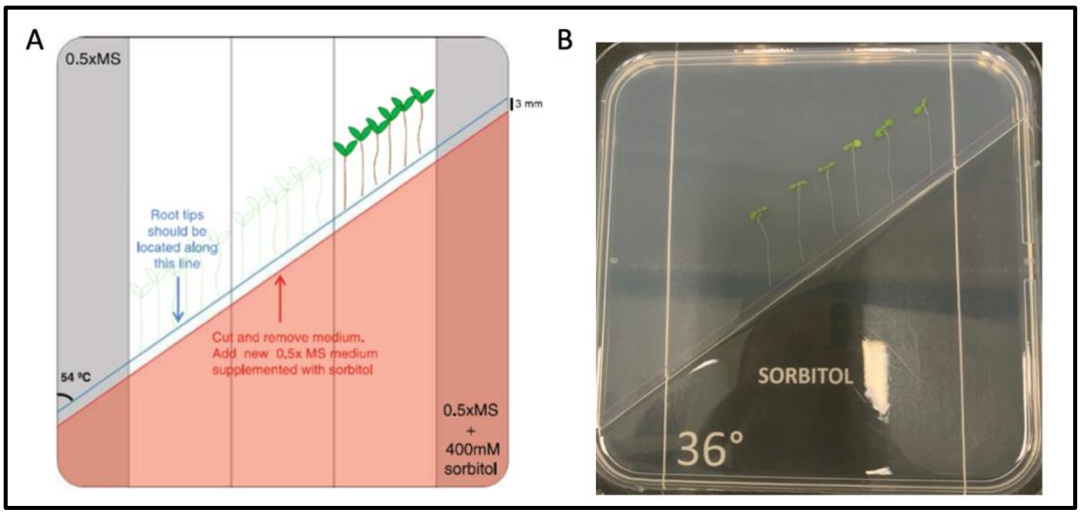


**Figure 2.2** Split agar plate for Arabidopsis roots hydrotropic responses based on water potential gradient. (A) Schematic for split agar plates show the upper part filled with 0.5 MS and the lower part filled with 0.5 MS and 400mM Sorbitol. (B) image for split plates assay (Dietrich et al., 2017).

### 2.2.1.3 Agar-Based Air-Gap Assay

Agar-based Air-gap Phenotyping assay was performed to examine the effects of short–term water stress on *Arabidopsis* seedlings. Optimization of the experimental setup is shown in (Figure 2.3), Square Petri dishes (12 cm x 12 cm) were filled with a mixture of 0.3% sucrose, 0.5 g/L MES, and 1% Bacto agar in half-strength MS media. Agar slants were made by holding Petri dishes at an angle of 15 degrees to a flat surface. Using a 10 cm length scraper blade, a clean cut was produced along the centre of the petri dish. With a 0.5 wide scalpel, agar was gently removed to make sufficient space for an air gap of 0.5 cm. The air gap distinguished the top and bottom halves of the agar (see Figure 2.3). On the 'top-half' of the plate, the root tips of five-day-old Arabidopsis seedlings were spaced about 2–3 mm from the agar-air interface. The plates were sealed and incubated vertically for 7 days in ideal growing circumstances at a continuous temperature of 21°C and 16 hours photoperiod (120 µmol $m^{-2}$ $s^{-1}$). Multiple rounds of optimisation revealed that a 'V- shape cut' into the agar allowed more than half of the roots to pass through the air gap and reach the 'bottom- half' of the plate in accordance with the gravity vector (Figure 2.3.B). On the other hand,

straight cut guided most of the root tips of *Arabidopsis* plants bent after being exposed to a hydrotropic stimulus (Figure 2.3.A). Furthermore, the agar slants made it easier for the root tips to gently touch down on the 'bottom half' of the plate. After a week in the air gap, the roots were evaluated for their branching response. The air gap was measured to determine how many lateral roots each primary root produced. As a baseline, the root development of both agar plates with and without an air gap was compared.

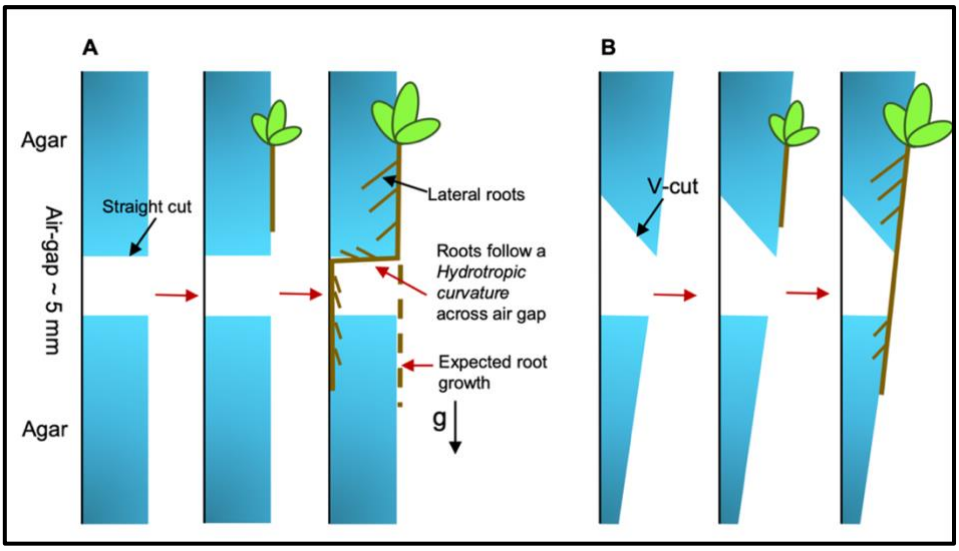


**Figure 2.3** (Agar-based Air-gap Assay) system for studying xerobranching in *Arabidopsis*.(A)Seedlings were placed on the top half of the agar with their primary root tips 2-3 mm from the edge. Plates were sealed and placed vertically to allow roots grow a cross air-gap. Most roots bent horizontally towards the moist agar side following a hydrotropic curvature rather than gravity. Bent roots formed lateral roots along the moist Petri dish wall. (B) To force primary root growth towards gravity, a 10 cm scraper blade V-cut the top side of agar. This moved the hydrotropic stimulus away from the root tip and allowed longitudinal root development.

### 2.2.2 Confocal Microscopy Imaging

The roots were placed on microscope slides and stained with propidium iodide ($15\mu gml^{-1}$) for one minute. Coverslips were used to protect the roots before they were photographed. A Leica SP5 confocal laser scanning microscope was used for the

fluorescent imaging (Leica Microsystems). To record the GFP signal, the wavelengths of excitation (488 nm) and emission (505-545 nm) were recorded. YFP was examined with excitation at 514 nm and emission at 525-545 nm.

## 2.3 Genotype Techniques

### 2.3.1 DNA Extraction

10 day old- seedlings which had a hydrotropic phenotype (show root lifting from agar plates surface as shown in **(**Figure 2.1) were transferred to 9 cm pots filled with Levington M3 compost and kept in a growth room (16 h light/8 h dark, 22°C day/18°C night). After two weeks, four to five leaves were harvested in micro centrifuge tubes (MCT) and immediately frozen in liquid nitrogen and ground to powder by pestle, 5oo µl of Edward's buffer (200 mM Tris-HCl pH 7.5, 250mM NaCl, 25 mM EDTA, 0.5% SDS) was added to ground tissue and had a brief vortex. Then, the mixture was spun down for 15 minutes at 13000 rpm, 200 µl of supernatant was added to fresh labelled MCT followed by precipitation using 1000 µl of chilled isopropanol. Samples were spun down for 10 minutes at 13000 rpm. The pellet was formed at the bottom of MCT, and all amount of supernatant was discarded. The pellet was washed twice by using 70% ethanol (v/v), MCT was centrifuged after discarding the wash solution and dried in a laminar flow hood before being resuspending in 50 µl of the mix of TE buffer and RNAse and kept in an incubator at 37 °C for at least one hour, then stored in 4°C for overnight. The next day, the concentration and purity of DNA were measured by using a Nanodrop™ spectrophotometer (2000, Thermo Scientific). A dilution of this extract was used to amplify DNA by using PCR technique.

### 2.3.1.1 Polymerase Chain Reaction (PCR)

A 20 µl reaction mixture containing 2 µl of DNA was used to amplify the gene of interest using a polymerase chain reaction (Table 2.2) with primers were used based on the gene of interest (Table 2.3).

**Table 2.2**Amount of components used in the different PCR reactions:

| Phusion® High-Fidelity DNA Polymerase | | | Q5® High-Fidelity DNA Polymerase | |
|---|---|---|---|---|
| | **Component** | **Amount** | **Component** | **Amount** |
| 1 | MQ Water | 10.8 µl | MQ Water | 7.4 µl |
| 2 | 5x GC Buffer | 4 µl | Q5 Reaction Buffer | 4 µl |
| 3 | 10 mM dNTPs | 0.4 µl | 10 mM dNTPs | 0.4 µl |
| 4 | DMSO | 0.6 µl | 5X Q5 High GC Enhancer | 4 µl |
| 5 | 10 µM Forward Primer | 1 µl | 10 µM Forward Primer | 1 µl |
| 6 | 10 µM Reverse Primer | 1 µl | 10 µM Reverse Primer | 1 µl |
| 7 | Phusion DNA Polymerase | 0.2 µl | Q5 High-Fidelity DNA Polymerase | 0.2 µl |
| 8 | Template DNA (50ng/ µl) | 2 µl | Template DNA (50ng/ µl) | 2 µl |
| 9 | Total | 20 µl | Total | 20 µl |

**Table 2.3** The list of primers used in PCR reaction.

| Primer Name | Sequence | Tm (° C) |
|---|---|---|
| gtr1_RP | CTTCGCACGAGATTTTGTTTC | 63.5 |
| gtr1_LP | ACGACTAACACCGATGTGGTC | 63.8 |
| dtx1-RP | AAGGCTTGAAGAGGAAACACC | 63.4 |
| dtx1- LP | GAACCAACGACTCCGAGAACAG | 63.0 |
| SAIL-LB 1 | GCCTTTTCAGAAATGGATAAATAGCCTTGCTTCC | 74.5 |
| M13_F | GTAAAACGACGGCCAG | 57.6 |
| M13_R | CAGGAAACAGCTATGAC | 50.7 |

### 2.3.1.2 Thermocycling

The components were mixed gently in PCR tubes and then had a brief centrifuge before being transferred to a PCR thermocycling machine running the following program (Figure 2.4). Different heat temperatures used in the annealing stage depend on primer Tm and the targeted gene amplicon size.

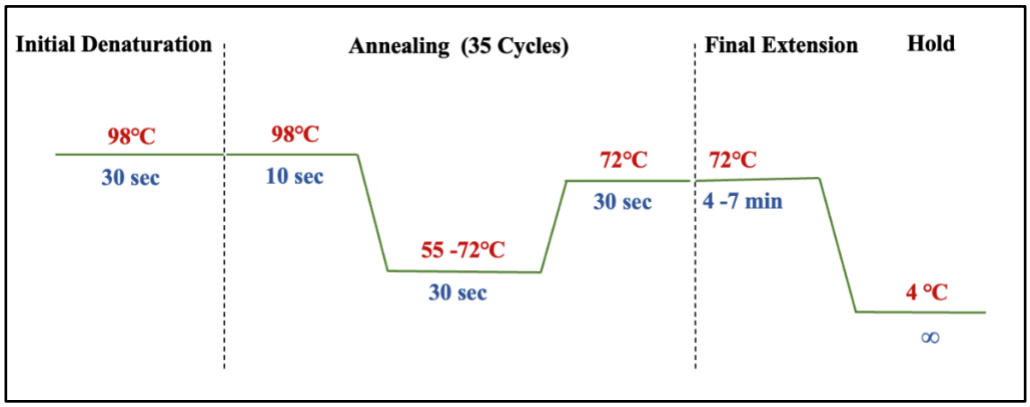


**Figure 2.4** Thermocycling Machine cycles setting.

### 2.3.1.3 Gel Electrophorasis

PCR reactions were mixed with 4 µl loading dye. To run the PCR reaction, 1% agarose was prepared in 1xTBE buffer solution by using the microwave to dissolve all agarose particles then cooled down before staining with 0.001% Ethidium Bromide. Gels were transferred to the gel electrophoresis tank. PCR reactions were loaded into gel wells and 1KB Plus DNA Ladder (New England Biolab – NEB) was used as a marker to determine the size of DNA fragments. Electrophoresis was done at 100 V for about 45 minutes. Bands were visualized under UV light and Image Lab Software was used to analyse results.

#### 2.3.1.4 DNA Gel Extraction

The UV light box (trans-illuminator) in a dark room was used to excise DNA fragments from an agarose gel. The band of interest was exposed by extremely brief visualisation of the DNA (to reduce DNA mutagenesis). The agarose gel's DNA was cut using a scalpel blade. A gel extraction kit was used to purify the excised DNA (GeneJET, Thermo Scientific). All samples were eluted into 20 µl of MQ water. After the purification step, DNA concentration was measured by a Nanodrop™ spectrophotometer (2000, Thermo Scientific) .When not in use, the pure DNA was stored at -20 °C.

### 2.3.2 RNA Extraction

To prepare RNA extraction, a fume hood was cleaned to work in and gloves were used in all steps to limit the degradation of precious RNA samples. The root tips of 7 days old seedlings were removed from the RAM and placed in a sterile, pre-labelled MCT tube. Liquid nitrogen was used to quickly freeze the root tissue, and then it was ground by autoclaved mortar and pestle into a powder. The immediate addition of 500 µl of Trizol reagent was followed by additional grinding. After minutes, ground samples were transferred to new pre-labelled MCT. This was followed by the addition and brief vertexing. The sample was centrifuged for 5 minutes at 14,000 rpm. The 500 µl of the supernatant was aliquoted into a clean labelled MCT, 250 µl of EtOH was added and mixed by inverting four times. A pink RNeasy spin column (Qiagen kit) had been filled with 750 µl of the sample. The RNA was then extracted using an RNeasy plant micro kit (Qiagen for total RNA purification). The purified RNA was eluted into 30 µl of RNase-free water to determine the concentration and purify. The RNA was

then either synthesised or stored at -20 °C (for short-term storage)/-80 °C (for long-term storage) until needed.

#### 2.3.2.1 Quality Estimation of DNA/ RNA

A Nanodrop TM spectrophotometer was utilised in order to determine both the DNA/RNA content and purity (Nanodrop 2000, Thermo Scientific). The NanodropTM was then blanked with the same buffer that was used to elute the DNA/RNA sample after the appropriate programme had been selected (either for DNA, RNA, or protein). One microliter of the sample material was measured, and the concentration was determined in ng µl $^{-1}$, with the purity determined as OD 260/280 nm; a ratio of 1.8 was deemed to be 'pure' for DNA and a ratio of 2.0 accepted as 'pure' for RNA.

#### 2.3.2.2 Complementary DNA (cDNA Synthesis)

Superscript II Reverse Transcriptase (Invitrogen; 2.4 µl (0.4 l Oligo-(dT) primer and 2 µl deoxy nucleotide triphosphates (dNTPs= 10 mM each dATP, dGTP, dCTP, and dTTP) was added to each RNA sample. The samples were vortexed and incubated at 65°C for 5 minutes before being refrigerated in ice for 1 minute. A reaction mixture (13 µl) containing SuperScript II, (SSII; 1 µl), 0.1 M dithiothreitol (DTT; 4 µl), and 5X First-Strand Buffer (8 µl) was added to each RNA sample, vortexed, and incubated at 42 °C for 50 minutes. To render the reaction inactive, the temperature was raised to 70 °C for 5 minutes.

#### 2.3.2.3 Reverse Transcriptase Polymerase Chain Reaction

Reverse transcriptase polymerase chain reaction (RT-PCR) was used to amplify complementary DNA (cDNA) samples (Table 2.4). At a total volume of 20 µl per PCR tube, we used the Gene Amp® PCR system 9700 (Applied Biosciences) with forward and reverse cDNA primers with At3G47960 primers as a positive control to confirm there was no expression in all knockout lines for homozygous lines and to detect any RNA contamination. Using a cDNA sequence, two gene-specific primers (forward: FP and reverse: RP) were built for each T-DNA insertion line. he LightCycler®480 System (Roche, USA) was used initially and qTower 384G was used in subsequent assays.

**Table 2.4** RT-PCR reaction mixture concentrations and volumes (in 20 µl).

| REAGENTS | VOLUME (µl) |
|---|---|
| cDNA (50 – 100 ng/ µl) | 2-4 |
| PCR Buffer (Sigma) with $MgCl_2$ (10×) | 2.0 |
| dNTPs (10 mM) | 0.4 |
| Forward primer; FP (10µM) | 1.0 |
| Reverse primer; RP (10µM) | 1.0 |
| Taq DNA Polymerase (Sigma) | 0.2 |
| Distilled water ($ddH_2O$) | x |
| Total volume | 20 |

## 2.4 CLONING

### 2.4.1 Gateway Cloning Protocol

The Gateway® BP clonaseTM II enzyme mix was used as the first step in the creation of pENTRY constructs (Invitrogen). The usual volume for a BP Clonase™ II reaction was 10 µl. Up to 8.0 µl of TE buffer (pH 8.0), 2.0 µl of BP clonaseTM II enzyme, and 1.0-7.0 µl of PCR product (15-150 ng $\mu l^{-1}$) were combined (kept on an ice block). After gently pipetting and centrifuging the reaction mixture, it was incubated at 25 °C for 1 hour. For the next 10 minutes, the response was slowed down by holding it at 37 °C. Afterwards, the reaction was either transformed into competent cells or frozen at -20 °C for later use.

Gateway® LR clonase™ II enzyme mix was used to move DNA from pENTRY to the destination constructs (Invitrogen). Conventional LR Clonase™ II reactions were conducted in volumes of 10 µl. Up to 8.0 µl of TE buffer (pH 8.0), 2.0 µl of LR clonase™ II enzyme, and 1.0 µl of each the ENTRY vector (50-150 ng $\mu l^{-1}$) and the destination vector (1.0 µl) were combined (kept on an ice block). After gently pipetting and centrifuging the reaction mixture, it was incubated at 25 °C for 1 hour. Following this, the mixture was left for 10 minutes at 37 °C to stop the reaction. The reaction was then either kept at -20 °C until needed or transformed into competent cells.

**Table 2.5** The List of Gateway ENTRY and Vectors

| Gene/Construct name | Locus |
|---|---|
| pCASP1 | Endodermis |
| pCO2 | Cortex |
| pWOL | Pericycle and Vasculature |
| pWER | Epidermis |
| pEN7 | Endodermis |
| pSCR | Endodermis |
| pSHR | Stele |
| pXPP | XPP |
| pGTR | GTR Promoter |
| GTR | GTR |
| VENUS | |
| P4-P1R | ENTRY (Promoter) Fragment |
| pDONR 221 | ENTRY (Gene Interests) |
| pDONR P2R-P3 | ENTRY (Encodes a protein tag) |
| pSWUs ( 015, 105, 205, 305, 405 505, 404) | Destination Vectors |

### 2.4.2 Competent Cell Transformation

After defrosting on ice for 10 minutes, competent cells (HB101, Dh5α, Top 10) were used. These cells were then incubated on ice for a further 20 minutes after receiving 1.0-2.0 µl of reaction mix was added (from LR Clonase II, DNA fragment, or plasmid). After the reaction was complete, it was transferred to a chilled 1.5 ml MCT and kept in an ice box for 30 minutes; the reaction was then immediately subjected to heat shock at 42 °C for 90 seconds. The reaction was then placed back on the ice for another 10

minutes. The reaction was continued by adding 450 µl of Luria-Bertani (LB) liquid medium. The reaction was incubated in 37°C shaker for 90 minutes. Following this, incubated MCT was centrifuged for 5 minutes at 5000 rpm. Placing 20 µl (aliquots of the reaction) on LB agar plates supplemented with the necessary antibiotic for the plasmid construct (for example, Ampicillin, Spectomycine and Kanamycin) was the next step. A 24-hour incubation period was performed at 37° C for selecting positive clones.

### 2.4.3 Bacterial Colonies

PCR was used to examine a sample of the colonies grown on the plates to validate whether or not they contained the appropriate insert. In other instances, it was also required to carry out a restriction enzyme digest in order to get a higher level of clarity. A shaker at 37° C was used to incubate liquid cultures of positive colonies for 24 hours. From the overnight cultures were utilised to isolate plasmid DNA was isolated using a plasmid mini-prep kit (GeneJET, Thermo Scientific). All the separation procedures were performed at room temperature, and the centrifuge settings were all higher than 12,000 rpm. Eluting the plasmid DNA into 30 µl of sterile water allowed us to attain the desired concentration and purity. The plasmid DNA was then either sent out for sequencing or incubated at -20 °C for later use.

### 2.4.5 DNA sequencing

PCR products, plasmid DNA and primers were prepared to send for Sanger sequencing (https://www.sourcebioscience.com) All samples were prepared in 5 µl volume in different concentrations. For PCR product it is 10ng/ µl while Plasmid DNA it is 100

ng/ µl and for Primers it is usually 3.2pmol/ µl. All data sending after DNA sequencing was analysed by alignments using Clustal Omega.

## 2.5 STATISTICAL ANALYSIS

When more than two groups were compared, data was analysed using the student's *t*-test or one-way ANOVA followed by Tukey's honestly significant difference (HSD) post hoc test ($p < 0.05$; 95% confidence interval). Comparable letters indicate statistically similar groups.

# 3 CHAPTER 3: DISCOVERING NOVEL TRANSPORTERS THAT REGULATE ROOT HYDROTROPISM IN ARABIDOPSIS

## 3.1 INTRODUCTION

Plants have developed adaptive mechanisms enabling their roots to locate and grow towards sources of water in soil, such as hydrotropism (Cassab et al., 2013; Dietrich, 2018; Kobayashi et al., 2007; Moriwaki et al., 2013). This root adaptive response modifies the direction of root growth, reorienting tip angle towards areas of soil where water availability is higher (Dietrich et al., 2017). Hydrotropism has fascinated researchers for over 100 years including Darwin and von Sachs (Takahashi,1997). However, the molecular mechanisms controlling this adaptive response have only recently been characterised using mutational approaches in the model plant Arabidopsis (Dietrich, 2018; Dietrich et al., 2017; Kiss, 2007; Moriwaki et al., 2013; N. Takahashi et al., 2002)

The water stress signal abscisic acid (ABA) has been demonstrated to play a key role regulating root hydrotropism (Anfang & Shani, 2021; Dietrich et al., 2017; H. Takahashi, 1997). Roots of mutants disrupting ABA synthesis (e.g. *aba2*;Eapen et al., 2005) and response (e.g. *snrk2.2, 2.3*; Dietrich et al., 2017) exhibit reduced hydrotropic root bending responses. However, to date, no ABA (or other) transporters have been identified that control this root adaptive response (Dietrich, 2018). This may reflect that multiple transporters have been described to transport ABA in Arabidopsis (Dietrich, 2018), hence masking their roles through genetic redundancy.

To determine the identity of the down-regulated Arabidopsis transporter sequence(s) likely causing the hydrotropic phenotypic defect, for each amiRNA line selected in

sections 3.3.2, leaf genomic DNA was isolated and then PCR fragments amplified using primers designed on either side of the amiRNA vector backbone.

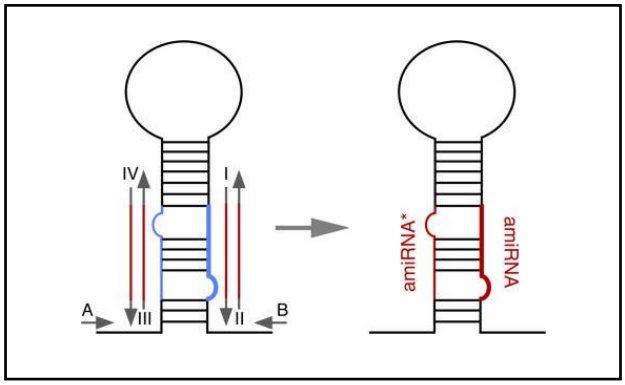


**Figure 3.1** AmiRNA engineering. Using overlapping PCR, site-directed mutagenesis was carried out on endogenous miRNA precursors. In order to replace the miRNA and miRNA* sections (blue) with synthetic sequences, oligonucleotide primers I through IV were utilised (red). On the sequence of the template plasmid, primers A and B were developed. In a single process with primers A and B, the PCR products A-IV, II-III, and I-B were combined to regenerate functional miRNA precursors (Schwab et al., 2006)

This chapter aims to dissect the genetic regulation of hydrotropism and whether transport of ABA (or other signals) play important roles during this adaptive response. The artificial microRNA inhibition-based (amiRNA) experimental strategy adopted in this Chapter is designed to overcome the inherent genetic redundancy found within plant transporter gene families by simultaneously down-regulating the expression of multiple related sequences (termed clades) in order to uncover which clades and/or genes are important for hydrotropism (Hauser et al. 2013; Zhang et al., 2018). Zhang et al.(2018) developed amiRNA PHANTOM Library to target *Arabidopsis* gene families. It is made up of 22,000 amiRNA constructions that are thought to quiet 18,117 genes in various combinations, with 96% of the amiRNAs silencing 2-5 closely related genes. In addition, for this investigation, a transporter-specific sublibrary of 1777 synthetic amiRNAs was bulk converted into wild-type Arabidopsis (Col-0) (Zhang et al., 2018). Each of the >1800 amiRNA lines expressed an artificial

microRNA targeting a distinct set of 1-6 transporter genes that collectively compose the entire 'transportome' of Arabidopsis (Zhang et al., 2018). In combination, a high throughput phenotypic screen is ideally suited to identify novel transporter-encoding genes regulating hydrotropism from the large collection of *Arabidopsis* amiRNA lines (Hauser et al., 2013). The hydrotropic screen involves exposing amiRNA seedlings to a water potential gradient, causing roots to grow towards the source of water instead of gravity. In this Chapter, results from screening the Arabidopsis amiRNA transportome population to identify hydrotropic mutant lines are described. Key results include initial optimisation of high throughput mutant screens, identification of promising lines and initial characterisation of the genes being targeted by amiRNA. The mutant screen successfully led to the identification of several classes of putative ABA (and other) transporters including NPF (NRT1/PTR FAMILY) and ABC sequences.

## 3.2 RESULTS

### 3.2.1 Optimisation of a high throughput hydrotropism mutant screen

A high throughput 'inverted' agar plate-based hydrotropic screening protocol designed to identify mutant roots no longer able to grow towards moisture and remain connected with the agar surface but grow in the direction of gravity (Takahashi et al., 2002) was initially optimised for genetic studies in this thesis.

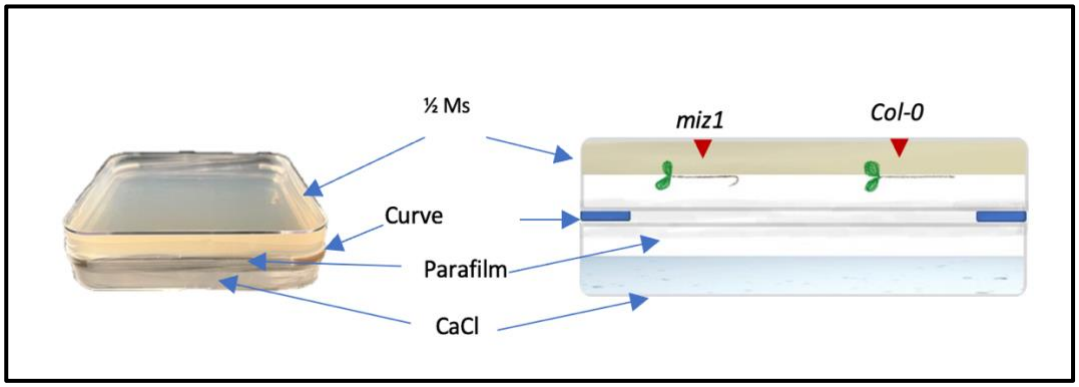


**Figure 3.2** The protocol for screening amiRNA library using ½ MS and different concentrations of salts (designed by Dietrich, 2018)

To optimise this hydrotropic mutant screen, 3 lines of *Arabidopsis* (*Col-0 wildtype, miz1* and *snrk2.2, 2.3*) were used. The *miz1* line was strongly impaired for hydrotropism, while the *snrk2.2 snrk2.3* double mutant had significantly reduced hydrotropism (Mustilli et al., 2002, Dietrich et al., 2017) . The initial aim was to assay these mutations and observe their altered hydrotropic responses.

Agar plates containing 5 days old seedlings were placed over different salt solutions. Sodium chloride and calcium chloride were used in different concentrations (starting from 1 M to 5 M). Based on previous studies (Dietrich et al. 2017), a positive response from *col-0* versus a negative response in *miz1* roots was expected to the hydrotropic screening conditions (Figure 3.2 , 3.3)

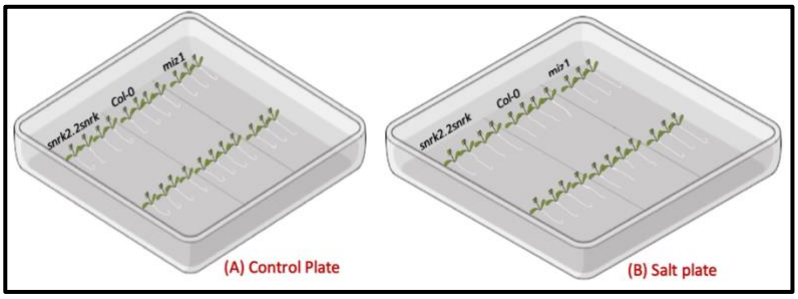


**Figure 3.3** High throughput hydrotropism mutant screen. Schematic diagram of seedings grown on ½ MS media plates following 2 days exposure over a salt solution, revealing differences in root direction between (A) control and (B) $CaCl_2$ (4M) treatments. (A) Seedlings of all 3 lines (Col-0 *wildtype, miz1* and *snrk2.2, 2.3*) curved towards the water due to a higher level of moisture in the water than 1/2 Ms media. (B)Col-0 seedlings showed horizontal growth on 1/2 MS media which indicated hydrotropism. *miz1* seedlings showed reverse behaviour towards saline solution following gravity which confirmed the absence of hydrotropism. Also, *snrk2.2/snrk2.3* seedlings showed variation in root growth direction according to salt concentrations, as they showed curvature towards low concentrations of saline solution.

Experimental results revealed the seedling roots exposed to a $CaCl_2$ saline solution exhibited a stronger effect on root responses than NaCl (Figure 3.4 , 3.5)

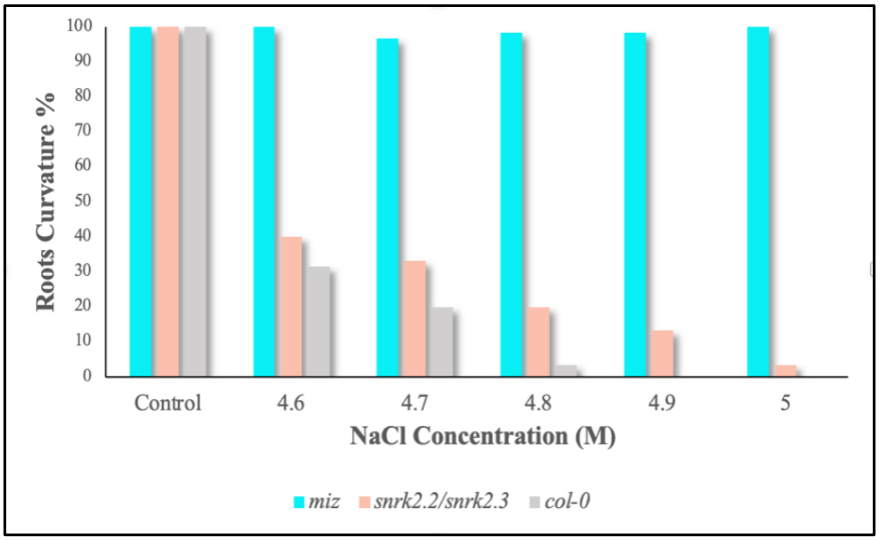


**Figure 3.4** The effect of different NaCl Concentrations used in assay. The graph illustrates the percentage of root curvature in different concentrations of NaCl. At a high concentration of the saline solution, a water potential gradient was stimulated (5M), and roots of *Col-0* and *snrk2.2/snrk2.3* grew in agar except for the slight percentage of *snrk2.2/snrk2.3* seedlings that show reduced hydrotropism (whereas all seedlings were directed towards water in control plates).

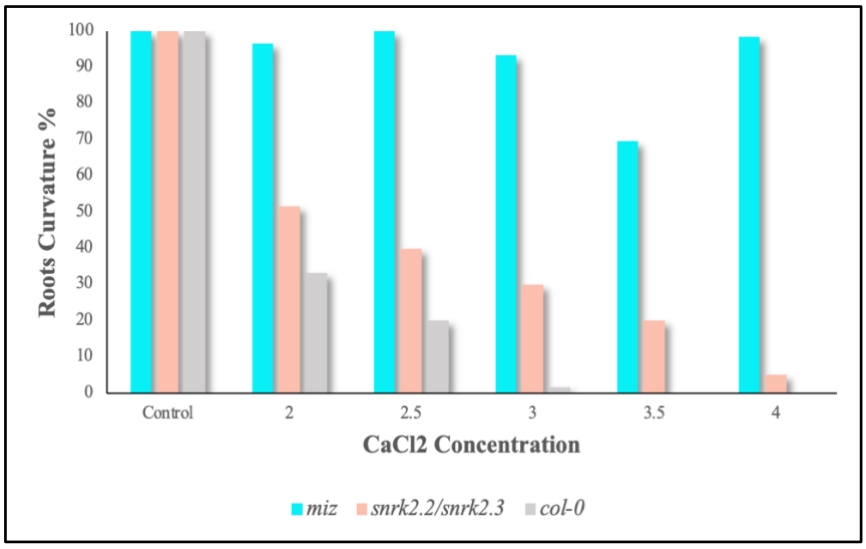


**Figure 3.5** The effect of different $CaCl_2$ Concentrations used in assay. Seedlings' hydrotropism response in different concentrations of Ca $Cl_2$ was similar to NaCl saline solution. *miz1* showed curvature at all concentrations due to the absence of a hydrotropism gene while *Col-0* and *snrk2.2/snrk2.3* exhibit hydrotropic responses in high concentrations of salt.

Based on the results, $CaCl_2$ proved more effective at lower concentrations of salt compared to NaCl, so the former was selected for high throughput bioassays. In this type of screening, a dry area around seedlings was needed to observe root growth direction and saline solution was used to dry air, the low concentration of $CaCl_2$ showed clear results without effected on media structure which made it the most appropriate to choose.

### 3.2.2 Initial Screen of amiRNA Lines Defective for Hydrotropism

A novel genetic resource was originally developed by US researchers to screen for redundant genes in Arabidopsis, consisting of a library of over 11000 amiRNA lines that target multiple related genes (Hauser et al., 2013). This approach proved successful when two amiRNAs targeting the PYR/RCAR ABA receptor genes and the SnRK2 genes, which are compose redundant essential genes required for ABA signal transduction, were discovered during screening for ABA-insensitive seed germination phenotypes (Ma et al., 2009; Park et al., 2009). Similarly, this amiRNA library resource

was used to identify functionally redundant auxin transporter genes such as ABCB6, ABCB20) (Y. Zhang et al., 2018). In this Chapter, a sub-set of amiRNA lines (each designed to silence 2-5 closely related transporter encoding genes) were screened to identify transporters sequences regulating root hydrotropism.

1876 Arabidopsis lines (each expressing an artificial microRNA targeting a distinct sub-set of transporter genes) were screened using the $CaCl_2$ based protocol (optimised in section 3.2.1). The principle of this experiment was to expose Arabidopsis seedlings ( grown on agar for 5 days) over a Calcium Chloride solution, then score root growth direction if lines can perform hydrotropism (or not). Positive and negative control lines of Arabidopsis (*col-0, miz1*) were included. From the original ~1900 lines, 40 of these exhibited root lifting (hydrotropism defective) phenotype and then transferred to soil to propagate. Of these 40 independent lines, 32 of these set seed and then their phenotypic defects were validated in section (3.3.3).

### 3.2.3 Validation of candidate amiRNA lined defective hydrotropic phenotypes

The hydrotropic defects of each of the 32 amiRNA hydrotropism defective lines were initially validated by repeating the high throughput screening conditions on the original batches of seed together with their next generation. All 32 independent lines retained their hydrotropic defects. However, despite the next generation retaining their hydrotropic defects, seedling growth was less vigorous than the original batch of seeds as the roots in the next generation were shorter than the previous generation.


**Figure 3.6** The number of seedlings showing the hydrotropic defect in the original amiRNA seeds and the first generation which the decrease in numbers related to the weak growth of the next generation or somewhat it will be silencing issue in the new generation.

To independently validate their hydrotropic defects, each line was phenotyped using an alternate hydrotropic screen employing split plates for the original batch of seeds only in control and sorbitol plates (due to the next generation of seedlings being very small and roots too short).

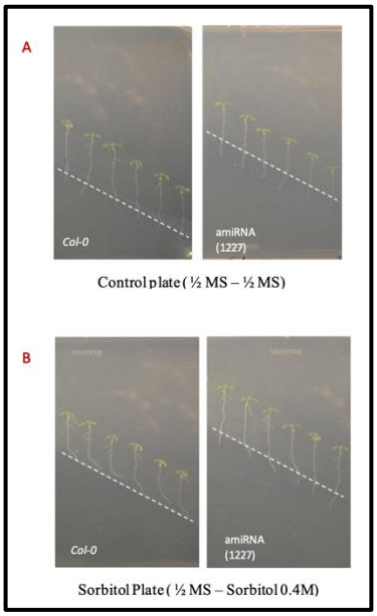


**Figure 3.7** Split plate screen used to validate hydrotropic defects in candidate lines.
(A) Control group had ½ MS media in the upper and the lower parts which exhibit gravitropic responses in the wild type (*col-0*) and target line (amiRNA line -1227) due to water potential equality in both parts. (B) sorbitol plates caused the wild type roots to undergo curvature to follow the higher water potential and repress gravitropism, whereas selected amiRNA lines (e.g. amiRNA line 1227) exhibited hydrotropic defective response and grew towards the direction of gravity.

### 3.2.4 Identification of Arabidopsis sequences encoded by hydrotropic mutants

PCR fragments from a total of 27 out of 32 lines were successfully amplified, then sequenced to pinpoint the identity of each amiRNA sequence. 23 of the sequenced lines generated sequence data sufficient to determine which Arabidopsis transporter gene(s) were targeted for down-regulation of expression by amiRNA.

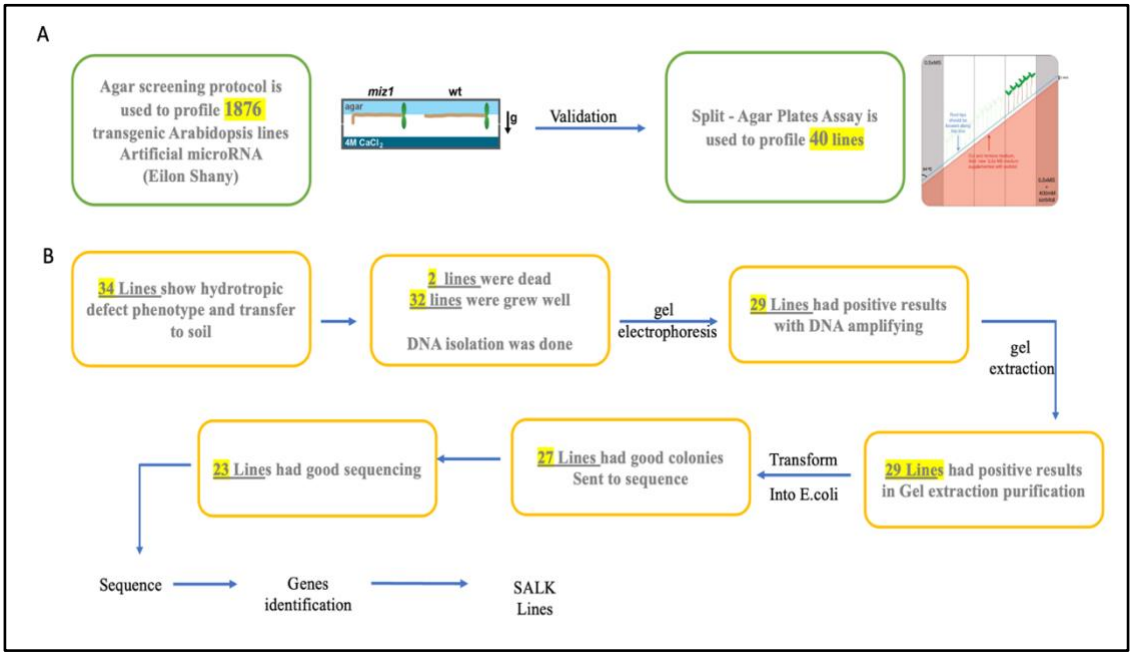


**Figure 3.8** Summarise of screening stages**.** (A) Phenotype stage. (B) Genotype stage

**Table 3.1** Summarised the Arabidopsis transporter sequence(s) identified as targets after the sequence of PCR products.

| amiRNA ID | TAIR ID | NASC ID | Function |
|---|---|---|---|
| **1466** | AT5G03260.1 | N662726 | Laccase11 |
| **833** | AT5G58910.2 | N668406 | Laccase16 |
| **790** | AT5G46370.1 | N666829 | Ca2+activated outward rectifying K+ channel2 |
| **784** | AT3G47960.1 | N923939 | Major facilitator superfamily protein |
| **693** | AT1G43470.1 | N69760 | mechanosensitive channel of small conductance-like 4 |
| **499 T3-1** | AT1G42470.1 | N654977 | Patched family protein |
| **633 -1** | AT5G46050.1 | N664402 | ARABIDOPSIS THALIANA PEPTIDE TRANSPORTER 3 |
| **1112 -1** | AT5G53130.1 | N547404 | ATCNGC1, CNGC1, , CYCLIC NUCLEOTIDE-GATED CHANNEL 1 |
| **523 -1** | AT4G09160.1 | N656113 | SEC14 cytosolic factor family protein / phosphoglyceride transfer family |
| **524** | AT1G76800.1 | N657639 | ATVTL2, VACUOLAR IRON TRANSPORTER-LIKE 2, VTL2 |
| **2077** | AT1G51460.1 | N662346 | ABC-2 type transporter family protein |
| **478** | AT5G40840.5 | N672286 | Rad21/Rec8-like family protein |
| **2690** | AT5G01190.2 | N678167 | Laccase10 |
| **1227** | AT1G66760.2 | N581560 | MATE efflux family protein |
| **1458** | AT5G49890.1 | N680169 | ATCLC-C, CHLORIDE CHANNEL C, CLC-C |
| **1484** | AT5G33280.1 | N686466 | ATCLC-C, CHLORIDE CHANNEL C, CLC-C |
| **2522** | AT3G47960.1 | N660899 | Major facilitator superfamily protein |
| **469** | AT5G01180.1 | N654100 | peptide transporter 5 |
| **2645** | AT3G45690.1 | N605411 | Major facilitator superfamily protein |
| **2078** | AT1G66760.2 | N599800 | MATE efflux family protein |
| **729** | AT5G12860.1 | N652687 | DICARBOXYLATE TRANSPORTER 1, DIT1 |
| **459** | AT5G57090.1 | N664960 | AGR, AGR1, ATPIN2, EIR1+B7 , MM31, PIN2, WAV6 |

In several cases such as major facilitator superfamily protein and MATE efflux family protein, amiRNA sequences were identified which targeted the same Arabidopsis transporters genes, validating the reproducibility and effectiveness of the screen (more details in Appendix).

### 3.2.5 Validation of Arabidopsis ABA transporter gene hydrotropic roles

Independent mutant lines (obtained using available T-DNA insertion mutants from NASC) were characterised for a limited number of Arabidopsis sequences to validate their roles in hydrotropic signalling which were originally Identified using the amiRNA approach. These sequences included GTR (see Chapter 4) and DTX1.

In section 3.3.4, selected MATE family and DTX50 sequences as ABA transporters. A T-DNA insertion mutant (SALK_081560; Table 3.2) was ordered from NASC to investigate if another *dtx1* allele exhibited a defect in hydrotropism. Like *miz1*, *dtx1* seedlings exhibited a hydrotropic defect (Figure 3.9 & 3.10).

In the split agar plates assay (Figure 3.10), 7 days old seedlings showed different responses in the root growth direction. In control plates which contains of half MS salts medium, all seedlings of all lines showed the same direction on growth, they were all grow forward gravity. In other hand, *Col-1* seedlings (WT) showed bending in root growth in split agar plates which had Sorbitol medium due to the different in water potential between plates two halves. Whereas *miz1* and *dtx1* seedlings showed hydrotropic defect by grew forward gravity in both cases (control and Sorbitol) due to hydrotropic mutation.

**Table 3.2** *dtx1* genetic identification

| Mutation | Gene ID | SALK_ID | Homozygous | NASC ID | Mutation Site |
|---|---|---|---|---|---|
| *dtx1* | At1g66760 | SALK_081560 | Segregating | N581560 | Promoter |

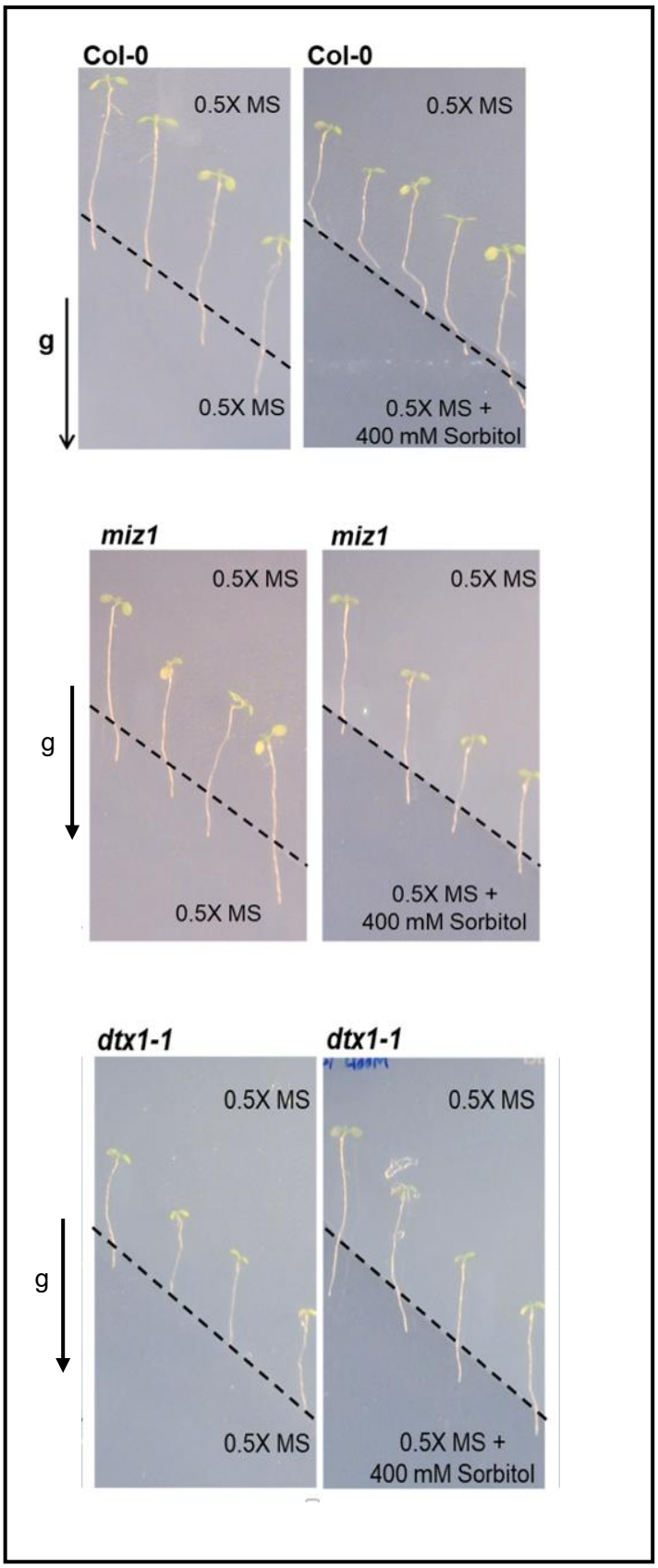


**Figure 3.9** *dtx1* mutation line in screening by use split agar. The phenotype *of dtx1* and *miz1* was characterised growth toward sorbitol media which is different from *col-0* growth which toward the high-water potential with root curvature. However, all three lines show same behaviour in control plates by grow towards gravity.

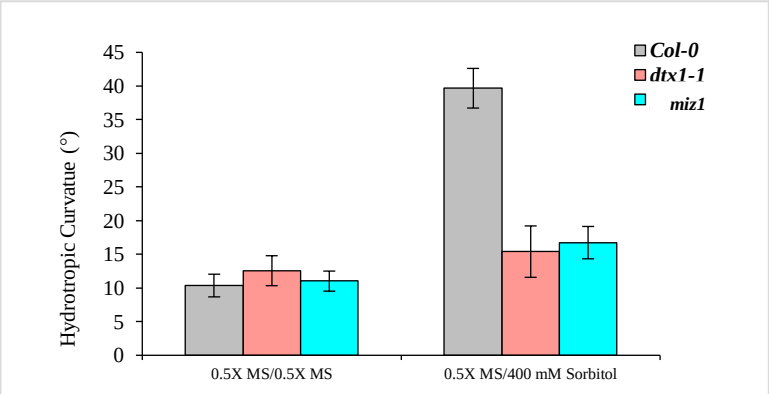


**Figure 3.10** Quantitative data for the growth of *dtx1* and *col-0* (WT) as measured by the angle degree of root growth. The increase of angle curvature was observed in *col-0* seedlings in sorbitol while *dtx1* keep growing toward gravity in both half MS and Sorbitol medium.

Positive *dtx1* seedlings which show hydrotropic defect by growing forward gravity were transferred to the soil. After 10 days, leaves samples were taken to extract DNA from them. The PCR reaction was prepared by using Phusion Protocol to amplify DNA fragments and discover the segregation in *dtx*1 alleles (more details in the material and method chapter). In gel electrophoresis, the DNA fragment of *dtx1* was amplified in both wild type (LR)and mutation (BR) which proved heterozygous mutation in *dtx1*.

**Table 3.3** The information of primers was used in PCR.

| Primer Name | Sequence | Insertion position | Orientation |
|---|---|---|---|
| dtx-RP | AAGGCTTGAAGAGGAAACACC | Promoter | Forword |
| dtx- LP | GAACCAACGACTCCGAGAACAG | | |
| LBb1.3 (SALK lines) | ATTTTGCCGATTTCGGAAC | | |

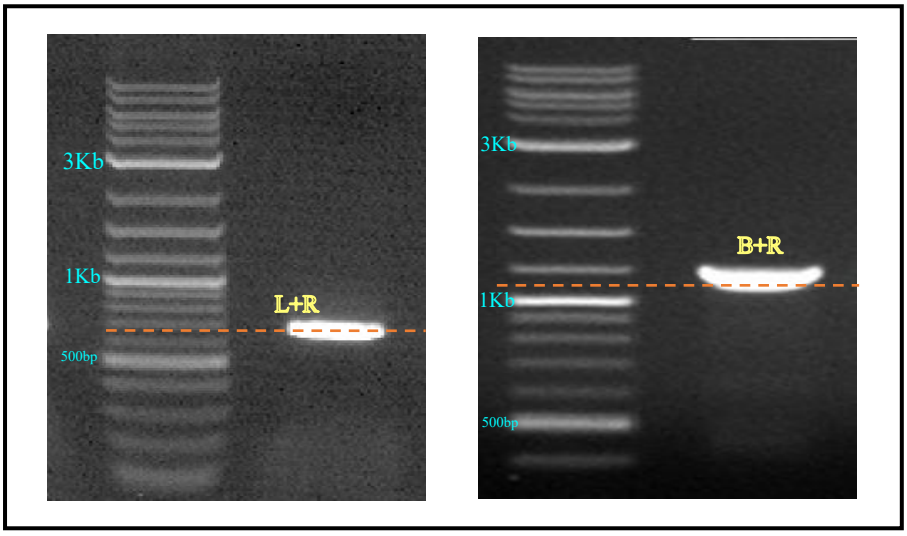


**Figure 3.11** Genotype results illustrate DNA amplification of *dtx1*. Phusion® High Fidelity DNA Polymerase was used to amplify DNA, the bands appear in specific band sizes (~ 670 bp) LR and (~1Kb) in BR primer which confirms heterozygous mutation lines.

## 3.3 DISSCUSION

Hydrotropism describes the tropic responses where roots exhibit the ability to grow towards the highest water availability (Cassab et al., 2013; Dietrich, 2018; Eapen et al., 2005; Kiss, 2007; Kobayashi et al., 2007; Takahashi, 1997). The hydrotropism response is controlled by the water stress signal ABA (Dietrich, 2018; Takahashi et al., 2002). Mutants disrupted in ABA synthesis or exhibit a hydrotropism defect (Kuromori et al., 2018), but no mutants in ABA transport have been identified to date. This Chapter describes the use of a high throughput hydrotropism mutant screen to screen ~1800 amiRNA lines targeting transporter-like sequences. Over 20 genes were identified had hydrotropic mutant defects (see Table 3.1).

The first class identified encoded members of the major facilitator superfamily. Two independent amiRNA lines targeting the same gene were identified. Based on previous studies, the *GTR1* gene was reported to encode as a glucosinolate transporter which is a member of the Nitrate Peptide transporter Family (NPF) (Nour-Eldin et al. 2012). In *Arabidopsis*, there are 53 NPF genes which include hormone transporters (e.g. AIT3 is an ABA transporter) (Léran et al., 2014). Saito et al. (2015) in (Figure 3.12) reported that GTR1 is a transporter with multiple substrate specificities that include glucosinolates, jasmonoyl-isoleucine and gibberellins, which may positively influence stamen development by mediating gibberellin supply.

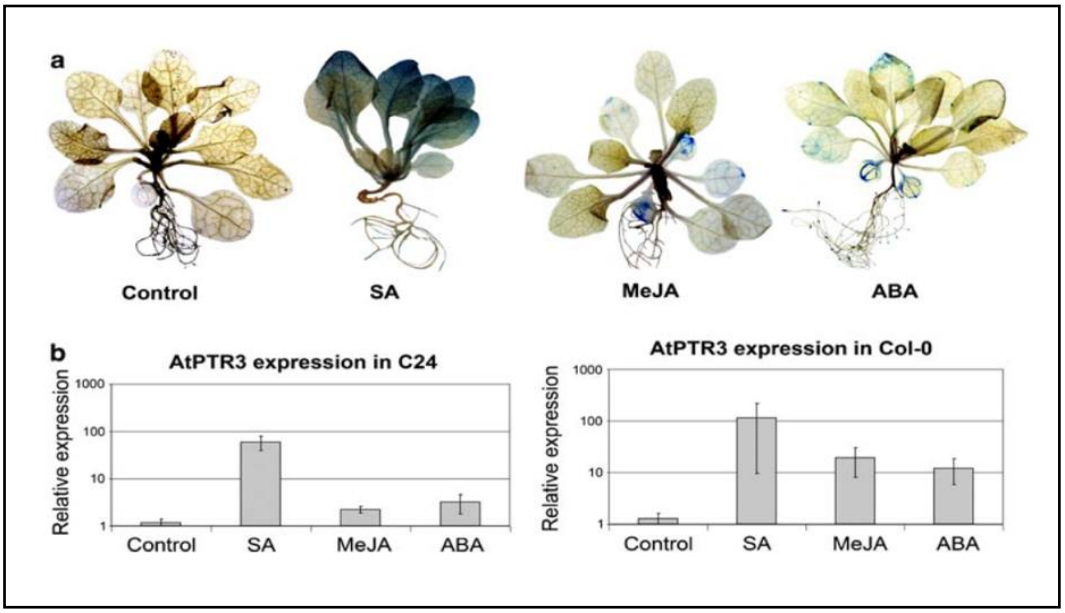


**Figure 3.12** The *gtr1*mutant is hypersensitive to JA. Expression of senescence-associated genes ingtr1seedlings. Ten-day-old liquid-cultured *Arabidopsis Columbia* WT orgtr1seedlings were treated with 0.02% ethanol(white bars) or 20mM MeJA (black bars) for 72 h, followed by quantitative–PCR.UBQ10was used as a reference gene. Values are the mean±s.d. of three biological replicates.(Saito et al. 2015)

The second class identified encoded members of the PEPTIDE transporter family which were found in two independent lines. AtPTR3 has been reported to be induced by many hormones including ABA. In addition, this gene is induced by salt and mutations decrease germination frequency in high concentrations of salt as it shown in (Figure 3.13) (Karim et al., 2005).

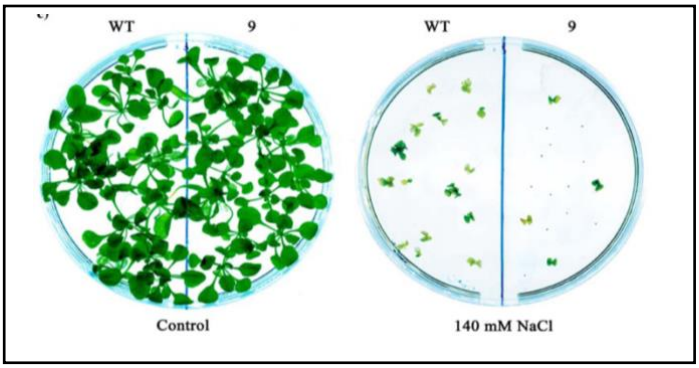


**Figure 3.13** Germination frequency ofAtptr3 knockout mutant line is reduced on salt medium. Atptr3knockout mutant (9) and wild-type C24 (WT) sown on MS medium (Control) and MS medium supplemented with salt (140 mM NaCl)(Karim et al., 2007)

The third class identified encoded members of the MATE efflux family. The *Arabidopsis thaliana* genome encodes 58 members of the DTX/MATE Family which function as transporters of organic acids and secondary metabolites (Li et al. 2002). Four independent lines were identified in this study. In (Figure 3.14), AtDTX50 has been reported as an ABA transporter in a study carried out by (Zhang et al., 2014), where the gene was found to be mostly expressed in vascular tissues and guard cells, with exogenous ABA significantly increasing its expression. Consistent with an ABA (efflux) transporter function, the AtDTX50:GFP fusion protein was mostly found in the plasma membrane and *dtx50* mutant plants responded to ABA growth inhibition with greater sensitivity.

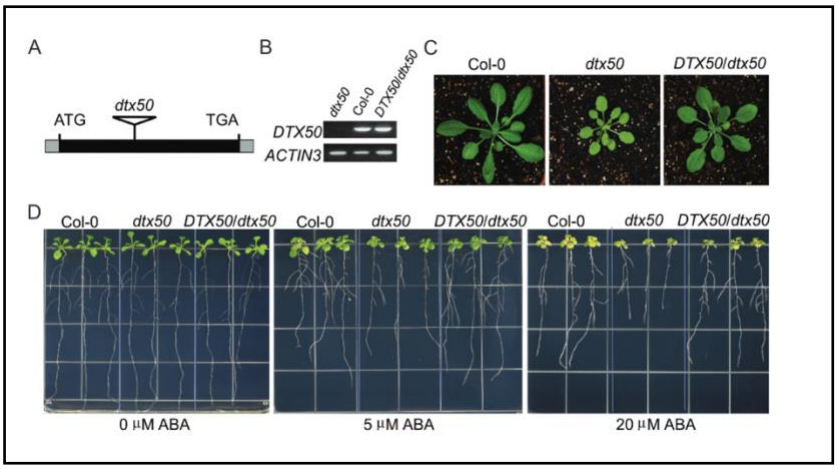


**Figure 3.14 The Arabidopsis *dtx50* T-DNA Insertion Mutant Phenotype**. (**A**) Genetic map of the *dtx50* insertion mutant used in this study.(**B**) RT–PCR results confirm *dtx50* mutant and the complementary line.(**C**) Phenotype of young seedlings (4 weeks old).(**D**) The *dtx50* mutant shows a growth inhibition by ABA.(Zhang et al., 2014)

In addition to several classes of putative ABA transporters, Ion Channels were identified including a chloride and calcium transporter, plus Vacuolar Iron and decaboxylate transporters. Most of the different ion transporters found were previously characterized for salt stress (Nguyen et al., 2016). For example, the gene *AtCLG* was

localized in the vascular membrane and mutations in this gene over-accumulates chloride in shoots in the present of sodium chloride.

In addition, a member of the ABC-transporter family (*ABCG13*) was identified in this screen (Table 3.1). Also, *ABCG13* transporter is highly expressed in flowers, predominantly in petals and carpels. Chemical analysis suggests that *ABCG13* is required mainly for flower cutin secretion (Panikashvili et al., 2011). More than 100 ABC-type proteins are found in *Arabidopsis*, and 53 genes produce the so-called full-size transporters (AGI, 2000). Studies have reported *ABCG25/WBC25* as an ABA transporter that transfers ABA from vascular to xylem cell, whereas *ABCG40/PDR12* acts to transport ABA from xylem to guard cells to control stomatal closure under drought stress (Kuromori et al., 2010). *abcg40* mutation effect on stomatal closure responses to ABA support the theory of the effect of *abcg40* on guard cells ability to uptake ABA(Kang et al., 2010). ABCG25 and ABCG40 cause stomatal closure during drought stress by delivering ABA from vascular cells to guard cells in (Figure 3.15)

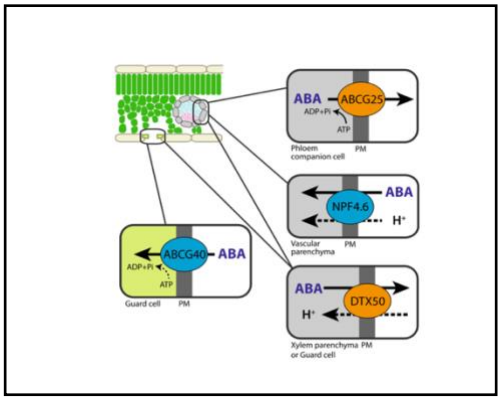


**Figure 3.15** ABA transporters in the leaf exposed to drought and in the dormant seed. Transporters that mediate efflux of ABA are marked in orange, and transporters that mediate influx of ABA are marked in blue. a When exposed to drought, ABA synthesized in vascular parenchymal cells is exported out of the cells via ABCG25 and DTX50. NPF4.6/AIT1 is reported to regulate the level of ABA in the vascular parenchymal cells. In the guard cell, ABCG40 takes up ABA, which induces stomatal closing (Park et al., 2017)

Likewise, ABA is also transported by ABCG25, ABCG40, and two more *Arabidopsis* ABCG-type transporters, ABCG30 and ABCG31, from the endosperm of seed coats to the embryo, sustaining seed dormancy (Kang et al. 2015).

The transportome screen also identified a Mechanosensitive (MS) ion channel of small conductance-like 4 (MSLs4). MSLs are non-selective anion channels whose activity is controlled by membrane stimulation with voltage or mechanically (Haswell et al., 2008). Ten MSLs genes are encoded in *Arabidopsis* genome (Haswell et al., 2008). MSL9 and MSL10 regulate mechanosensitive anion channel activity in the plasma membrane of root protoplasts. The precise integrated function of these channels has remained a mystery because neither the double *msl9, msl10* mutant nor the quintuple *msl4, msl5, msl6, msl9 and msl10* mutant showed altered responsiveness to a range of stimuli, such as osmotic, salt, mechanical, or dehydration (Haswell et al. 2008). The mechano-sensitivity of MSL10 was established through heterologous expression (Maksaev and Haswell, 2012), MSL10 enhances cell responses to swelling by interacting with both cell wall inhibitors that loosen the cell wall and osmoticum to modify cell turgor (Basu et al., 2020). In a recent study, researchers studied the interaction between osmosis and ABA abundance and the effect of different gene families which can control the process and MSLs was one of those families as it shown in (Figure 3.16) but they did not mention MSL4 (Gorgues et al., 2022).

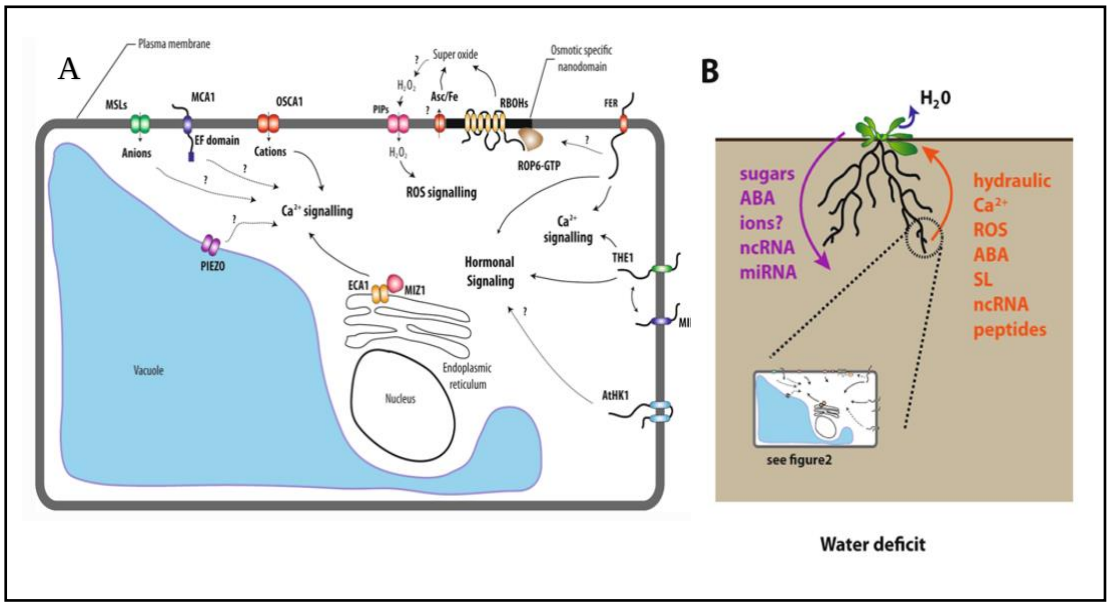


**Figure 3.16** Long-distance and developmental response to homogeneous or local water deficit. (A) Changes in membrane tension induced by osmolarity imbalance can be perceived by membrane mechanosensory such as OSCA1, MSLs, MCA1, PIEZO, and ECA1/MIZ1. By transporting cations or anions, these sensors initiate cell calcium signalling by as yet unknown mechanisms. (B) When a plant lacks water, it first drastically reduces transpiration before changing root and shoot growth to match the water supply. As shown in.(Gorgues et al. 2022)

The last transporter gene identified was *PIN2* which is an auxin efflux carrier(Wan et al., 2012). PINs frequently mediate root tropic responses in Arabidopsis, and the root is extremely responsive to environmental signals. Proteasome-mediated asymmetrical degradation of PIN2 in the root cells regulates root gravitropism(Abas et al., 2006). Along with controlling positive phototropism, PIN2 also controls root heliotropism (Wan et al., 2012; Galvan-Ampudia et al., 2013). Roots in PIN2-deficient mutants are unable to quickly bend away from salt locations. External inputs cause asymmetrical auxin build-up and cell elongation by triggering PIN2 intracellular trafficking (Galvan-Ampudia et al., 2013b; Wan et al. 2012). In a recent study (Xie et al., 2021), an ABA double mutant *cyp707a1,3* displayed growth patterns similar to agravitropism (wavy growth trajectory) which might be caused by the accumulation of exogenous and

endogenous ABA. The agravitropism-like phenotype was brought on by ABA's reduction of the quantity of PIN2.

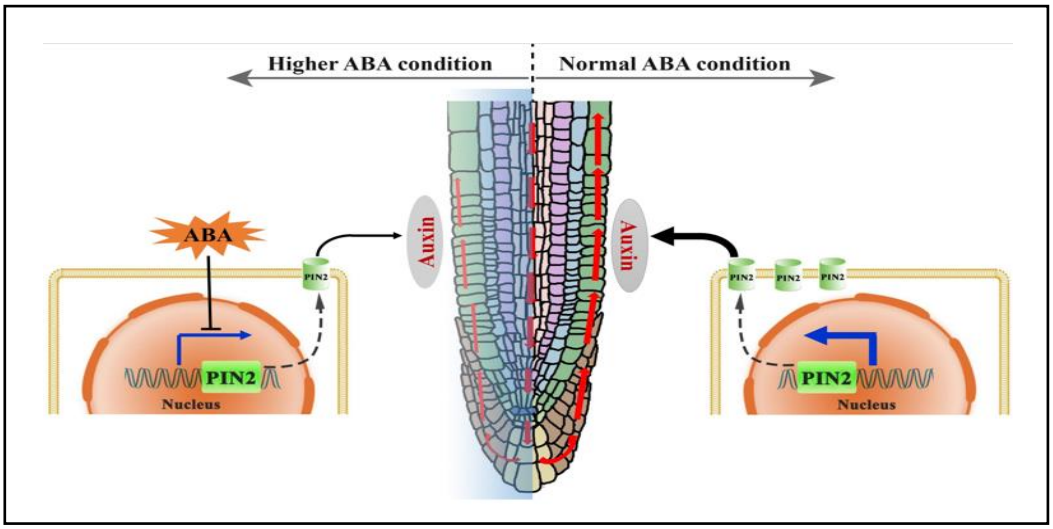


**Figure 3.17** An idea for a mechanistic model to explain how ABA controls the trajectory of root growth**.** Auxin can travel from the lateral root caps to the elongation zone under normal (ambient) climatic conditions, primarily via the polar-distributed auxin efflux carrier PIN2. However, under unfavourable environmental conditions, increased ABA levels inhibit PIN2 transcription, decreasing PIN2 abundance, which impairs SAT (red upward arrowheads). Asymmetric cell elongation in the Elongation Zone is ultimately brought on by a deficiency in auxin content, which results in wavy growth (Xie et al, 2021).

In conclusion, an amiRNA transportome library was screened for new genes that regulate ABA mobilisation in Arabidopsis roots in this chapter. ATP binding cassette family (ABCG), DTX1, and GTR1 are putative ABA transporters. In the next results Chapter, I will explain more about GTR1 and its relation with ABA.

# 4 CHAPTER 4: CHARACTERISATION OF NOVEL MFS TRANSPORTER REGULATING HYDROTROPISM

## 4.1 INTRODUCTION

ABA (abscisic acid) acts as a key signal that regulates the hydrotropic bending of *Arabidopsis* roots. Several ABA signalling mutants have been shown to disrupt root hydrotropism in the presence of moisture gradients (Dietrich et al., 2017; Takahashi et al., 2002). Apart from ABA signalling, ABA biosynthesis is essential for hydrotropism. The loss-of-function ABA biosynthesis mutant *aba1-1* exhibits significant defects in its hydrotropism response (Takahashi et al., 2002) whereas exogenous application of ABA restores the sensitivity of *aba1-1* to a hydrotropism stimulus (Takahashi et al., 2002). Previous studies carried out by (Dietrich et al., 2017) revealed that hydrotropic bending requires the activity of ABA signalling component SnRK2.2 kinase which is specifically required to act in elongation zone cortical cells to perceive moisture gradients, ABA responsive gene *MIZ1* regulates hydrotropism via preferential expression in cortical cells (Moriwaki et al., 2013). These findings suggest that the cortex is an important target site for ABA-dependent root adaptive responses such as hydrotropism.

Intriguingly, most ABA biosynthesis genes are expressed in vascular tissues (Kuromori et al., 2014). This observation led us to hypothesize that moisture-regulated root responses such as hydrotropism requires movement of ABA from inner to outer root tissues through an, as yet, unknown hormone transport pathway(s). Therefore, to discover the putative ABA transporters involved in root hydrotropism, an extensive screen of 1876 *Arabidopsis* amiRNA lines (each expressing an artificial microRNA targeting a distinct sub-set of transporter genes) (see Chapter 3). This screen led to the

identification of 34 amiRNA lines defective in hydrotropism response (see Chapter 3). Interestingly, two independent amiRNA lines (L784 and L 2522) were found to express identical amiRNA that targets transcripts of a gene encoding major facilitator superfamily (MFS) protein, AT3G47960. Given the reproducibility of these hydrotropic defects in multiple independent lines, we hypothesized that the identified MFS protein might be a putative ABA transporter involved in hydrotropic bending. Therefore, in this chapter, functional characterization of the candidate MFS (AT3G47960) was carried out to investigate its putative role in ABA transport and hydrotropism.

## 4.2 RESULTS

### 4.2.1 Hydrotropic regulator AT3G47960 encodes NPF transporter AtNPF2.10

Two independent amiRNA lines (L784 and L2522) expressed identical amiRNA targeting major facilitator superfamily (MFS) protein, AT3G47960 (see Chapter 3 for details). To discern the possible function of this MFS transporter, I screened the TAIR database as well as performed extensive literature searches. This revealed the MFS encodes AtNPF2.10 (NRT1/PTR FAMILY), a member of NITRATE TRANSPORTER 1/PEPTIDE TRANSPORTER (NRT1/PTR) family (Léran et al., 2014).

The NPF class of transporters are known to transport a broad range of substrates including peptides, amino acids, nitrate, dicarboxylates as well as hormones. So far, 53 NPF proteins have been identified in *Arabidopsis*. Based on sequence similarity, *Arabidopsis* NPFs are subdivided into eight subfamilies (NFP1 to NPF8) (Léran et al., 2014). Interestingly, two NPFs belonging to NPF4 subfamily, NPF4.1 (AIT3) and

NPF4.6 (NRT1.2/AIT1) are able to transport ABA(Léran et al. 2014). Many members of the NPF2 subfamily including AtNPF2.10 are involved in long-distance transport of nitrate and glucosinolates (Nour-Eldin et al., 2012). However, several studies have noted that the sequence homology of NPFs does not correlate with their substrate selectivity as members of different subfamilies may transport similar substrates, whereas members of the same subfamily may transport different substrates (Le´ran et al., 2014).

AtNPF2.10 was initially identified as *GTR1* (*Glucosinolate transporter1*) which encodes a 636 amino acid length transmembrane-spanning protein. Previous studies have shown that AtNPF2.10 also transports hormones such as bioactive JA (JA-Ile) and GA in heterologous systems such as yeast and *Xenopus* oocytes (Saito et al., 2015). Thus, given the broad substrate specificity of AtNPF2.10, it is highly likely that AtNPF2.10 (hereafter described as GTR1) is capable of transporting other substrates including hormones such as ABA.

### 4.2.2 GTR1 Is localized to the plasma membrane

The GTR1 protein consists of 12 transmembrane helices and has been previously detected in plasma membranes of onion epidermal and mesophyll cells (Nour-Eldin et al., 2012; Saito et al., 2015). To assess its role as an ABA transporter in roots, the expression of *pGTR1:GTR1-GFP/gtr1-1* in 5-day old *Arabidopsis* roots was tested. Consistent with previous studies in shoot cells, GFP tagged GTR1 was localised at the plasma membranes of root cells (Figure 4.1 ). In addition, nearly every root cell type expressed *GTR1*, but, higher GTR1-GFP levels were detected in the epidermis, lateral root cap and vasculature. The observed expression patterns of *pGTR1:GTR1-GFP*

varied significantly from the available single cell transcriptomics datasets (discussed below). It is noteworthy that the intergenic region upstream of *GTR1* is >7 kb, whereas only a ~2.8 kb promoter sequence was cloned to drive *GTR1* expression. Therefore, it is possible that elements required for *GTR1* spatial expression were missing in the *pGTR1:GTR1-GFP* promoter-reporter construct.

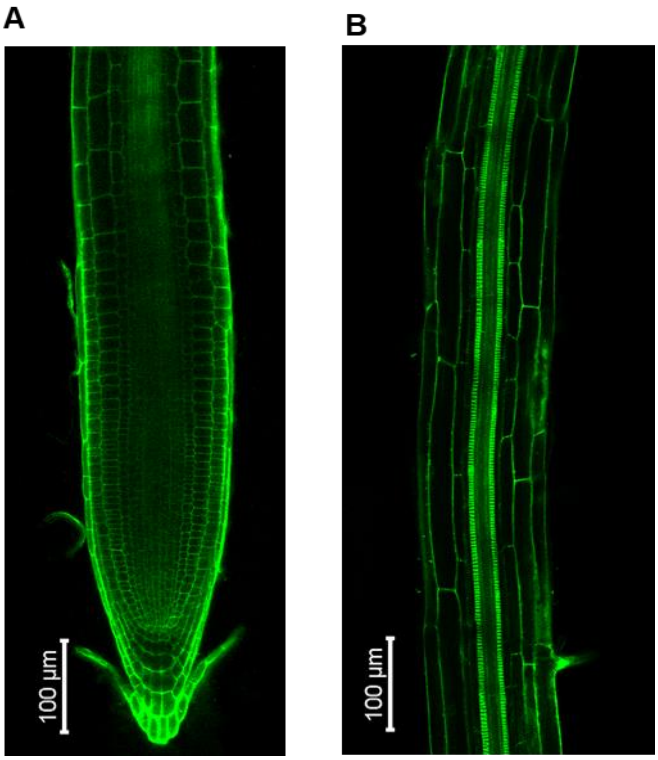


**Figure 4.1** Expression patterns of GTR1 in roots**.** Representative confocal images showing expression of *pGTR1:GTR1-GFP* in **A.** meristem and early elongation zone, and **B.** differentiation zone of *Arabidopsis* root tips. Scale bar = 100µm.

Analysis of available single-cell gene expression datasets revealed very high mRNA levels of *GTR1* in the root cortex (Figure 4.2), an important cell-type for ABA-mediated hydrotropic bending (Dietrich et al., 2017). Strikingly, *GTR1* mRNAs are highly enriched in cortical cells at the start of the transition zone. The mRNA pattern of *GTR1* in this key root tissue supports a role in the ABA-dependent hydrotropic response pathway. In the root differentiation zone, *GTR1* shows very high expression in stele consistent with its role in long distance transport of metabolites such as GLSs.

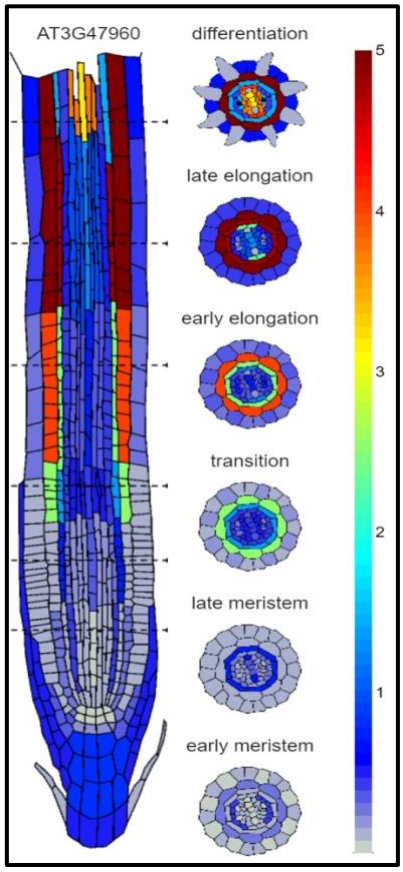


**Figure 4.2** Visualization of *GTR1* expression profiles at cell-scale. Integrated single cell expression dataset of *Arabidopsis* roots mapping expression domains of *GTR1* in longitudinal and transverse root sections. Single-cell transcriptomics data was retrieved from root cell atlas (https://rootcellatlas.org/). Colour scale indicates level of expression in different cell types.

### 4.2.3 *GTR1* is crucial for the root hydrotropism response

The *GTR1* amiRNA line L784 (identified in Chapter 3) exhibited a significantly reduced hydrotropism response in the 'root-lift assay'. These findings were tested using another hydrotropism assay termed the 'split-agar assay'. The latter method relies on water potential gradients generated by high concentrations of diffusing sorbitol (400mM). Roots of WT and amiRNA L784 were then placed on MS agar plates close to an agar-Sorbitol supplemented agar junction. 24 hours after a hydrotropic stimulus, roots of WT showed hydrotropic bending (Figure 4.3) whereas roots of amiRNA line L784 failed to produce any significant hydrotropic curvature.

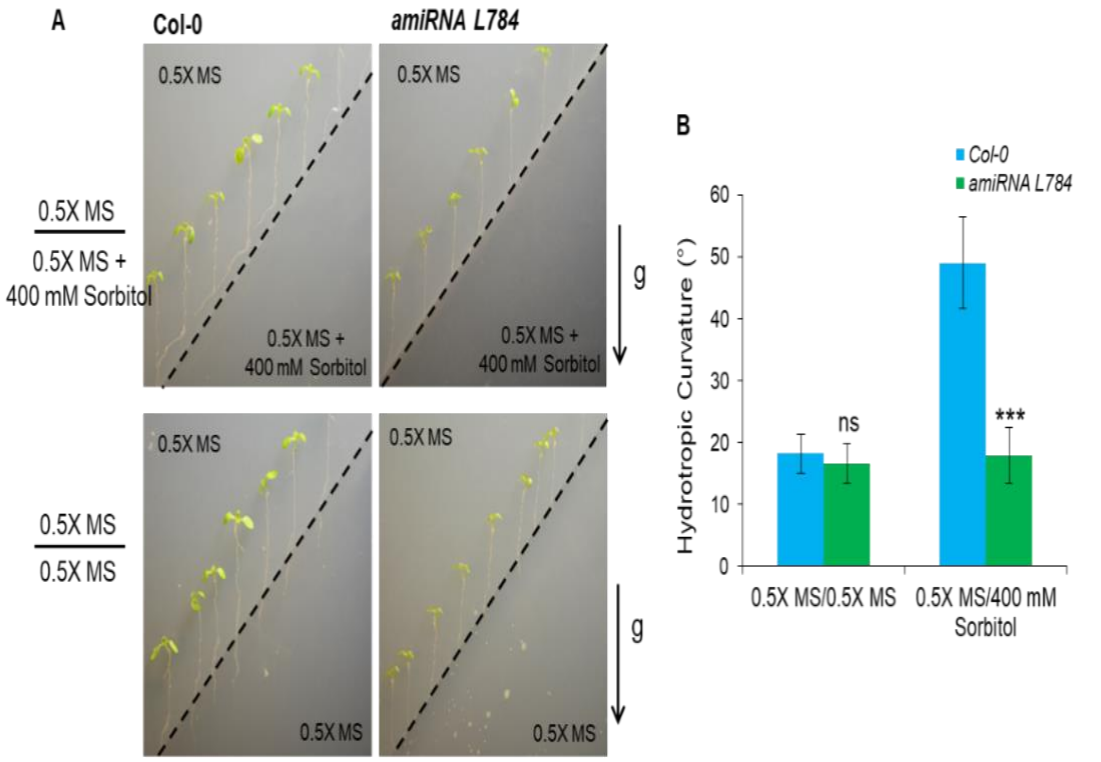


**Figure 4.3** Hydrotropic response of amiRNAL784 vs wild-type A. Root bending phenotypes and B. Hydrotropic curvature of WT and amiRNA L784 roots exposed to split-agar plates with or without 400 mM sorbitol. Level of significance was determined by Student's *t*-test. *** and ns indicate $p < 0.001$ and non-significant, respectively. Error bars represent standard error.

Artificial miRNA can silence more than one target gene due to partial base pairing with related sequences (Arroyo et al., 2014). Therefore, the observed phenotypes of amiRNA lines may be a complex output of silencing multiple gene targets. To confirm the hydrotropic defect was related to silencing of *GTR1* (and not other related genes), I utilized a loss-of-function *gtr1* T-DNA allele (Nour-Eldin et al., 2012; Saito et al., 2015). Similar to amiRNA L784, *gtr1-1* (SAIL_801_G03, N879742) also exhibited an attenuated hydrotropism response in the split-agar hydrotropism assay (Figure 4.4).

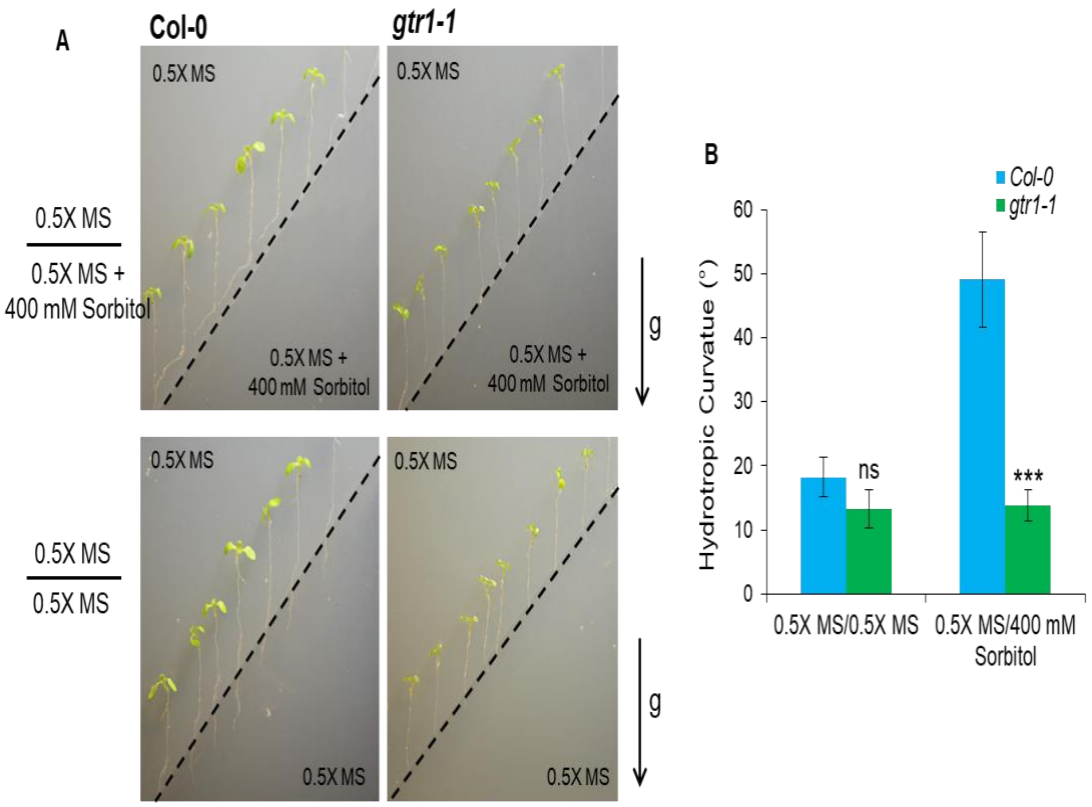


**Figure 4.4** Hydrotropic response of *gtr1-1* vs wild-type *Arabidopsis*. Root bending phenotypes and B. Hydrotropic curvature of WT and *gtr1-1* roots exposed to split-agar plates with or without 400 mM sorbitol. Level of significance was determined by Student's *t*-test. *** and ns indicate $p<0.001$ and non-significant, respectively. Error bars represent standard error.

Additionally, a *GTR1* mutant allele, *gtr1-2* (SALK_090694.2, N923939) was characterised and observed similar defects in its hydrotropism response (Figure 4.5). Both T-DNA mutant lines were confirmed for their homozygosity by PCR based genotyping. Collectively, these results reveal that *GTR1* is an essential component of the hydrotropic signalling machinery in the *Arabidopsis* roots.

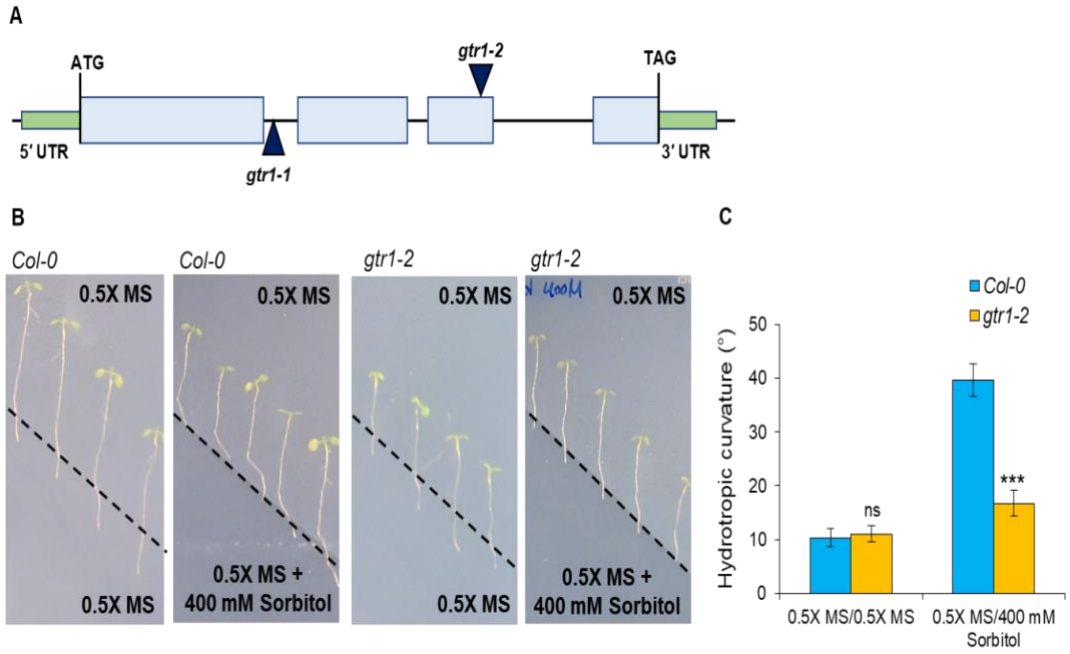


**Figure 4.5** Hydrotropic response of *gtr1-2* vs wild-type *Arabidopsis*. Site of T-DNA insertion in *gtr1-1* and *gtr1-2* mutants. Blue-coloured boxes represent exons. **B.** Root bending phenotypes and **C.** Hydrotropic curvature of WT and *gtr1-2* roots exposed to split-agar plates with or without 400 mM sorbitol. Level of significance was determined by Student's *t*-test. *** and ns indicate $p<0.001$ and non-significant, respectively. Error bars represent standard error.

### 4.2.4 Mutants lacking GTR1 also disrupt the ABA-dependent xerobranching response

In addition to hydrotropism, ABA regulates another moisture-driven root adaptive response termed xerobranching (see Chapter 5; Mehra et al, 2022). Xerobranching refers to the complete suppression of lateral root branching during the transient absence of water (e.g., in soil air-gaps) (Orman-Ligeza et al., 2018). Therefore, to explore the potentially wider role of *GTR1* in moisture-regulated root branching responses, an 'agar-based' xerobranching assay (see Chapter 5) was test the branching response of *gtr1* knock-out/knock-down lines. Interestingly, both *gtr1* mutants and amiRNAL784 exhibited defects in their xerobranching responses and (unlike wild-type) continued to produce lateral roots in air-gaps (Figure 4.6).

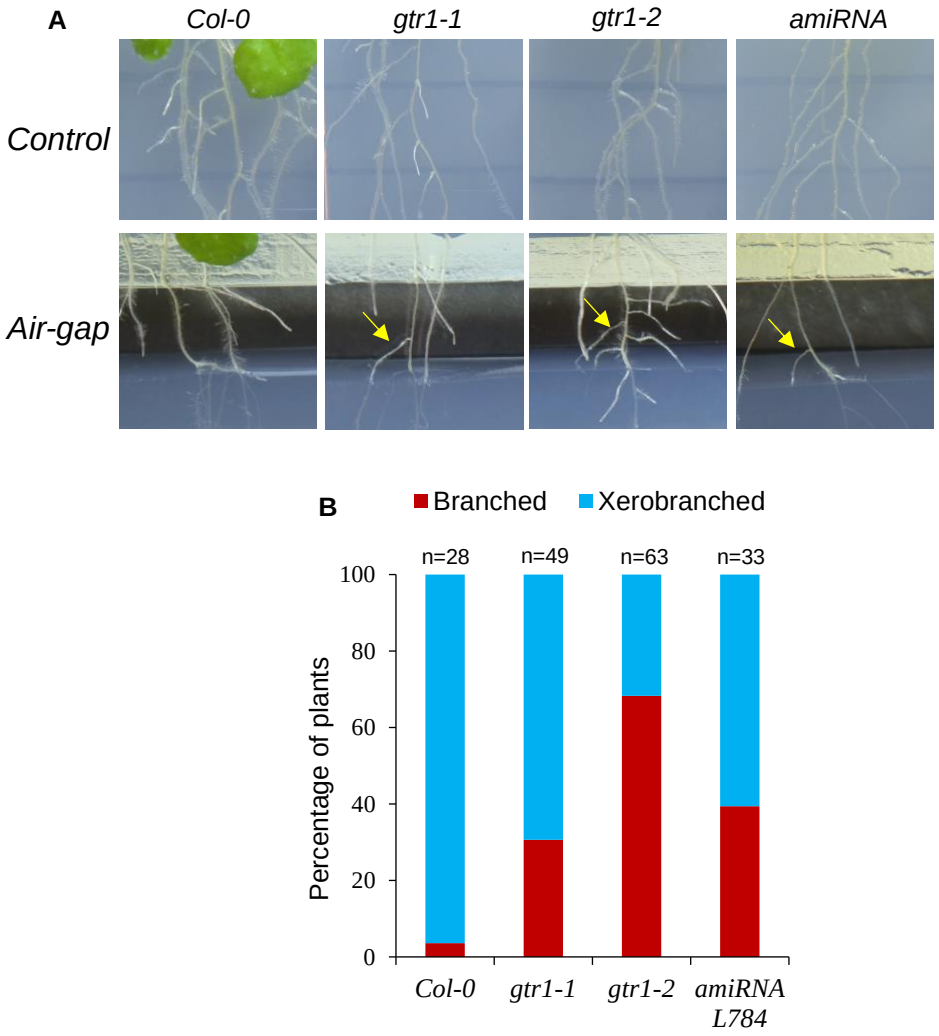


**Figure 4.6** *gtr1* disrupts xerobranching response. A. Branching phenotype of WT (Col-0), loss-of-function *gtr1* mutants (*gtr1-1*, *gtr1-2*) and *GTR1* amiRNA line (L784) in air-gaps. Air-gap ~ 5mm. Yellow arrow marks lateral roots produced in ai-gaps. B. High frequency of *GTR1* knock-out/knock-down lines branched in air-gap as compared to wild-type. Number of plants analysed (n) has been indicated at the top of each bar.

It was notable that *gtr1-2* exhibited a higher frequency of roots disrupted for xerobranching. Such phenotypic variability may arise due to the differences in the site of T-DNA insertion in *gtr1-1* (intron 1) vs *gtr1-2* (exon 3) (Figure 4.5). However, any variability in GTR1 transcription or translation between both mutant alleles still needs to be confirmed. It is also important to note that *gtr1-2* (SALK_090694.2) is a derivative of parent line SALK_090694 which harbours additional mutations in three genes; UDP-Glucosyl Transferase (AT1G07260), Response Regulator 15 (ARR15,

AT1G74890) and Response Regulator 5 (ARR5, AT3G48100). Genotyped *gtr1-2* was genotyped for these three additional mutations, confirming *gtr1-2* is a knock-out for all three additional mutations, which might contribute to stronger xerobranching defects. In future, it would be interesting to investigate the effect of cytokinin signalling on xerobranching. Overall, xerobranching assays reveals that GTR1 is a component of several moisture-driven ABA dependent root adaptive response pathways. Given the likely role of ABA transport in xerobranching (Mehra et al., 2022), it is highly plausible that GTR1 may acts as a putative ABA transporter in this (and other) root adaptive response pathways.

The quantitative reverse transcriptase polymerase chain reaction (qRT-PCR) technique was used to quantify cDNA sequences and confirm whether T-DNA insertion lines showed overexpression or no expression, as this method provides a very accurate analysis of any gene expression at very low levels, and the expression in *gtr1-2* mutation downregulated the gene.

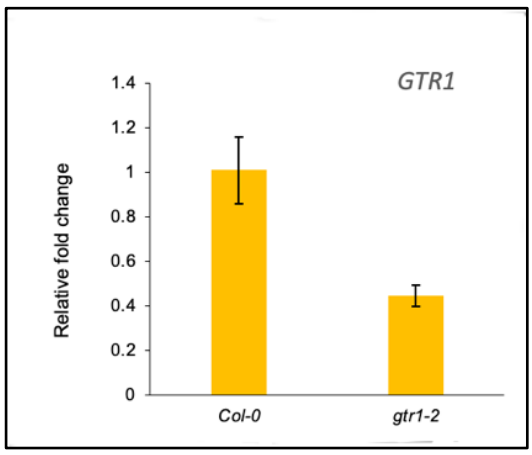


**Figure 4.7** Quantitative reverse transcriptase polymerase chain reaction (PCR**)** for GTR1 expression in gtr1-2 mutant expression in gtr1 mutation downregulated the gene.

### 4.2.5 Characterisation of GTR1 dependent hydrotropism using the ABACUS2 biosensor

Many of the ABA biosynthetic enzymes such as ABA2, NCED and AAO3 are specifically expressed in vasculature, suggesting synthesis of this key abiotic signal primarily occurs in these key tissues (Kuromori et al., 2014). However, ABA is required to be transported from its site of synthesis in the root vasculature to target cells (e.g. cortex) to trigger a hydrotropic response. To discover when and where ABA movement occurs following a hydrotropic stimulus (Rowe et al.,2022), a next generation highly sensitive Förster resonance energy transfer (FRET)–based ABA biosensor, nlsABACUS2 was used. nlsABACUS2-100 displays an increased fluorescence emission ratio upon ABA binding and can detect as low as 100 nM of physiological ABA concentrations. Strikingly, roots of nlsABACUS2-100 showed significantly enhanced emission ratio just one hour after a hydrotropic stimulus (Figure 4.8) suggesting rapid sensing of water potential gradients in growing root tip tissues. Spatially, ABA accumulated specifically in basal meristem and early elongation (but not root tip) zones, consistent with previous ABA response mapping studies (Dietrich et al, 2017). These zones have also been reported as key sites of ABA-mediated responses such as xerobranching (Chapter 5).

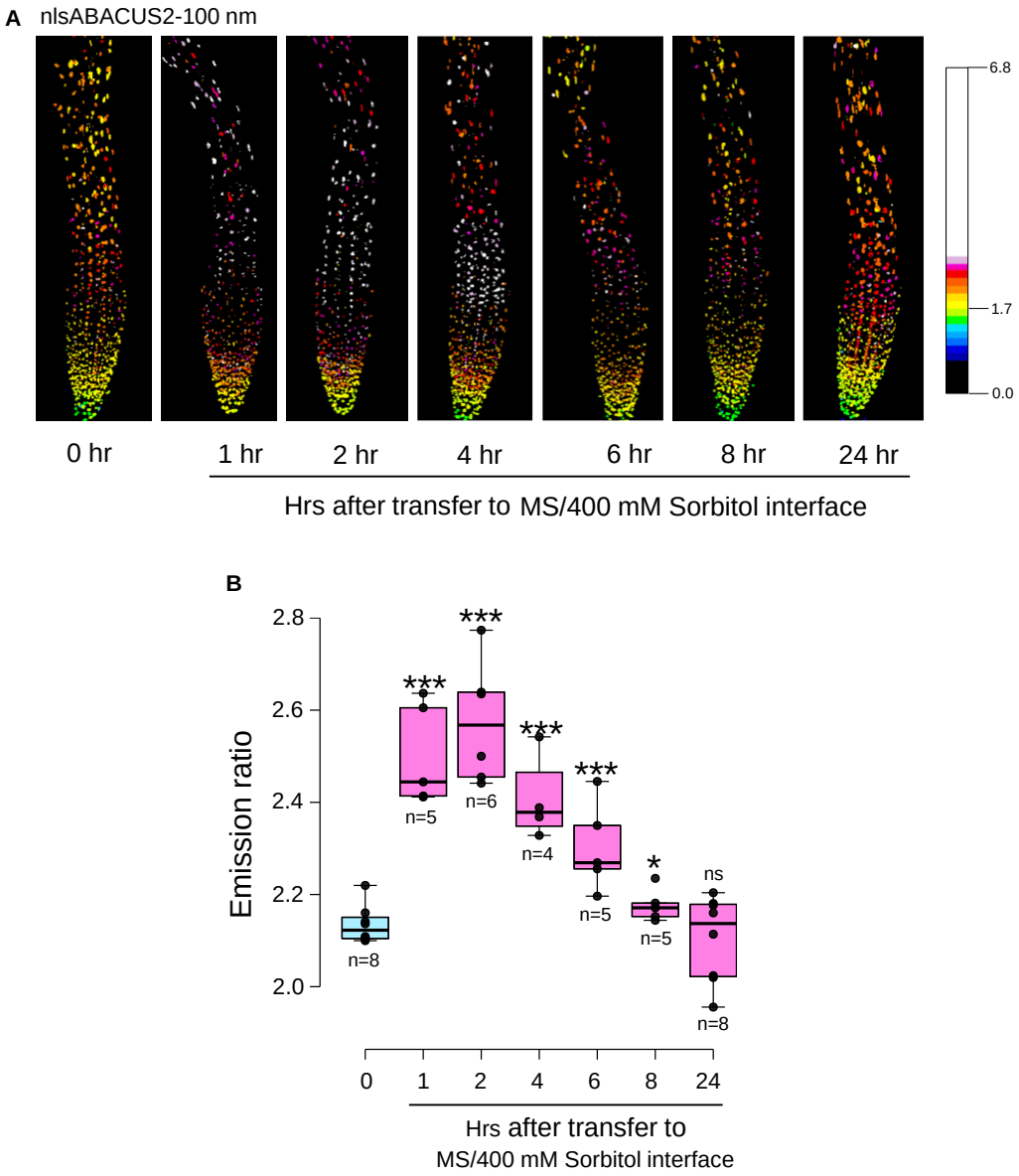


**Figure 4.8** High-affinity ABA biosensor (nlsABACUS2-100n) localisation reveals dynamic changes in ABA accumulation following hydrostimulation. A. Emission ratio maps and B. box-plots of *Arabidopsis* root tips expressing ABA biosensor nlsABACUS2-100n reveal dynamic changes in endogenous ABA levels during hydrotropism. Colour scale bars represent emission ratios. Higher ratios correspond to higher ABA concentrations. *, *** and ns represent $P \leq 0.05$, $P \leq 0.001$ and non-significant changes, respectively.

ABACUS2 FRET measurements revealed ABA levels gradually declined 2 hrs after a hydrotropic stimulus and were restored to normal levels after 24 hrs. Surprisingly, no asymmetry in ABA distribution were visualized in the root tips showing hydrotropic bending. Nevertheless, the ABACUS2 biosensor revealed the rapid accumulation of endogenous ABA in elongation zone target tissues following a hydrotropic stimulus.

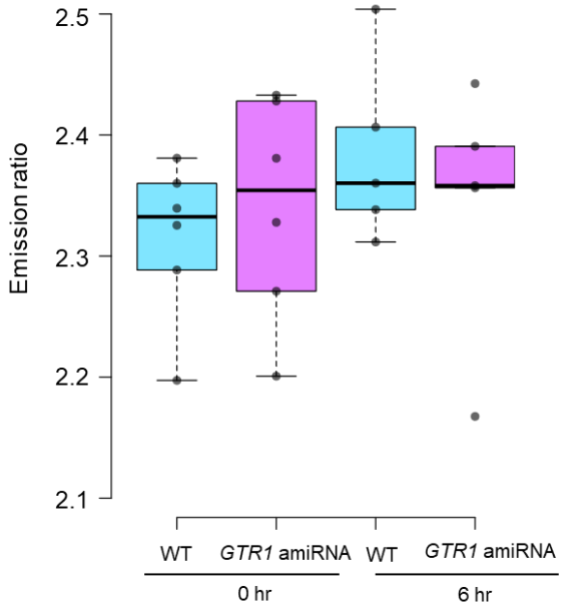


**Figure 4.9** Endogenous ABA levels in *GTR1* amiRNA line. Emission ratios of *Arabidopsis* root tips expressing ABA biosensor nlsABACUS2-100n in background of wild-type or *GTR1* amiRNA L784. Higher ratios correspond to higher ABA concentrations. Emission ratios were determined at 0 hr and after 6 hr of hydrotropism stimulus. Analysis was made in F1 progenies.

GTR1 may be involved in facilitating this rapid accumulation of ABA following a hydrotropic stimulus. To directly visualize whether GTR1 regulates ABA transport, the nlsABACUS2-100 biosensor was expressed in the *gtr1* amiRNA L784 background. F1 plants were compared with wild-type before and 6 hrs after a hydrotropic stimulus. No significant differences were observed in ABA levels between wild-type and amiRNA line (Figure 4.9) suggesting GTR1 may be involved in regulating the transport (directly or indirectly) of signals other than ABA. However, these results need to be cross-validated using nlsABACUS2-100 expressed in the background of homozygous *gtr1* knock-out lines.

### 4.2.6 Determination of key root tissues important for GTR1 dependent hydrotropism

To pinpoint which root cell types GTR1 functions to control hydrotropism, a tissue-specific complementation strategy of *gtr1-1* was adopted. Different cell-type specific promoters, e.g. *pCASP1*, *pSCR*, *pEN7* (endodermis), *pCO2* (cortex), *pWOL*, *pSHR* (stele), *pWER* (epidermis), p*XPP* (xylem pole pericycle), were selected to drive expression of *GTR1*. All promoters including the *GTR1* native promoter (*pGTR1*) were successfully amplified from *Arabidopsis thaliana* genomic DNA (Figure 4.10) and cloned in the MultiSite Gateway® Donor vector, pDONR™ 221 P4-P1r. *GTR1* genomic amplicon a VENUS reporter was also successfully cloned in pDONR™ 221 and pDONR™ 221 P2r-P3, respectively. All clones were confirmed by Sanger sequencing (Table 4.1).

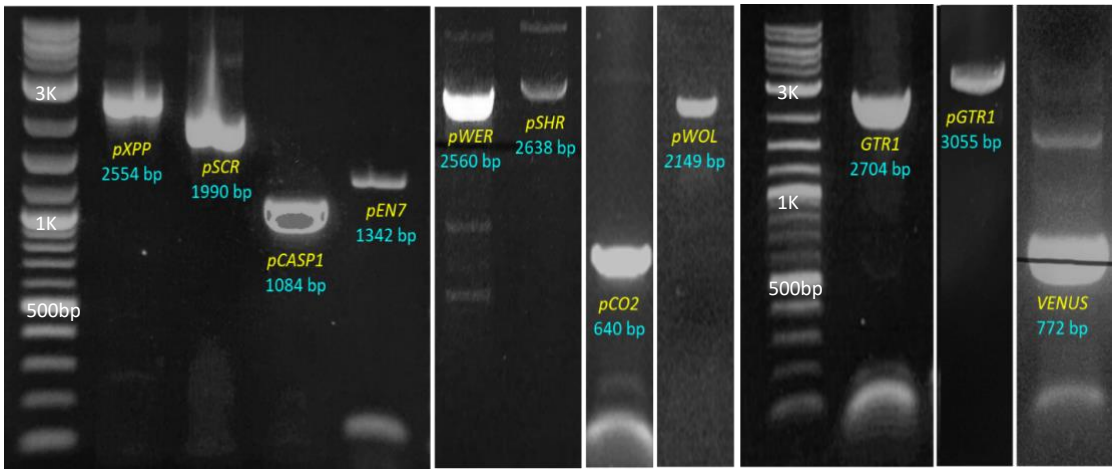


**Figure 4.10** Amplification of promoters, *GTR1* and reporter for MultiSite Gateway cloning. Gel electrophoresis image showing PCR amplification of tissue-specific promoters (*pXPP*, *pSCR*, *pCASP1*, *pEN7*, *pWER*, *pSHR*), *GTR1* native promoter (*pGTR1*), *GTR1* gene and *VENUS* reporter sequence. Amplicon sizes have been indicated in blue font.

**Table 4.1** Primers used in cloned MultiSite Gateway® and expected amplicon size

| Locus | Primers | Length of Primer | TM | Expected amplicon size |
|---|---|---|---|---|
| Endodermis | pCASP1_F<br>pCASP1_R | 54<br>45 | 75<br>76 | 1084 bp |
| Cortex | pCO2_F<br>pCO2_R | 48<br>48 | 74<br>73 | 640 bp |
| Precycle and vasculature | pWOL_F<br>pWOL_R | 48<br>48 | 74<br>74 | 2149 bp |
| Epidermis | pWER_F<br>pWER_R | 52<br>50 | 73<br>73 | 2560 bp |
| Endodermis | pEN7_F<br>pEN7_R | 52<br>49 | 75<br>75 | 1342 bp |
| Endodermis | pSCR_F<br>pSCR_R | 52<br>44 | 73<br>76 | 1990 bp |
| Stele | pSHR_F<br>pSHR_R | 46<br>55 | 72<br>71 | 2638 bp |
| XPP | pXPP_F<br>pXPP_R | 52<br>50 | 74<br>75 | 2554 bp |
| GTR promoter | pGTR_F<br>pGTR_R | 52<br>42 | 75<br>77 | 3055bp |
| AT3G47960 | GTR_F<br>GTR_R | 56<br>54 | 79<br>80 | 2704 bp |

Appropriate combinations of pDONOR clones will be assembled into destination vectors to create cell-type specific *GTR1* constructs. Transgenic *Arabidopsis* lines will be finally generated by *Agrobacterium*-mediated floral dip.

## 4.3 Discussion

GTR1/NPF2.10 is a well-known glucosinolate (GLS) transporter (Nour-Eldin et al., 2012). GLSs are a group of sulfur-rich secondary metabolites, primarily involved in herbivore defence (Anderson 2013). From an evolutionary perspective, GLSs confer a selective advantage to *Brassicales* due to their insect antifeedant/attractant, nematicidal and fungicidal properties (War et al. 2012; Reichelt et al. 2001). GTR1 along with its close homolog, GTR2 are involved in long-distance bidirectional transport of GLSs between root and shoot tissues (Nour-Eldin et al., 2012). A few studies have also proposed GTR1 as a multifunctional transporter (Ishimaru et al. 2017; Saito et al., 2015). Impaired GA transport is the proposed reason that *gtr1* mutants are defective in stamen development and anther dehiscence (Saito et al., 2015). Saito et al. (2015) also showed that GTR1 transports hormones such as JA-Ile and GA in the heterologous oocyte system. Interestingly, JA-Ile and GA share no structural resemblance to GLSs, which suggests that GTR1 can transport a wide range of metabolites. In this thesis, a new role for GTR1 regulating ABA-mediated root adaptive responses is shown in hydrotropism and xerobranching.

Previous studies have shown that *GTR1* is expressed in phloem companion cells and imports glucosinolates into phloem for long-distance transport to roots (Nour-Eldin et al., 2012). Analysis of single cell expression datasets revealed strong expression of *GTR1* in cortical cells of root transition and elongation zones. This tissue and these zones are considered critical for ABA-mediated root adaptive responses such as hydrotropism and xerobranching (Mehra et al., 2022; Dietrich et al., 2017). Therefore, use of tissue-specific complementation lines of *gtr1* would shed more light on the functional importance of GTR1 at a cell-scale. Also, GTR1 can express in different

tissue in different stages based on information of several studies in TAIR (https://www.arabidopsis.org/), (Figure 4.11)

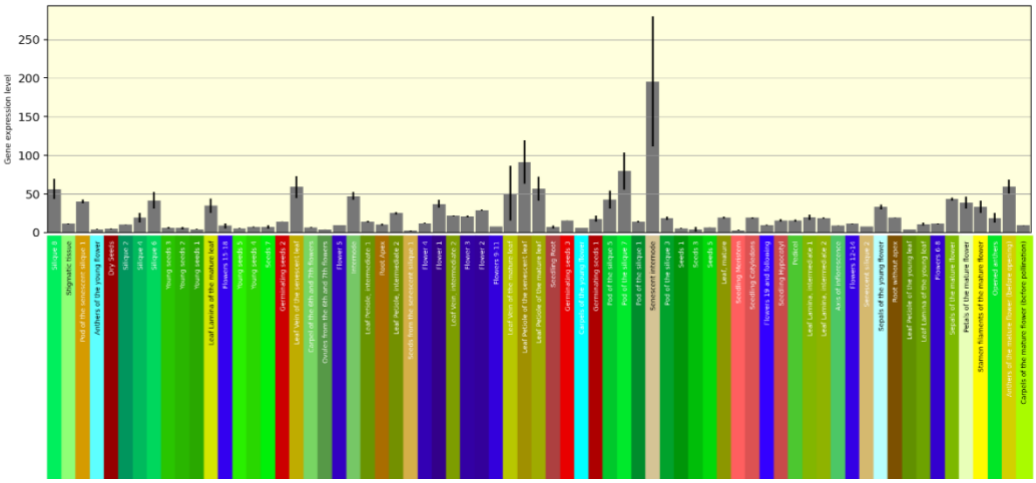


**Figure 4.11** AT3G47960 (GTR1) expression tissues and the level of expression. (https://www.arabidopsis.org/)

Until very recently ABA research suffered technical constraints due to the absence of sensitive tools/biosensors capable of monitoring ABA levels in root tissues at a cell-scale resolution. This is evident from the fact that all previous studies solely relied on the heterologous systems such as insect cells or oocytes to characterize transport activity of ABA transporters (Kuromori et al., 2010). To overcome this limitation, a highly sensitive next-generation ABA biosensor, ABACUS2 (kindly donated by our collaborators Jim Rowe and Alexander Jones, SLCU) was used. Notably, nlsABACUS2-100 is sensitive enough to report levels as low as 100nM of physiological ABA (Rowe et al., 2022). Interestingly, ABACUS2 was used to revealed dynamic changes in ABA specifically in root basal meristem following a hydrotropic stimulus. However, unlike auxin during gravitropism. no asymmetry in ABA redistribution was observed within root tip tissues. This suggests that ABA signalling

triggers some as yet unknown cell-specific signalling, to create an asymmetric tropic growth response during hydrotropism.

Phenotypic studies suggest GTR1 may function as a putative ABA transporter. However, preliminary ABACUS2 biosensor studies revealed no significant difference in endogenous ABA levels between wild-type and amiRNA lines following a hydrotropic stimulus. It should be noted that the expression of *GTR1* was not confirmed in the analysed F1 lines. Insignificant silencing of *GTR1* or less dynamic range of biosensor in F1 amiRNA lines (compared to WT) may attribute to unaltered FRET ratios. Therefore, the present results need to be confirmed by biosensor studies in homozygous *gtr1* knock-out backgrounds. Alternatively, GTR1 may regulate hydrotropism via indirect mechanisms or through transport of other possible 'hydro-signals'.

As GTR1 primarily transports glucosinolates, it is possible GLSs act as hydro-signals. Normally seeds display the highest level of GLSs as compared to other plant parts (Brown et al., 2003). However, at the vegetative stage of plant development, roots act as the primary sink of GLSs with higher concentrations of GLSs as compared to shoot (Borpatragohain et al., 2016)suggesting important functions of GLSs in roots. Apart from the nematidical action of GLSs in roots, GLSs also affect water uptake/transport across plasma membranes. Administration of sinigrin (aliphatic GLS) has been shown to increase hydraulic conductance, water permeability and abundance of PIP2 (Plasma membrane intrinsic proteins) aquaporins in roots under salt stress conditions (Martínez-Ballesta et al., 2014). Moreover, *Arabidopsis* mutants lacking aliphatic GLSs (*myb28myb29*) also exhibited significant reduction in root hydraulic

conductivity and aquaporin abundance under salt stress (Martínez-Ballesta et al., 2015); Aquaporins are specialized water channels that are essential for cellular transport of water (Biswas et al., 2021). This evidence suggests that GLSs are important for maintaining plant's water balance or osmotic adjustments. Therefore, it would be interesting to explore how GSLs regulate aquaporins to determine root tropic responses.

GLSs are predominant in *Brassicales* (*Capparales*) (Fahey et al., 2001). Few GLSs have been reported in non-cruciferous dicotyledonous angiosperms (Rodman et al.,1996). This further begs the question about functional conservation of GTR1-mediated water sensing mechanisms across broader range of plant species. It would be fascinating to understand how and why dicotyledonous angiosperms acquired selective advantage to adapt to water stress through GSLs or GTR1 dependent molecular pathways?

In conclusion, the present study revealed novel roles of GTR1 in water sensing and raises several interesting questions to investigate in future.

# 5 CHAPTER 5: HYDRAULIC FLUX RESPONSIVE HORMONE REDISTRIBUTION DETERMINES ROOT BRANCHING

## 5.1 INTRODUCTION

Crop plant foraging capacity is determined by root branching (Lynch, 2011; Muller et al., 2019). Roots have acquired versatility in their branching patterns to maximise access to soil water resources, which are frequently distributed in a heterogeneous manner (Morris et al., 2017). Extreme weather (such as drought or flooding) affects root branching, as do transient or local spatial changes in soil moisture (Zhan et al. 2015; Karlova et al., 2021). (Orman-Ligeza et al., 2018; Bao et al., 2014) Water scarcity's negative effects on contemporary agriculture will be compounded as climate change affects hydrological cycles and soil water resources (Lobell and Gourdji 2012; Grusson et al., 2021). Improved resilience in the face of climate change will necessitate a better understanding of how plant roots sense and respond to changing water supply.

## 5.2 RESULTS

### 5.2.1 Dissecting Root Water Sensing Using Xerobranching

Xerobranching (Orman-Ligeza et al., 2018) provides an experimental model to study root adaptive responses to transient water stress. A xerobranching response is triggered when growing root tips temporarily lose contact with moist soil (e.g., in an air-gap), causing branching to temporarily cease until roots re-enter moist soil. To discover the mechanistic basis of xerobranching, an agar-based air gap assay ( for more details see section 2.2.1.3) was used in experiments with *Arabidopsis* seedlings.

In which tissue(s) does ABA originate from to trigger a xerobranching response? ABA biosynthesis genes like *ABA2* are expressed in phloem-related root vascular tissues (Kuromori et al., 2014). *Arabidopsis aba2-1* mutant roots exhibit a xerobranching defect, which can be rescued by expressing WT *ABA2* using the phloem companion cell-expressed *SUC2* promoter (Figure 5.1, A to C). A *SUC2:YFP-ABA2* translation fusion was used to confirm that the ABA2 protein can act in a phloem companion cell-autonomous manner. Phloem provides water for growing roots in the temporary absence of an external supply (Wiegers et al., 2009).

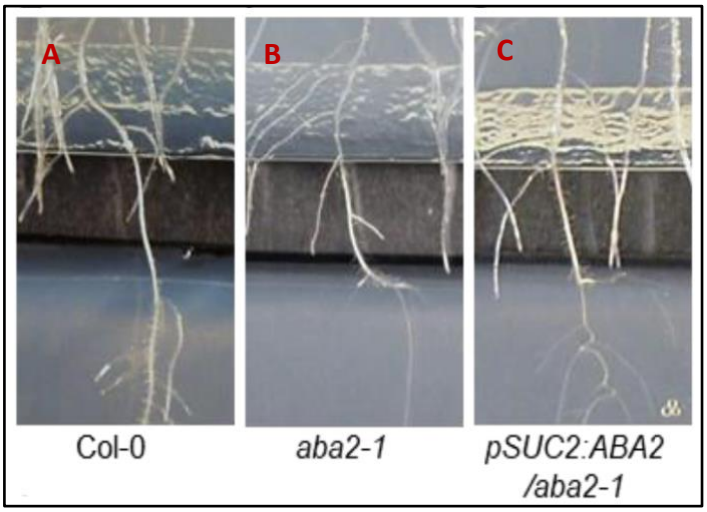


**Figure 5.1** Agar-based Air-gap Assay system showing xerobranching response in *Arabidopsis*. (A) Col-0 is a WT. (B) mutant *aba2-1*. (C) *pSUC2:ABA2/aba2-1* is a promoter. (air-gap ~5 mm) (Mehra et al., 2022).

Hydraulic modelling (Couvreur et al., 2018; Pascut et al., 2021)predicts radial water fluxes within root tissues change direction from predominately inwards to outwards following a xerobranching stimulus (Figure 5.2). Simulations reveal that an inwards water flux dominates under normal externally hydrated conditions, and phloem-derived water is limited to close to companion cells (Figure 5.2). However, following a xerobranching stimulus (when the external water source is temporarily lost), root tip

tissues rely on an outwards flux of phloem-derived water to maintain growth, requiring ~8 hours for outer root tissues to receive phloem water (Figure 5.2). Phloem-derived ABA is likely to travel with this outwards flow of water during a xerobranching response.

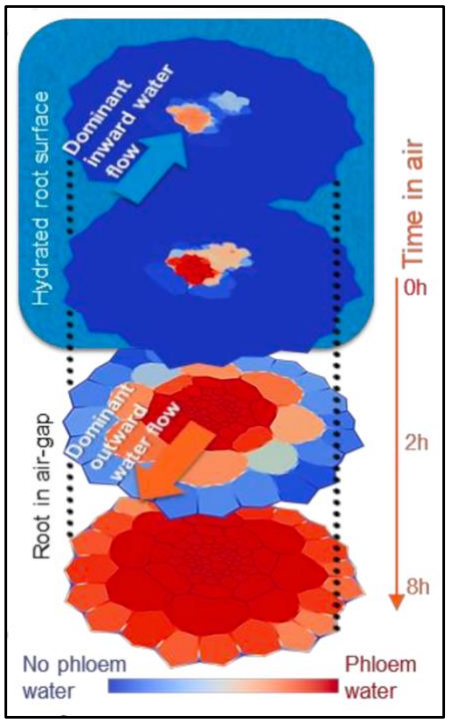


**Figure 5.2** The MECHA hydraulic model predicts phloem as the main source of water in *Arabidopsis* root elongation zone only when located in an air-gap. Simulated water advection maps show dominating phloem water in root epidermal cells within 8 hours (Mehra et al., 2022).

### 5.2.2 ABA moves outwards following a xerobranching stimulus

To visualise *whether*, *when* and *where* ABA movement occurs following a xerobranching stimulus, we utilised a sensitive FRET-based hormone biosensor (Rowe et al., 2022), nlsABACUS2 which displays an increased fluorescence emission ratio upon ABA binding. Seedlings expressing a nuclear localised nlsABACUS2 biosensor revealed dynamic changes in ABA distribution and levels during our agar-based

xerobranching bioassay (Figure 5.3, A to C). Spatially, nlsABACUS2 accumulates in epidermal cells in the basal meristem and elongation zones (Figure 5.3 B). Quantifying temporal emission ratio changes revealed that ABA levels initially increase in root epidermal tissues >12 hours after a xerobranching stimulus. Considering the sensitivity of the biosensor, these results are also consistent with our hydraulic simulations that predict the outward flux of phloem-derived water after ~8 hours of xerobranching stimulus (Figure 5.2). Once root tips re-connect with the agar (recovery phase), ABA levels fall rapidly in epidermal cells (Figure 5.3 C).

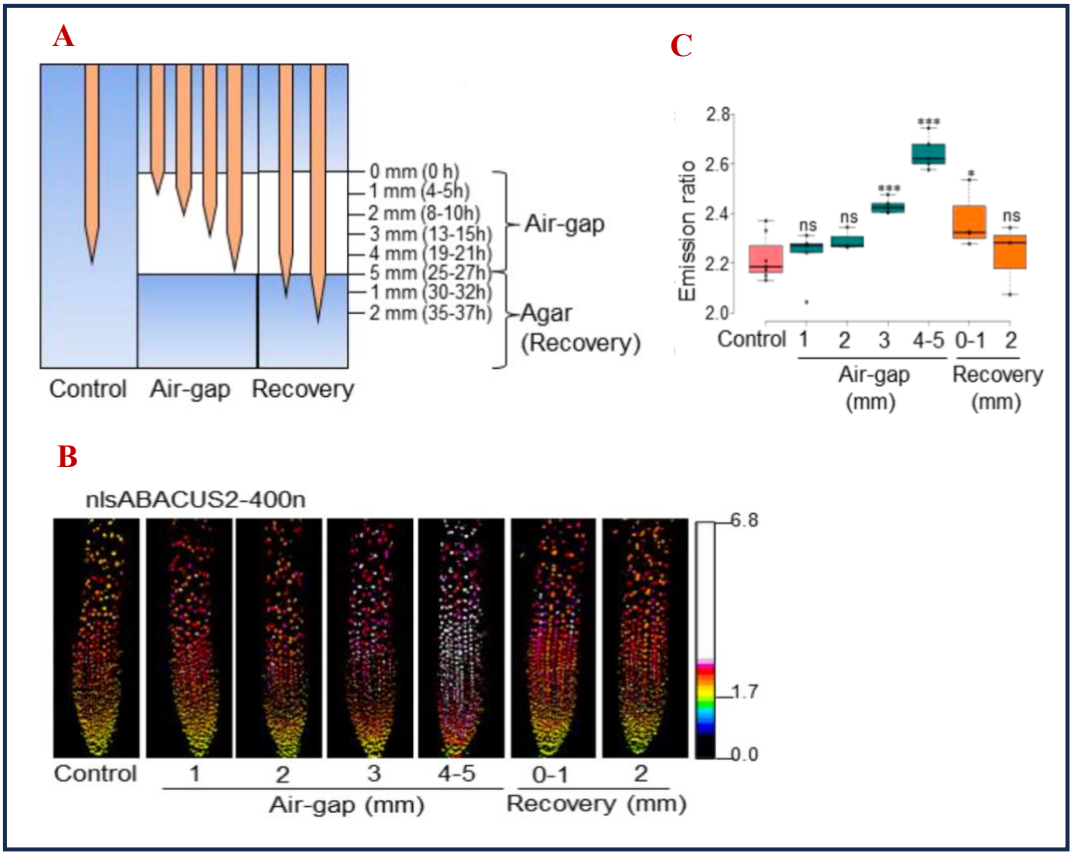


**Figure 5.3** Temporal response of reporters during xerobranching. (A) primary root tips were grown to different lengths in air-gap (0-5 mm) and recovery (up to 2 mm in moist agar) conditions. (B) Emission ratio images and (C) box-plots of nlsABACUS2-400n reveal dynamic changes in endogenous ABA levels as root tips grow across air-gap and after recovery. Colour scale represent emission ratios. *, *** and ns represent $P \leq 0.05$, $P \leq 0.001$ and non-significant changes, respectively (Mehra et al., 2022).

To directly visualise *whether* ABA moves radially outwards ("piggy-backing" the re-direction of water flux) following a xerobranching stimulus, we generated cross-sectional images of nlsABACUS2 root tip tissues (Figure 5.4) from three key zones. These zones included meristem and early elongation zone tissues (zone 1), mid to late elongation and early differentiation zone tissues (zone 2) and fully differentiated root tissues (zone 3). Radial images of these three zones (taken at different time points during the xerobranching response) revealed contrasting patterns of ABA redistribution. For example, an increase in ABA levels can initially be detected in inner root tissues that is later seen in outer tissues in zone 2 (compare nlsABACUS2 signals in 3mm versus 4mm root tip sections for zone 2 in (Figure 5.4) consistent with ABA movement from inner to outer root tissues. In contrast, radial cross sections through nlsABACUS2 zone 1 root tissues revealed an increase in ABA in outer (but not inner) tissues, suggesting this signal originates from phloem unloading in zone 2 and then undergoes redistribution via symplastic continuity. ABA accumulated much less in outer root tissues of zone 3 versus zones 1 and 2 following a xerobranching stimulus (Figure 5.4). The results are consistent with the phloem unloading patterns of solutes described earlier (Rowe et al., 2022) suggesting that zone 2 overlaps with the protophloem unloading zone where solutes are transferred laterally via symplastic continuity. In contrast, zone 3 is active in solute translocation through phloem but inactive in phloem unloading (Ross-Elliott et al. 2017) Another parallel study also reports similar expression patterns of nlsABACUS, when exogenously applied ABA unloads through phloem (Rowe et al., 2022). The pattern of elevated ABA in outer root tissues of zones 1 and 2 also coincides with the root tip region where new lateral root primordia initiate (termed the basal meristem or oscillatory zone) (De Smet et al., 2007). Elevated levels of ABA in zones 1 and 2 rapidly reduce once root tip tissues

contact a new moisture source during the recovery phase (Figure 5.4). Endogenous ABA levels in cotyledons of nlsABACUS2 plants did not change following a xerobranching stimulus, suggesting that ABA accumulation is locally confined to root tips exposed to air-gaps. Hence, during a xerobranching response, ABA accumulates in the root zone associated with the earliest stage of lateral root development.

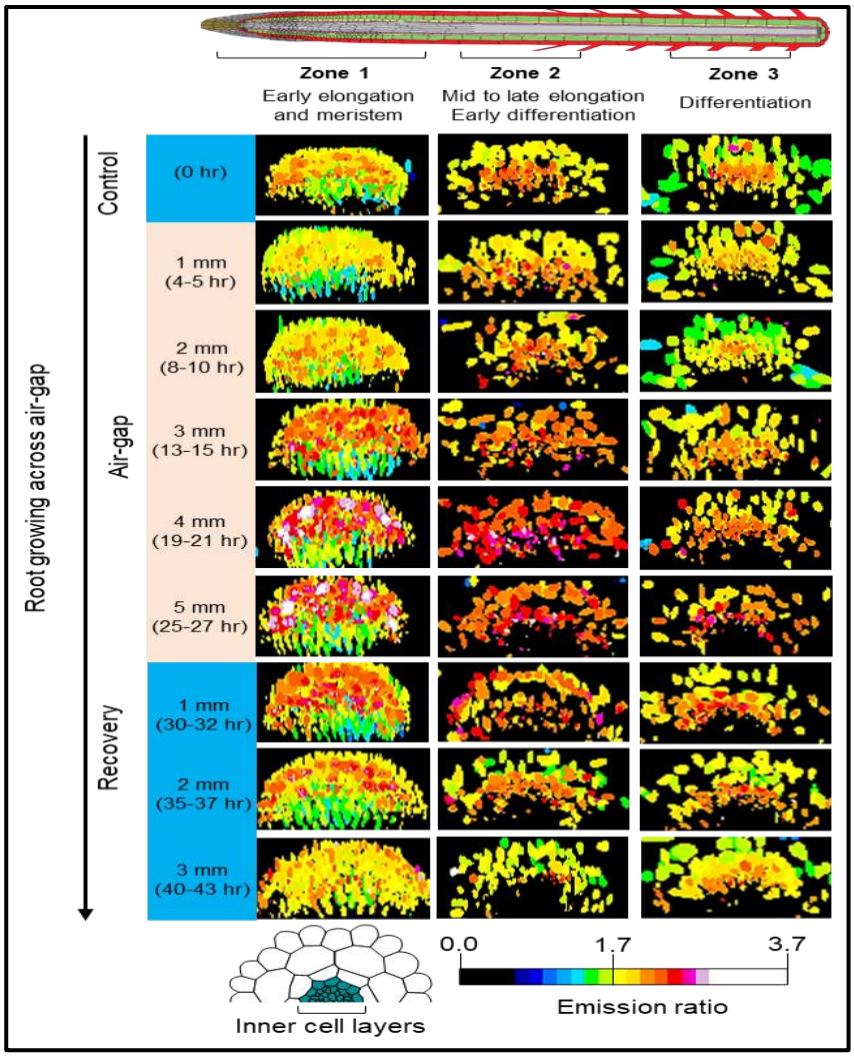


**Figure 5.4** ABA moves radially outwards following a xerobranching stimulus**.** Ratio images of nlsABACUS2-400n-expressing Arabidopsis roots growing across an air-gap reveal ABA spatiotemporal dispersion. The images are maximum projection ratio maps from many radial cross-sections. Roots were observed at various hours as they left moist agar (control), developed in a 5mm air-gap, and returned to agar (recovery). Root tip length (mm) on the vertical axis shows air-gap and recovery. Root zones 1 (early elongation and meristem), 2 (mid-to-late elongation/early differentiation), and 3 (differentiation) were cross-sectioned at each time point. After xerobranching stimulation, zone 2 phloem unloading enhances ABA in outer tissues but not interior tissues. Colour-coded FRET emission ratios. Ratios raise ABA levels. Each timepoint has four replicates (n=4).rations. The experiment has four replicates per timepoint per zone (n=4) (Mehra et al., 2022).

To test the function of the observed changes in ABA following a xerobranching stimulus, we examined the impact of mutations in key components of the ABA signalling machinery for this adaptive response. ABA insensitive mutants disrupting ABA receptors (*pyr/pyl*) and ABA-activated SnRK2 kinases (*snrk2.2/2.3*, *snrk2.2/2.3/2.6*) exhibited lateral root branching in a xerobranching bioassay (Figure 5.5 A), whilst ABA hypersensitive *pp2c* mutants failed to produce lateral roots in the air-gap. Detailed analysis with *snrk* triple/septuple/nonuple mutants as well as *snrk2.2* complementation lines revealed that *SnRK2.2* is required for xerobranching (Figure 5.5 D). Roots of a *snrk* nonuple mutant (lacking nine out of ten members of the SnRK2 family except SnRK2.2) behaved like WT in a xerobranching bioassay. Furthermore, a GFP-tagged SnRK2.2 reporter *pSnRK2.2: SnRK2.2-GFP* revealed that a xerobranching stimulus induced the fusion protein in the basal root meristem (Figure 5.5 B&C), which overlaps with the site of largest emission ratio changes of ABA biosensor nlsABACUS2 (Figure 5.3 B). Hence, SnRK2.2 regulates ABA (and in turn the xerobranching) response in *Arabidopsis* root tissues.

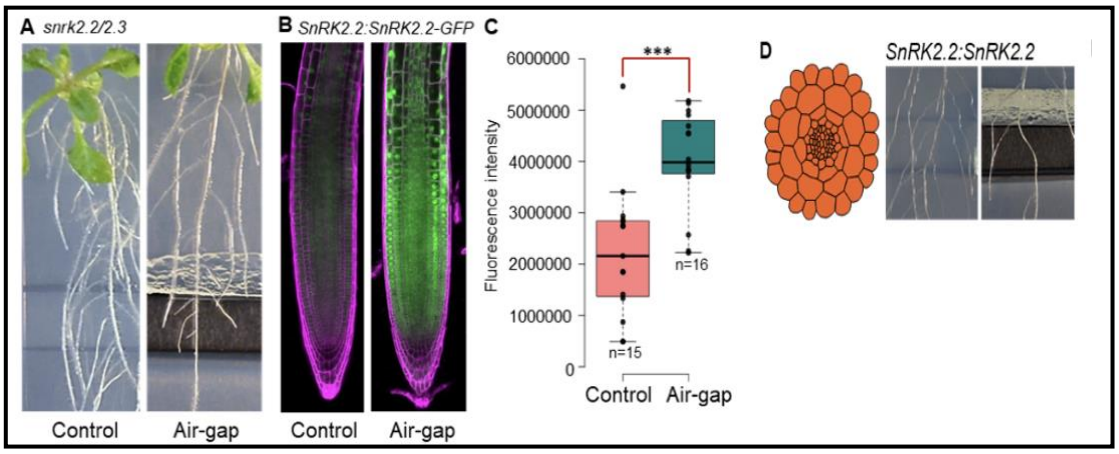


**Fig. 5.5** Xerobranching is dependent on ABA perception in *Arabidopsis* primary root transition zone tissues. (A) ABA signalling mutant *snrk2.2/2.3* disrupts xerobranching in AAA system. Air-gap ~ 5 mm. (B and C) Elevated response of *pSnRK2.2:SnRK2.2-GFP* in root tips subjected to air-gap vs control conditions. Scale bar = 100 µm.

## 5.3 Discussion

Our research shows that xerobranching occurs in both eudicot and monocot species and is an ABA-dependent root adaptation response to localised loss of contact with soil water. Additionally, Genetic and biosensor-based studies revealed that ABA moves from its inner root (phloem) source to outer root tissues during a xerobranching response (Figure 5. 1, Figure 5. 2 and Figure 5.3 B). However, it remains unclear which root tissue(s) ABA targets to repress lateral root development during a xerobranching response. To determine this, we attempted to rescue the xerobranching defect of the ABA response mutant *snrk2.2/2.3* by expressing the WT *SnRK2.2* sequence under a series of root tissue/zone specific promoters (Figure 5. 6, E to J). Expressing *SnRK2.2* in either root epidermal, cortical, endodermal, or basal meristem (but not lateral root cap) tissues rescued the *snrk2.2/2.3* xerobranching defect (Figure 5. 6, E to J). This result led us to ask, is there a common target important for xerobranching that the ABA signalling pathway regulates in each of these outer root tissues? ABA modulates hydraulic conductivity by inducing aquaporin expression to affect water movement out of the vasculature (Prado et al., 2013). To investigate possible roles of aquaporins in ABA-dependent repression of branching in air-gaps, we analysed a *pip* (Plasma membrane Intrinsic Proteins) quadruple mutant in our xerobranching bioassay system. However, analysis of *pip* mutant disrupting the most highly expressed *PIP* genes in roots did not show any significant difference compared to the WT control.

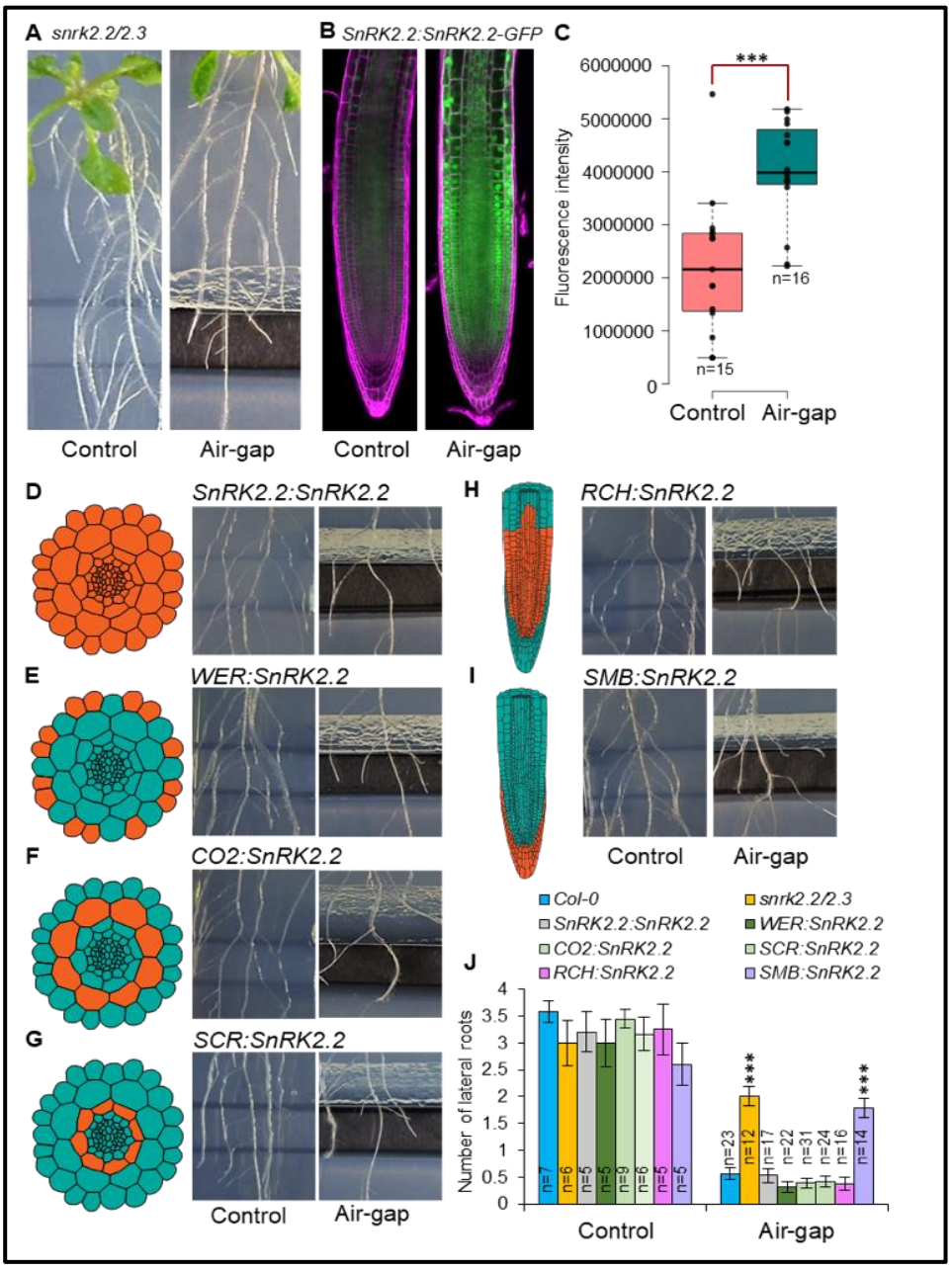


**Fig. 5.6** Arabidopsis primary root transition zone tissues perceive ABA for xerobranching. (A) ABA signalling mutant snrk2.2/2.3 impairs AAA system xerobranching. Air-gap ~5 mm. (B, C) Air-gap-exposed root tips showed increased pSnRK2.2:SnRK2.2-GFP response. 100 µm. (D) SnRK2.2's own promoter restores the xerobranching deficiency of snrk2.2/2.3. (E–G) Tissue-specific expression of SnRK2.2 in epidermis, cortex, and endodermis with WER, CO2, and SCR promoters complements snrk2.2/2.3. (H) Root zone-specific SnRK2.2 expression in root meristem/transition zone utilising RCH promoter restores snrk2.2/2.3 xerobranching deficiency. (I) SMB promoter-driven SnRK2.2 expression in columella and lateral root cap in snrk2.2/2.3 background. (J) Number of lateral roots produced by wild-type (Col-0), snrk2.2/2.3, and tissue/zone-specific rescue lines in the air-gap region compared to roots developed under control conditions. Root schematics show the tissue/zone of complementation promoter expression in orange. Student's t-test determined significant changes from control (C) or wild-type (J). *** indicates $P < 0.001$(Mehra et al., 2022).

ABA has been reported to trigger reversible closure of intercellular pores termed plasmodesmata (PD) (Benitez-Alfonso, 2019). Does ABA regulate the xerobranching response by gating plasmodesmata between root tissues? To address this, the symplastic fluorescent tracer carboxyfluorescein (CF; derived from CFDA, carboxy-fluorescein diacetate) was used to monitor whether plasmodesmata were open or closed in root tissues during a xerobranching response. Within plant cells, non-fluorescent CFDA is cleaved by cellular esterases to release membrane-impermeable fluorescent CF that travels exclusively through the plasmodesmata. Following CFDA application to cotyledons, we observed decreased protophloem unloading in *Arabidopsis* WT root tips exposed to a xerobranching stimulus. Delayed unloading was also observed in the root tips of a *pSUC2:GFP* line that expresses free GFP in phloem companion cells. Collectively, both lines of evidence reveal that root tips experience decreased plasmodesmata permeability following a xerobranching stimulus.

To assess the role of ABA in root PD gating during xerobranching, CFDA was locally applied to root tips. WT roots exhibited reduced intercellular fluxes of the tracer, indicating closed plasmodesmata following a xerobranching stimulus (Figure 5.7, A and B). In contrast, CFDA treatment of root tips of the ABA response mutant *snrk2.2/2.3* revealed that plasmodesmata remained open following a xerobranching stimulus. Plasmodesmata aperture is regulated by modifying the size of a callose 'ring' encircling each end of the inter-cellular pore. The callose stain aniline blue revealed higher callose deposition in basal meristem cells of WT roots compared to *snrk2.2/2.3*

following a xerobranching stimulus. Taken together, the evidence indicates that ABA regulates gating of plasmodesmata in key root tissues during a xerobranching response.

To determine the function of plasmodesmata gating during a xerobranching response, *Arabidopsis* mutants no longer able to gate their plasmodesmata were characterised. Plasmodesmata aperture is regulated through the action of enzymes including a family of Callose Synthases (CS) and associated regulatory proteins like plasmodesmata-located proteins (PDLPs) ( Xie et al., 2011). Mutating individual members of the *Arabidopsis* CS gene family resulted in nine of these lines exhibiting a xerobranching defect, including *CALS7* which is primarily associated with phloem sieve pores (Xie et al., 2011), as did mutating both *PDLP2* and *PDLP3* genes .Hence, blocking the ability to close plasmodesmata disrupts a root's ability to activate a xerobranching response.

How does ABA trigger plasmodesmata closure following a xerobranching stimulus? Transgenic lines expressing GFP reporters fused to either PDLP2 or PDLP3 proteins under their native promoters were upregulated in response to a xerobranching stimulus (Figure 5.7, C & D). In the case of PDLP3, its mRNA and *PDLP3:PDLP3-GFP* reporter were upregulated in root tip and specifically basal meristem cells during a xerobranching response, exhibiting a punctate pattern in apical, basal and side walls, consistent with its plasmodesmata regulatory function (Figure 5.5, C & D ).

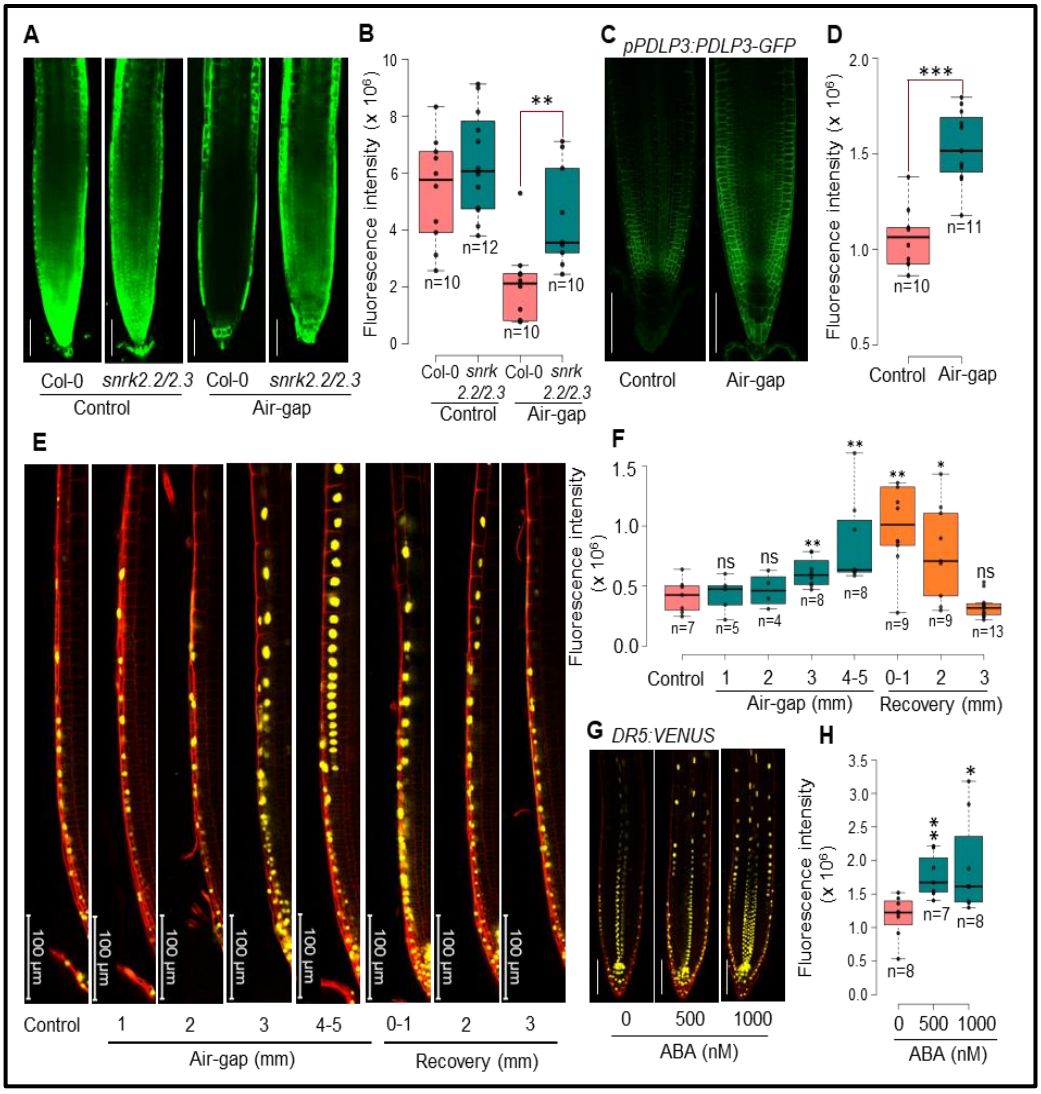


**Figure 5.7** ABA reduces PD permeability, preventing radial auxin flow and xerobranching. (A) Xerobranching stimulation slows CF (carboxyfluorescein) movement in wild-type Arabidopsis (Col-0) primary root tips. ABA signalling mutant snrk2.2/2.3 CF migration was unaffected by xerobranching. Before imaging, root tips received CFDA (carboxyfluorescein diacetate). (B) Air-gap-exposed wild-type and snrk2.2/2.3 root tip CF fluorescence intensity vs. control. Xerobranching induces pPDLP3:PDLP3-GFP. (D) Box-plots revealing that pPDLP3:PDLP3-GFP responds better in air-gap than control circumstances. (E, F) Auxin response reporter DR5:VENUS fluoresces more in air-gap-exposed root tip epidermis than control/recovery circumstances. (G, H) (G, H) ABA mimics DR5:VENUS xerobranching reaction. 100 µm. *, **, ***, and ns are non-significant (Student's t-test). (Mehra et al., 2022).

Unlike WT, *abi1-1* roots exhibit branching in air-gaps. However, ectopic expression of *PDLP1* (using *35S* rather than its native promoter) rescued the xerobranching defect of *abi1-1*. Hence, ABA triggers plasmodesmata closure following a xerobranching stimulus by upregulating expression of *PDLP*s. Additionally, GAL4-mediated transactivation of *abi1-1* in root ground tissues (cortex and endodermis) led to maximal disruption of xerobranching response as compared to induction of *abi1-1* in single root cell layers . Hence, ABA mediated PD closure in root ground tissues is essential for a xerobranching response.

ABA-mediated plasmodesmata gating disrupts root branching. Closing plasmodesmata during xerobranching prevents the inwards (symplastic) transport of auxin, which is essential to induce lateral root branching. Exposing DR5:VENUS auxin reporter roots to xerobranching increases auxin responsiveness in root basal meristem epidermal cells (Figure 5.7, E & F). The changed DR5:VENUS reporter pattern is consistent with xerobranching-induced PD closure in basal meristem epidermal cells preventing radially-inward auxin transport (Figure 5.7, E &F ). DII-VENUS showed greater auxin abundance in root tips during xerobranching. Exogenous ABA application to roots mimics xerobranching on DR5:VENUS and DII-VENUS (Figure 5.7, G & H). During xerobranching, ABA-mediated plasmodesmata gating limits radial auxin transport and lateral root induction. Switching down ABA signalling in the *abi1-1* mutant (which kept plasmodesmata open) inhibited any change in DII-VENUS auxin response following xerobranching. Suppression of lateral root initiation in roots exposed to xerobranching was visualised using the DR5:LUC reporter, which normally demarks groups of lateral root stem cells in the basal meristem (or oscillation zone) that go on to form new branches in control roots, but

were not detected in roots exposed to xerobranching. Therefore, xerobranching limits radially-inward auxin transport essential for lateral root induction.

AUX1/LAX, ABCB, and PIN auxin influx and efflux transporters were assumed to determine root auxin distribution (Petrášek and Friml, 2009). To assess the impact of xerobranching on carrier-mediated auxin transport, reporter lines for auxin influx (pAUX1:AUX1-YFP) or efflux (pPIN2:PIN2-GFP) carriers were analysed. No spatial changes were detected in AUX1-YFP or PIN2-GFP expression in the outermost root tissues following xerobranching, consistent with the observed elevated auxin response (Figure 5.7, E & F) being due to gating of hormone movement through plasmodesmata rather than modulation of apoplastic auxin transport. Ectopic expression of AUX1 or PIN2 in every elongation zone tissue led to a synthetic radial apoplastic auxin route, bypassing plasmodesmata-mediated inhibition of symplastic auxin flow and leading to lateral root branching in air-gaps.

ABA-mediated plasmodesmata gating of radial symplastic auxin flow regulates xerobranching. Roots co-mobilize water and hormones via plasmodesmata to 'sense' water availability. Water, ABA, and auxin co-mobilize through aquaporins, ABCG, and PINs. Because plasmodesmata are non-selective big inter-cellular pores, radial hydraulic fluxes co-mobilize hormones inwards (like auxin) or outwards (like ABA) whether water is available or not. When co-mobilized via plasmodesmata with water, auxin and ABA are "hydro signals."

Additionally, we detail the molecular and cellular mechanisms by which plant roots inhibit lateral root growth in response to a xerobranching stimulus (see schematic in

Figure 5.6). With the right amount of moisture present, roots co-transport auxin and water inward between root basal meristem tissues via plasmodesmata, generating a symplastic pathway for the radial mobilisation of this crucial hormone signal via hydraulic fluxes from epidermal to pericycle cells. However, the root tips combine the outward radial flow of water from the phloem with the movement of the hormone ABA (Wiegers et al., 2009) when the external source of water is temporarily missing, allowing the roots to continue growing. This essential indicator of water stress decreases the size of plasmodesmata, preventing auxin from reaching the stem cells' of the lateral roots via their radial transport. When an external water source is reinstated (during the reset/recovery phase), the concentration of ABA in the root's outer tissues drops rapidly (within three hours), allowing plasmodesmata to open and symplastic auxin transport to resume. When a plant's roots are re-established in a watering system, the amount and distribution of these signals in the root tip tissues return to their pre-xerobranching stimulus levels. Hydrosignalling refers to the dynamic regulatory events that allow plant roots to calibrate spatial root branching responses in heterogeneous soil conditions, which are more common than not.

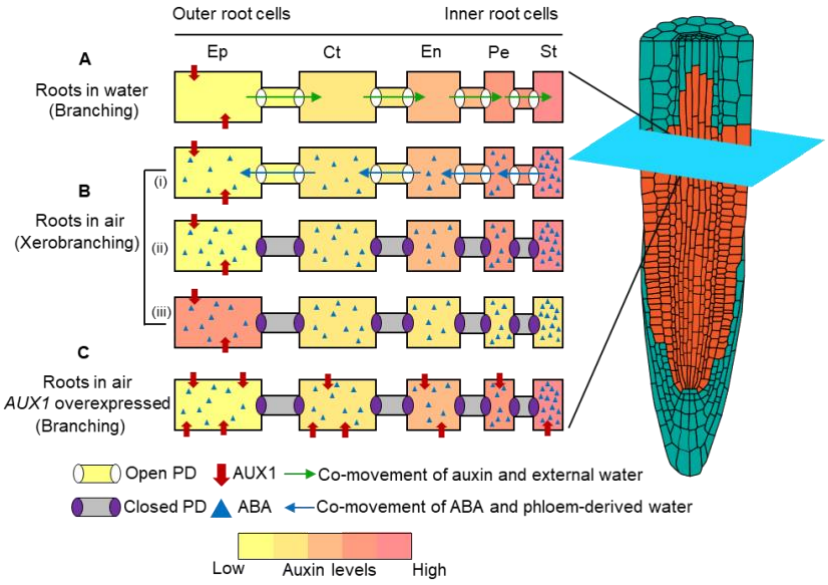


**Figure 5.8** Hormone redistribution controls xerobranching**.** Root basal meristem, auxin, ABA, and water flow diagrams. (A) Under normal moisture conditions, roots co-transport water and auxin radially inwards via plasmodesmata (PD) to pericycle (Pe) cells, which drive lateral root initiation. (B) Xerobranching stimulus increases ABA in inner root tissues (St; stele) preventing root branching. In the absence of external water, plasmodesmata (i) co-mobilize ABA from inner (St; stele) to outer root cells (Ep; epidermis) via phloem-derived water. PDLPs and Cals shut plasmodesmata, preventing pericycle symplastic radial auxin transport (iii). (C) Ectopic auxin carriers like AUX1 in all elongation zone tissue create a synthetic radial apoplastic auxin channel that bypasses disrupted symplastic auxin flow, inducing air-gap root branching. Epidermis, cortex, endodermis, pericycle, and stele (Mehra et al., 2022)

# 6 CHAPTER 6: GENERAL DISCUSSION

## 6.1 A WORLD DEPENDENT ON WATER

Climate change is modifying global precipitation and temperature patterns, causing biological and agricultural systems to move, transform, or fail (Chen and Gong, 2021). Desertification (Huang et al., 2020) and salinization (Harper et al., 2021) are predicted to rise in the future, further endangering crop productivity, food security, and plant biodiversity. Drought, salinity, heat, cold, and flooding represent abiotic stresses that are having a major impact on plant development and survival (Boursiac et al., 2022).

Land plants have evolved root adaptive responses which facilitate water exploration by sensing soil moisture availability, then modifying traits such as the orientation and velocity of primary root growth, as well as the frequency and patterning of root branching (Klein et al., 2020; Maurel & Nacry, 2020). Exploiting such plant root traits conferring resilience to water stress provides a novel way to close the yield gap (Raza et al., 2019), but requires new knowledge about these adaptive processes and their underlying molecular mechanisms.

This PhD thesis addresses the molecular mechanisms underpinning two water stress adaptive root responses, namely hydrotropism (Chapter 3 & 4) and xerobranching (Chapter 5; Mehra et al, 2022). Hydrotropism orients root growth towards the best available soil moisture source (Moriwaki et al., 2013; Dietrich, 2018). In contrast, the xerobranching response prevents the initiation of lateral roots when roots lose contact with moist soil (Orman-Ligeza et al., 2018). Despite their obvious developmental differences, this thesis studies have demonstrated both root adaptive responses are

regulated by the same abiotic stress hormone, ABA (Chapter 3 & 5; Mehra et al, 2022). This observation raises important questions about whether ABA regulates both root water stress adaptive responses using identical, related or distinct molecular mechanisms and/or components? My thesis studies have focused on revealing how ABA is transported during each of these root adaptive responses.

## 6.2 HAS ABA TRANSPORTED APOPLASTICALLY DURING A ROOT HYDROTROPIC RESPONSE?

ABA is a key signal that regulates hydrotropic bending of *Arabidopsis* roots (Dietrich et al., 2017; Takahashi et al., 2002). ABA signalling mutants have been shown to disrupt root hydrotropism and are required to function in the cortex (Dietrich et al., 2017; see Figure 6.1). ABA biosynthesis is also essential for hydrotropism (Takahashi et al., 2002). In root tissues, ABA biosynthesis takes place in phloem companion cells (PCC; see Figure 6.1). Hence, ABA is required to be mobilized from PCC to cortex tissues during a hydrotropic response.

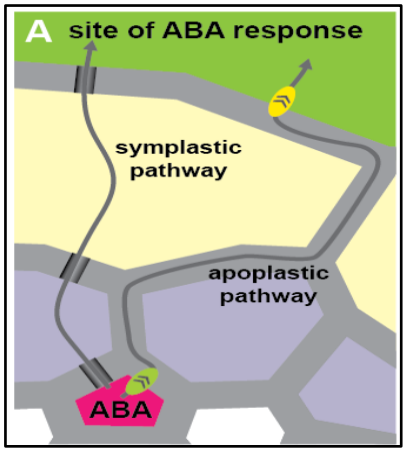


**Figure 6.1** Hydrotropism and ABA transport. In the early elongation zone (which does not contain a Casparian strip) ABA can move from its phloem companion cell source (PCC; denoted in pink) to surrounding cells either symplistically or apoplectically. Apoplastic ABA movement implies the activity of an efflux transporter in PCC source tissue and an influx transporter in the responding tissue (cortex, denoted in green). Pericycle and endodermal tissue layers are denoted in mauve and yellow. Plasmodesmata pores are shown in black, with ABA efflux and influx carriers in green and yellow (Dietrich et al.,2017).

During a root hydrotropic response, ABA must move from its PCC source to target cortex cells either symplastically (via inter-cellular pores termed plasmodesmata) or apoplastically (via specialised influx and efflux carriers) (see Figure. .1). To address this question, an amiRNA transportome library was screened in this study to discover novel genes and their transporters that regulate ABA mobilisation in *Arabidopsis* roots (Chapter 3). ABA transporters were identified such as ATP binding cassette family (ABCG). This includes the *ABCG13* transporter which is highly expressed in flowers, predominantly in petals and carpels (Panikashvili et al., 2011). Other groups have identified ABCG genes that encode ABA transporters; these include (Kuromori et al., 2018) who identified *ABCG25* as a vascular ABA exporter, and *ABCG40* as a guard cell ABA importer, which likely functions as proposed in Fig. 6.1, but within leaf tissues. In addition, a MATE transporter family member termed *dtx1* was identified which had a strong root hydrotropic defective phenotype. A related member of the same MATE family, *DTX 50*, is reported to be an ABA efflux transporter (Léran et al., 2020). Hydrotropic mutant screens also identified GTR1 which encodes a glucosinolate influx transporter that belongs to the Nitrate Peptide Transporter Family (NPF) (Nour-Eldin et al., 2012). Several NPF genes in Arabidopsis have been identified as hormone transporters (for example, AIT3 encodes an ABA influx transporter) (Léran et al., 2014).

The amiRNA based transportome screen identified a number of promising influx and efflux carriers that regulate hydrotropism. However, functionally demonstrating that these genes regulate (either directly or indirectly) ABA transport *in planta* is challenging. The development of highly sensitive hormone biosensors such as ABACUS2 (Rowe et al, 2022) that are capable of detecting changes in physiologically

relevant levels of ABA in roots, provides the tools required to probe whether the genes identified in this genetic screen do indeed regulate ABA transport. Preliminary ABACUS2 studies suggest that *GTR1* does not regulate hydrotropism by transporting ABA but could instead mobilise another regulatory signal (Chapter 4).

As GTR1 primarily transports glucosinolates, it is possible GLSs act as novel water stress signals. Intriguingly, *Arabidopsis* mutants lacking aliphatic GLSs (*myb28myb29*) also exhibit significant reduction in root hydraulic conductivity and aquaporin water channel abundance under salt stress (Martínez-Ballesta et al., 2015). This suggests that GLSs are important for maintaining plants' water balance or osmotic adjustments. Therefore, it would be interesting to explore how GSLs regulate aquaporins to determine root tropic responses. However, GLSs predominantly occur in *Brassicales* (Fahey et al., 2001). Few GLSs have been reported in non-cruciferous dicotyledonous angiosperms (Rodman et al.,1996). This further begs the question about the functional conservation of GTR1-mediated water sensing mechanisms across a broader range of plant species. It would be fascinating to understand whether dicotyledonous angiosperms acquired a selective advantage in adapting to water stress through GSLs or GTR1 dependent molecular pathways? Overall, the present study (Chapter 4) reveals novel roles of GTR1 in water sensing and raises several interesting questions to investigate in future. Further studies using ABACUS2 are also required on other transporters identified in genetic screened in Chapter 3 to determine whether they function as ABA influx or efflux carriers during the root hydrotropic response.

## 6.3 IS ABA MOBILISED SYMPLASTICALLY DURING A XEROBRANCHING RESPONSE?

These PhD studies have revealed that ABA is a key regulator of the root adaptive response Xerobranching (Chapter 5; Mehra et al, 2022). This represents an ABA-dependent root adaptive response to loss of contact with moist soil, that is conserved in eudicot and monocot species, which inhibits lateral root development after a xerobranching stimulus. ABA functions as a phloem-derived stress hormone disrupting intercellular communication between inner and outer cell layers via plasmodesmata. The closure of these intercellular pores prevents lateral root branching by impeding the inward passage of the hormone signal auxin (summarized in Figure 6.2; Mehra et al., 2022).

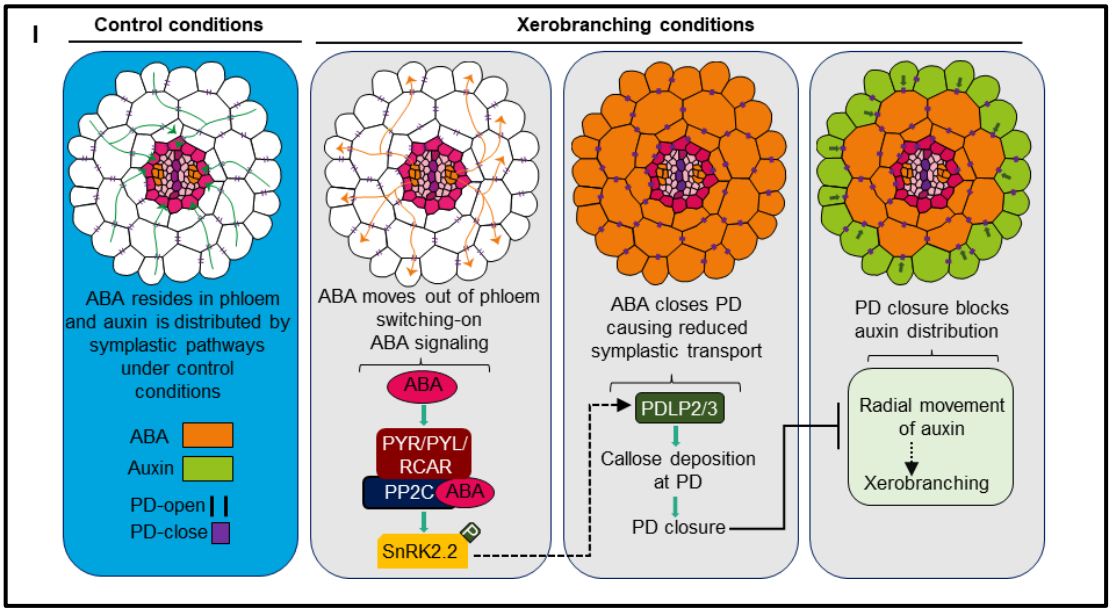


**Fig. 6.2** ABA and auxin transport regulation controls Xerobranching. Model showing proposed molecular mechanisms underlying xerobranching. Xerobranching stimulus induces ABA movement out of phloem tissues towards the root epidermis triggering ABA signalling through key components including SnRK2.2. ABA signalling reduces PD permeability via PDLP-mediated callose deposition, which impedes symplastic auxin flow from the epidermis towards the stele (Mehra et al., 2022).

Under normal moisture circumstances, roots co-transport auxin and water inwards between root transition zone tissues via plasmodesmata, enabling a symplastic mechanism to radially deploy this key hormone signal with hydraulic fluxes from epidermal to pericycle cells, where auxin triggers lateral root initiation. When the external source of water is temporarily missing, root tips rely on internal (phloem) water to continue growing and couple radial outflow with abiotic stress signal ABA. This water stress signal acts by reducing plasmodesmata aperture, preventing symplastic in-flow of the branching signal auxin to activate lateral root stem cells, when reconnected to an external water source, the abundance and distribution of these important signals rapidly re-set in root tip tissues to pre-xerobranching stimulus levels.

## 6.4 COMPARING AND CONTRASTING HYDROTROPIC AND XEROBRANCHING RESPONSES.

The dynamic regulatory events taking place during Xerobranching (Figure 6.2) that couple changes in hydraulic fluxes, between inner and outer tissues with hormone redistribution, allow plant roots to calibrate root branching responses in heterogeneous soil conditions. Whilst it is tempting to extrapolate this hydraulic mechanism to other ABA-regulated water stress responses, it remains unclear whether a similar cascade of ABA-related events takes place during a root hydrotropic response. Initial ABACUS2 based hydrotropic experiments reveal a rapid mobilization of ABA to outer root tissues in the transition zone, similar to xerobranching. However, the ABACUS2 biosensor reveals ABA remobilization takes place within an hour after a hydrotropic stimulus (Chapter 4). An equivalent level of ABA re-mobilization takes over 10 hours after a Xerobranching stimulus (Chapter 5; Mehra et al, 2022).

Mutant studies have revealed that hydrotropism and xerobranching share a number of common signaling components that mediate these ABA-dependent root adaptive responses. In addition to confirming the importance of core components of the ABA synthesis and signaling machinery (Chapter 5), this thesis studies have also revealed that GTR1/ AtNPF2.10 is required for both root adaptive responses (Chapter 4). Given GTR1 primarily transports glucosinolates, it is possible GLSs act as novel water stress signals (hydro-signal) during both adaptive responses. Further studies are required to explore this question in *Arabidopsis* and a wider range of plant species.

In the future, climate change is very likely to increase water shortage (Ahuja et al. 2010; Sykes et al. 2005), which means that water distribution in soils is likely to become substantially more uneven than it already is. These results provide information that may also present an important opportunity to increase our knowledge of ABA transporters and ABA regulation in hydrotropism and xerobranching which may be of benefit for the improvement of other plants technology, productivity and in the conservation of crop genetics research. Likewise, the generation of GTR1 constructs is unique to individual cell types, the appropriate pDONOR clones will be combined and integrated into final vectors, will allow for the generation of transgenic strains of Arabidopsis. It would be interesting to investigate the effect of cytokinin signalling on xerobranching. Also, many of AmiRNA lines can be a good target for future studies in water stress and other stress. Future crop climate resistance could be enhanced by understanding the molecular and cellular mechanisms by which roots acclimatise under these conditions.

# 7 APPENDIC

My contribution in (Hydraulic flux – responsive hormone redistribution determines root branching) was as investigator.



PLANT SCIENCE

## Hydraulic flux–responsive hormone redistribution determines root branching

Poonam Mehra[1]*, Bipin K. Pandey[1], Dalia Melebari[1], Jason Banda[1], Nicola Leftley[1], Valentin Couvreur[2], James Rowe[3], Moran Anfang[4], Hugues De Gernier[5,6], Emily Morris[1]†, Craig J. Sturrock[1], Sacha J. Mooney[1], Ranjan Swarup[1], Christine Faulkner[7], Tom Beeckman[5,6], Rishikesh P. Bhalerao[8], Eilon Shani[4], Alexander M. Jones[3], Ian C. Dodd[9], Robert E. Sharp[10], Ari Sadanandom[11], Xavier Draye[2], Malcolm J. Bennett[1]*

Plant roots exhibit plasticity in their branching patterns to forage efficiently for heterogeneously distributed resources, such as soil water. The xerobranching response represses lateral root formation when roots lose contact with water. Here, we show that xerobranching is regulated by radial movement of the phloem-derived hormone abscisic acid, which disrupts intercellular communication between inner and outer cell layers through plasmodesmata. Closure of these intercellular pores disrupts the inward movement of the hormone signal auxin, blocking lateral root branching. Once root tips regain contact with moisture, the abscisic acid response rapidly attenuates. Our study reveals how roots adapt their branching pattern to heterogeneous soil water conditions by linking changes in hydraulic flux with dynamic hormone redistribution.

Root branching determines foraging capacity of crop plants (*1*, *2*). Roots have evolved plasticity in their branching patterns to maximize access to soil water resources, which are often distributed heterogeneously (*3*, *4*). Root branching is affected both by extreme weather (such as drought or flooding) (*5*, *6*) and by transient or local spatial differences in soil moisture (*7*, *8*). Negative effects of water scarcity on modern agriculture will be exacerbated as climate change affects hydrological cycles and soil water resources (*9*, *10*). Increased resilience in the face of climate change will require better insight into how plant roots sense and adapt to fluctuating water availability.

### Dissecting roots' water sensing using xerobranching

Xerobranching (*7*) provides an experimental model to study root adaptive responses to transient water stress. A xerobranching response is triggered when growing root tips temporarily lose contact with moist soil (e.g., in an air gap), which causes branching to temporarily cease until roots reenter moist soil (Fig. 1A). To discover the mechanistic basis of xerobranching, an agar-based xerobranching bioassay was developed (fig. S1) that phenocopies the original x-ray computed tomography (CT) soil-based bioassay (Fig. 1A) in experiments with *Arabidopsis* and tomato seedlings. As levels of the abiotic stress signal abscisic acid (ABA) increase in root tips during transient water stress (*7*), we tested whether tomato ABA biosynthesis mutants (*flacca* and *notabilis*) (*11*, *12*) are disrupted in xerobranching response. Both soil- and agar-based bioassays revealed that, unlike wild-type (WT) controls, primary roots of both *flacca* and *notabilis* continue to branch when growing across an air gap (Fig. 1, A to D, and fig. S2). Similarly, the ABA-deficient maize mutant *vp14* (*13*) disrupted xerobranching in both paper-based and soil-based bioassays (figs. S3 and S4). Hence, ABA is a widely conserved regulator that represses lateral root development during a xerobranching response in these monocot and eudicot plant models.

From which tissue(s) does ABA originate to trigger a xerobranching response? ABA biosynthesis genes, such as *ABA2*, are expressed in phloem-related root vascular tissues (*14*). *Arabidopsis aba2-1* mutant roots exhibit a xerobranching defect, which can be rescued by expressing WT *ABA2* using the phloem companion cell–expressed *SUC2* promoter (Fig. 1, E to G, and fig. S5A). A *SUC2:YFP-ABA2* translation fusion confirmed that the ABA2 protein can act in a phloem companion cell–autonomous manner (fig. S5B). Phloem provides water for growing roots in the temporary absence of an external supply (*15*). Hydraulic modeling (*16*, *17*) predicts that radial water fluxes within root tissues change direction from predominately inward to outward after a xerobranching stimulus (Fig. 1H). Simulations reveal that an inward water flux dominates under normal externally hydrated conditions, and phloem-derived water is limited to close to companion cells (Fig. 1H). However, after a xerobranching stimulus (when the external water source is temporarily lost), root-tip tissues rely on an outward flux of phloem-derived water to maintain growth, requiring ~8 hours for outer root tissues to receive phloem water (Fig. 1H). Phloem-derived ABA is likely to travel with this outward flow of water during a xerobranching response.

### ABA moves outward after a xerobranching stimulus

To visualize whether, when, and where ABA movement occurs after a xerobranching stimulus, we used a sensitive Förster resonance energy transfer (FRET)–based hormone biosensor (*18*), nlsABACUS2, which displays increased fluorescence emission ratio upon ABA binding (fig. S6). Seedlings expressing a nuclear-localized nlsABACUS2 biosensor revealed dynamic changes in ABA distribution and levels during our agar-based xerobranching bioassay (Fig. 1, I to K, and figs. S7 and S8). Spatially, nlsABACUS2 accumulates in epidermal cells in the basal meristem and elongation zones (Fig. 1J). Quantifying temporal changes in emission ratios revealed that ABA levels initially increase in root epidermal tissues >12 hours after a xerobranching stimulus. Considering the sensitivity of the biosensor, these results are also consistent with our hydraulic simulations that predict the outward flux of phloem-derived water after ~8 hours of xerobranching stimulus (Fig. 1H). Once root tips reconnect with the agar (recovery phase), ABA levels fall rapidly in epidermal cells (Fig. 1, J and K, and fig. S8).

To directly visualize whether ABA moves radially outward ("piggy-backing" the redirection of water flux) after a xerobranching stimulus, we generated cross-sectional images of nlsABACUS2 root-tip tissues (Fig. 2) from three key zones. These zones included meristem and early elongation zone tissues (zone 1), mid- to late elongation and early differentiation zone tissues (zone 2), and fully differentiated root tissues (zone 3). Radial images of these three zones (taken at different time points during the xerobranching response) revealed contrasting patterns of ABA redistribution. For example, an increase in ABA levels can initially be detected in inner root tissues that is later seen in outer tissues in zone 2 (compare nlsABACUS2 signals in 3- versus 4-mm root-tip sections for zone 2 in Fig. 2), consistent with ABA movement from inner to outer root tissues. By contrast, radial cross sections through nlsABACUS2 zone 1 root tissues revealed an increase in ABA in outer (but not inner) tissues, which suggests that this signal originates from

[1]Plant and Crop Sciences, School of Biosciences, University of Nottingham, Nottingham, UK. [2]Earth and Life Institute, Université catholique de Louvain, 1348 Louvain-la-Neuve, Belgium. [3]Sainsbury Laboratory, University of Cambridge, Cambridge, UK. [4]School of Plant Sciences and Food Security, Tel Aviv University, Tel Aviv, Israel. [5]Department of Plant Biotechnology and Bioinformatics, Ghent University, 9052 Ghent, Belgium. [6]Center for Plant Systems Biology, VIB-UGent, 9052 Ghent, Belgium. [7]Crop Genetics, John Innes Centre, Norwich Research Park, Norwich, UK. [8]Umeå Plant Science Centre, Department of Forest Genetics and Plant Physiology, Swedish University of Agricultural Sciences, SE-901 87 Umeå, Sweden. [9]Lancaster Environment Centre, Lancaster University, Lancaster, UK. [10]Division of Plant Science and Technology, University of Missouri, Columbia, MO, USA. [11]Department of Biosciences, University of Durham, Durham, UK.
*Corresponding author. Email: p.mehra@nottingham.ac.uk (P.M.); malcolm.bennett@nottingham.ac.uk (M.J.B.)
†Present address: Oxford University Innovation, Oxford, UK.

phloem unloading in zone 2 and then undergoes redistribution through symplastic continuity. ABA accumulated much less in outer root tissues of zone 3 versus zones 1 and 2 after a xerobranching stimulus (Fig. 2). The results are consistent with the phloem unloading patterns of solutes described earlier (*19*), which suggests that zone 2 overlaps with the protophloem unloading zone, where solutes are transferred laterally through symplastic continuity. By contrast, zone 3 is active in solute translocation through phloem but inactive in phloem unloading (*19*). Another parallel study also reports similar expression patterns of nlsABACUS when exogenously applied ABA unloads through phloem (*18*). The pattern of elevated ABA in outer root tissues of zones 1 and 2 also coincides with the root-tip region, where new lateral root primordia initiate (termed the basal meristem or oscillatory zone) (*20*, *21*). Elevated levels of ABA in zones 1 and 2 rapidly decrease once root-tip tissues contact a new moisture source during the recovery phase (Fig. 2). Endogenous ABA levels in cotyledons of nlsABACUS2 plants did not change after a xerobranching stimulus, which suggests that ABA accumulation is locally confined to root tips that are exposed to air gaps (figs. S7 to S9). Hence, during a xerobranching response, ABA accumulates in the root zone that is associated with the earliest stage of lateral root development.

To test the function of the observed changes in ABA after a xerobranching stimulus, we examined the impact of mutations in key components of the ABA signaling machinery for this adaptive response. ABA-insensitive mutants disrupting ABA receptors (*pyr/pyl*) and ABA-activated SnRK2 kinases (*snrk2.2/2.3*, *snrk2.2/2.3/2.6*) exhibited lateral root branching in our xerobranching bioassay (Fig. 3A and figs. S10 and S11), whereas ABA-hypersensitive *pp2c* mutants failed to produce lateral roots in the air gap (fig. S12). Detailed analysis with *snrk* triple, septuple, and nonuple mutants as well as *snrk2.2* complementation lines revealed that *SnRK2.2* is required for xerobranching (Fig. 3D and fig. S11). Roots of a *snrk* nonuple mutant (which lacked 9 of 10 members of the SnRK2 family except SnRK2.2) behaved like WT in our xerobranching bioassay (fig. S11). Furthermore, a green fluorescent protein (GFP)–tagged SnRK2.2 reporter *pSnRK2.2:SnRK2.2-GFP* revealed that a xerobranching stimulus induced the fusion protein in the basal root meristem (Fig. 3, B and C, and fig. S13), which overlaps with the site of largest emission ratio changes of the ABA biosensor nlsABACUS2 (Fig. 1J). Hence, SnRK2.2 regulates ABA (and in turn, the xerobranching) response in *Arabidopsis* root tissues.

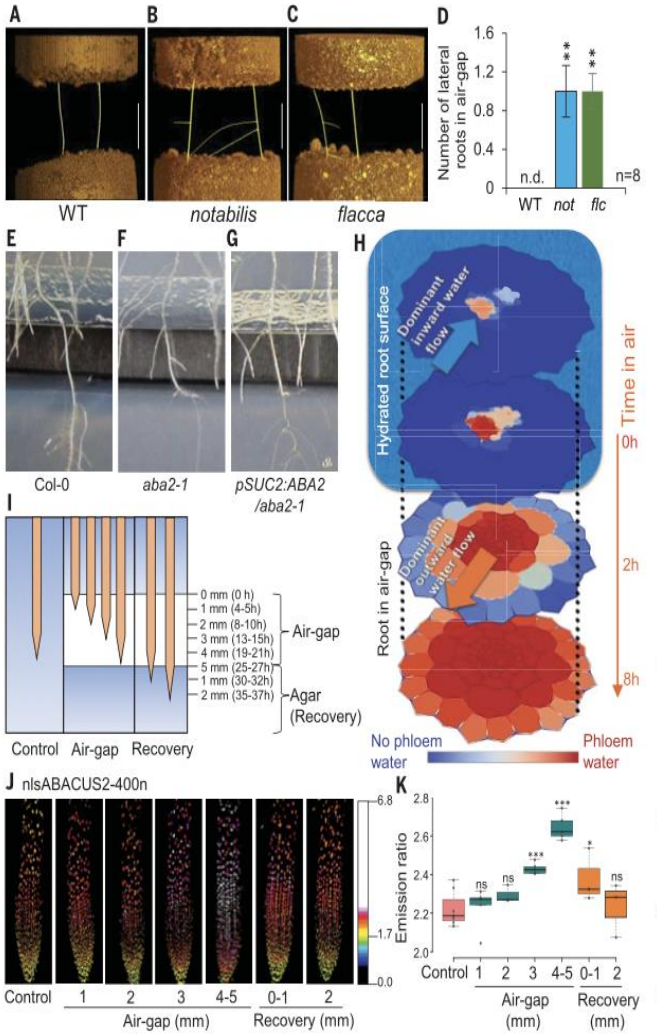


**Fig. 1. ABA functions as a repressive signal during xerobranching response.** (**A** to **D**) Representative CT images [(A) to (C)] and a bar graph (D) showing xerobranching defect in ABA-deficient tomato mutants (*notabilis* and *flacca*) versus WT (Ailsa Craig). Air gap, ~1.5 cm. Scale bar, 1 cm. n.d., not detected. (**E**) Agar-based air-gap assay system showing xerobranching response in *Arabidopsis* WT (Col-0) (air gap, ~5 mm). (**F**) *Arabidopsis* ABA biosynthetic mutant *aba2* produces lateral roots in air gap. (**G**) Expression of *ABA2* in phloem companion cells rescues xerobranching defect of *aba2*. (**H**) The MECHA hydraulic model predicts phloem as the main source of water in *Arabidopsis* root elongation zone only when located in an air gap. Simulated water advection maps show dominating phloem water in root epidermal cells within 8 hours. (**I**) For studying temporal response of reporters during xerobranching, primary root tips were grown to different lengths in air-gap (0 to 5 mm) and recovery (up to 2 mm in moist agar) conditions. (**J** and **K**) Emission ratio images (J) and box plots (K) of nlsABACUS2-400n reveal dynamic changes in endogenous ABA levels as root tips grow across air gap and after recovery. Color scale represents emission ratios. *$P \leq 0.05$; ***$P \leq 0.001$; ns, nonsignificant changes.

### ABA regulates xerobranching by closing plasmodesmata

Genetic and biosensor-based studies revealed that ABA moves from its inner root (phloem) source to outer root tissues during a xerobranching response (Fig. 1, E to H and J; Fig. 2; and Fig. 3B). However, it remains unclear which root tissue(s) ABA targets to repress lateral root development during a xerobranching response. To determine this, we attempted to rescue the xerobranching defect of the ABA response mutant *snrk2.2/2.3* by expressing the WT *SnRK2.2* sequence under a series of root-tissue and/or zone-specific promoters (Fig. 3,

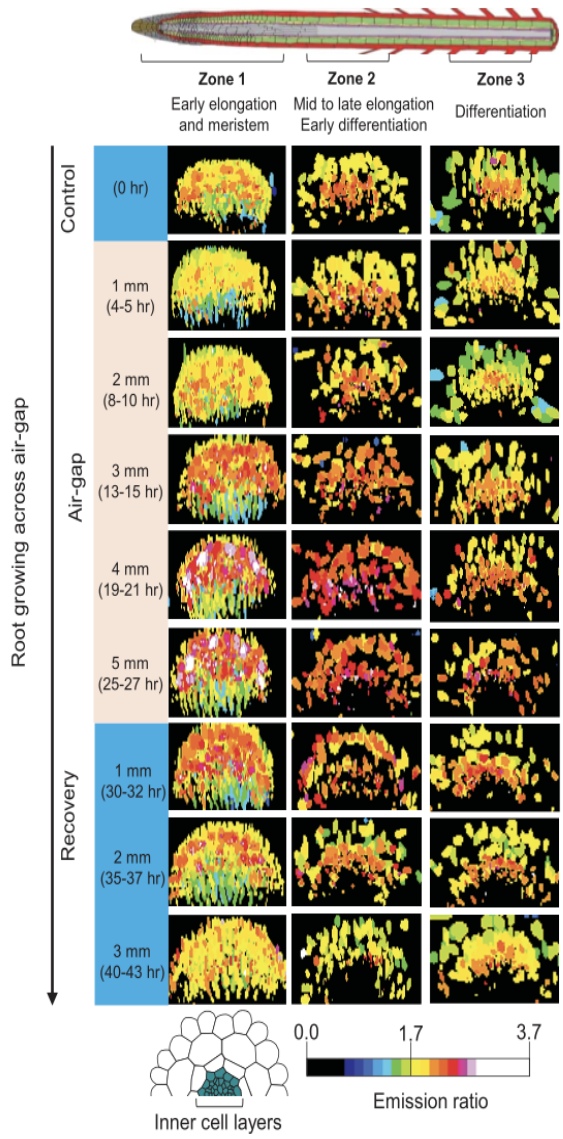


**Fig. 2. ABA moves radially outward after a xerobranching stimulus.** Ratio images of *Arabidopsis* roots expressing nlsABACUS2-400n reveal spatiotemporal distribution of ABA as the roots grow across an air gap. Each image is a representative maximum projection ratio map generated from a stack of several radial cross sections. Roots were imaged at different time points (indicated with hours) as they exit moist agar (control), grow in a 5-mm air gap, and reconnect with agar (recovery). Length (in millimeters) on the vertical axis indicates the length of root tips in air-gap and recovery conditions. For each time point, cross sections were generated from different zones of roots marked as zone 1 (early elongation and meristem), zone 2 (mid- to late elongation and early differentiation), and zone 3 (differentiation). Radial cross sections from zone 1 (compare cross sections from 1 to 5 mm) reveal an increase in ABA in outer (but not inner) tissues, which appears to originate from phloem unloading in zone 2 after a xerobranching stimulus. Color scale represents FRET emission ratios. Higher ratios correspond to higher ABA concentrations. Experiment was performed with at least four replicates per time point per zone ($n$ = 4).

E to J). Expressing *SnRK2.2* in either root epidermal, cortical, endodermal, or basal meristem (but not lateral root cap) tissues rescued the *snrk2.2/2.3* xerobranching defect (Fig. 3, E to J). This result led us to ask, is there a common target important for xerobranching that the ABA signaling pathway regulates in each of these outer root tissues? ABA modulates hydraulic conductivity by inducing aquaporin expression to affect water movement out of the vasculature (*22*). To investigate possible roles of aquaporins in ABA-dependent repression of branching in air gaps, we analyzed a *pip* (plasma membrane intrinsic proteins) quadruple mutant in our xerobranching bioassay system. However, analysis of the *pip* mutant disrupting the most highly expressed *PIP* genes in roots did not show any significant difference compared with the WT control (fig. S14).

ABA has been reported to trigger reversible closure of intercellular pores, termed plasmodesmata (PD) (*23*). Does ABA regulate the xerobranching response by gating PD between root tissues? To address this, the symplastic fluorescent tracer carboxyfluorescein (CF) [derived from carboxyfluorescein diacetate (CFDA)] was used to monitor whether PD were open or shut in root tissues during a xerobranching response. Within plant cells, nonfluorescent CFDA is cleaved by cellular esterases to release membrane-impermeable fluorescent CF that travels exclusively through the PD. After CFDA application to cotyledons, we observed decreased protophloem unloading in *Arabidopsis* WT root tips that were exposed to a xerobranching stimulus (fig. S15). Delayed unloading was also observed in root tips of a *pSUC2:GFP* line that expresses free GFP in phloem companion cells (fig. S16). Collectively, both lines of evidence reveal that root tips experience decreased PD permeability after a xerobranching stimulus.

To assess the role of ABA in root PD gating during xerobranching, CFDA was locally applied to root tips. WT roots exhibited reduced intercellular fluxes of the tracer, which indicated closed PD after a xerobranching stimulus (Fig. 4, A and B). By contrast, CFDA treatment of root tips of the ABA response mutant *snrk2.2/2.3* revealed that PD remained open after a xerobranching stimulus (fig. S17). PD aperture is regulated by modifying the size of a callose ring encircling each end of the intercellular pore. The callose stain aniline blue revealed higher callose deposition in basal meristem cells of WT roots compared with *snrk2.2/2.3* after a xerobranching stimulus (fig. S18). Taken together, the evidence indicates that ABA regulates gating of PD in key root tissues during a xerobranching response.

To determine the function of PD gating during a xerobranching response, *Arabidopsis* mutants no longer able to gate their PD were characterized (figs. S19 and S20). PD aperture

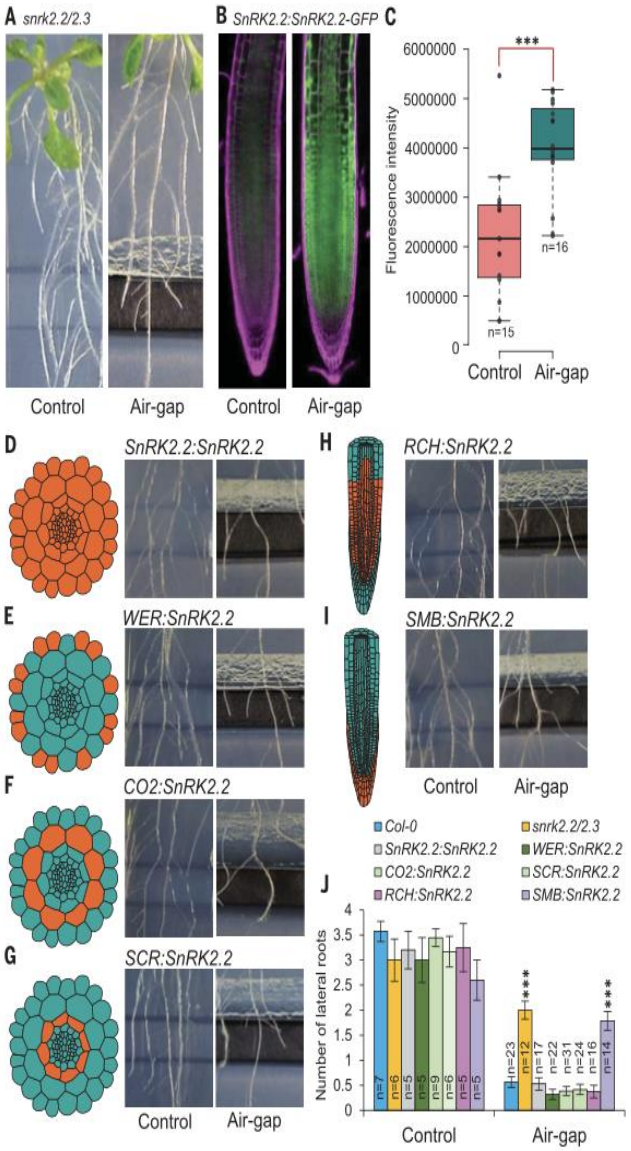


**Fig. 3. Xerobranching is dependent on ABA perception in *Arabidopsis* primary root transition zone tissues.** (**A**) ABA signaling mutant *snrk2.2/2.3* disrupts xerobranching in agar-based air-gap assay system. Air gap, ~5 mm. (**B** and **C**) Elevated response of *pSnRK2.2:SnRK2.2-GFP* in root tips subjected to air-gap versus control conditions. Scale bar, 100 μm. (**D**) Expression of *SnRK2.2* under its own promoter rescues the xerobranching defect of *snrk2.2/2.3*. (**E** to **G**) Functional complementation of *snrk2.2/2.3* by tissue-specific expression of *SnRK2.2* in epidermis, cortex, and endodermis using the *WER*, *CO2*, and *SCR* promoters, respectively. (**H**) Root zone–specific expression of *SnRK2.2* in root meristem and transition zone (using *RCH* promoter) rescues the xerobranching defect of *snrk2.2/2.3*. (**I**) Expression of *SnRK2.2* in columella and lateral root cap using SMB promoter in *snrk2.2/2.3* background. (**J**) Number of lateral roots produced by WT (Col-0), *snrk2.2/2.3*, and different tissue- and/or zone-specific rescue lines in the air-gap region versus the corresponding region of roots grown under control conditions. Orange color in root schematics defines the tissue and/or zone of expression of selected promoters used for complementation. Significant changes with respect to control (C) or WT (J) were calculated by Student's *t* test. ***$P \leq 0.001$.

is regulated through the action of enzymes, including a family of callose synthases and associated regulatory proteins such as PD-located proteins (PDLPs) (*24*). Mutating individual members of the *Arabidopsis* callose synthase gene family resulted in nine of these lines exhibiting a xerobranching defect, including *CALS7*, which is primarily associated with phloem sieve pores (fig. S19) (*25*), as did mutating both *PDLP2* and *PDLP3* genes (fig. S20). Hence, blocking the ability to close PD disrupts a root's ability to activate a xerobranching response.

How does ABA trigger PD closure after a xerobranching stimulus? Transgenic lines expressing GFP reporters that were fused to either PDLP2 or PDLP3 proteins under their native promoters were up-regulated in response to a xerobranching stimulus (Fig. 4, C and D, and figs. S21 to S23). In the case of PDLP3, its mRNA and *PDLP3:PDLP3-GFP* reporter were up-regulated in root tip and, specifically, basal meristem cells during a xerobranching response, exhibiting a punctate pattern in apical, basal, and side walls, consistent with its PD regulatory function (Fig. 4, C and D, and figs. S21 and S23). Treating roots of *PDLP3:PDLP3-GFP* with low levels of ABA (50 nM) phenocopied a xerobranching stimulus (fig. S24), in agreement with the presence of several ABA-responsive elements (ABREs) in its promoter sequence (table S1). We also noted that many other *PDLP* and *callose synthase* genes contained ABREs in their promoter sequences (tables S1 and S2). Comparing spatiotemporal response curves of nlsABACUS2 and PDLP3-GFP (during xerobranching and subsequent recovery) reveals that ABA accumulation precedes PDLP3 induction (Fig. 1K and fig. S23). To test the functional importance of ABA-regulated PDLP up-regulation during xerobranching, we characterized the ABA-insensitive mutant *abi1-1*. The dominant negative *abi1-1* allele disrupts ABA-dependent PD closure and maintains high frequencies of open PD (*26*). Unlike WT, *abi1-1* roots exhibit branching in air gaps (fig. S25). However, ectopic expression of *PDLP1* (using *35S* rather than its native promoter) rescued the xerobranching defect of *abi1-1* (fig. S25). Hence, ABA triggers PD closure after a xerobranching stimulus by up-regulating expression of *PDLP*s. Additionally, GAL4-mediated transactivation of *abi1-1* in root ground tissues (cortex and endodermis) led to maximal disruption of xerobranching response as compared with induction of *abi1-1* in single root cell layers (fig. S26). Hence, ABA-mediated PD closure in root ground tissues is essential for a xerobranching response.

### PD closure blocks inward auxin movement

How does ABA-mediated PD gating disrupt lateral root branching? Our reporter studies reveal that closing PD during a xerobranching response blocks the inward (symplastic) movement of another plant hormone signal, auxin, which is required to initiate lateral root branching. Exposing roots of the *DR5:VENUS* auxin reporter line to a xerobranching stimulus results in an elevated auxin response in epidermal cells within the root basal meristem zone (Fig. 4, E and F). The altered *DR5:VENUS* reporter pattern is consistent with xerobranching-induced PD closure in basal meristem epidermal cells transiently blocking the radially inward symplastic movement of auxin (Fig. 4, E and F, and fig. S27).

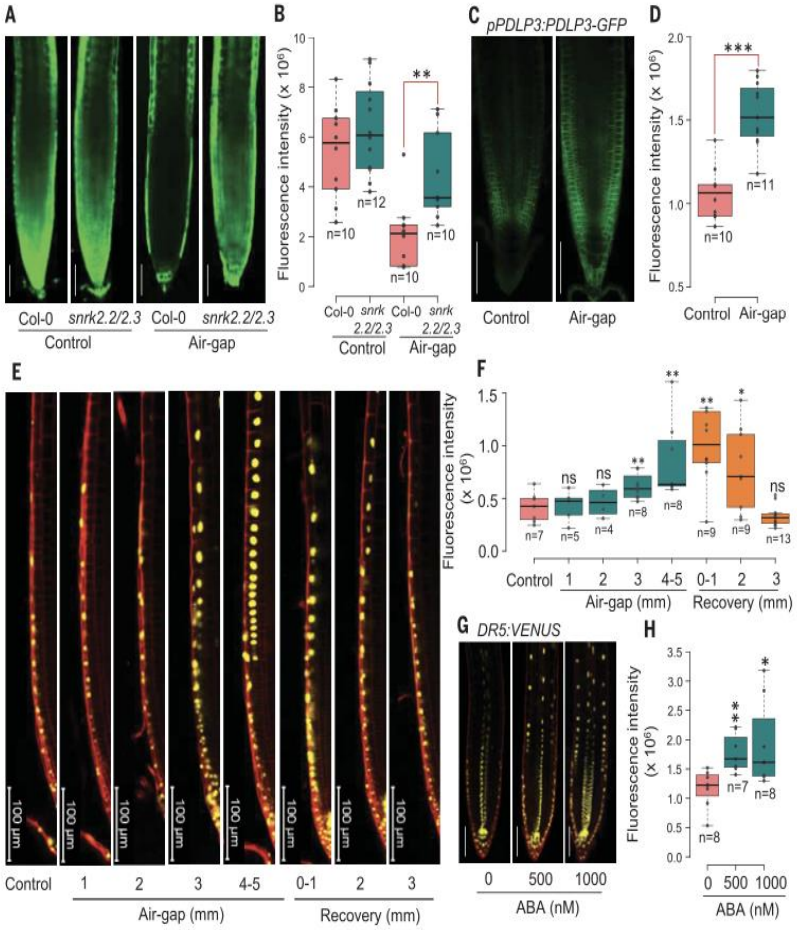


**Fig. 4. ABA blocks radial auxin flow by reducing PD permeability causing xerobranching.** (**A**) Slower migration of symplastic tracer CF in WT *Arabidopsis* (Col-0) primary root tips subjected to xerobranching stimulus versus control conditions. CF migration was indistinguishable in ABA signaling mutant *snrk2.2/2.3* with or without the xerobranching stimulus. Root tips were treated with CFDA before imaging. (**B**) CF fluorescence intensity in WT and *snrk2.2/2.3* root tips exposed to air-gap versus control conditions. (**C**) Xerobranching stimulus induces expression of *pPDLP3:PDLP3-GFP*. (**D**) Box plots showing significantly enhanced response of *pPDLP3:PDLP3-GFP* in air-gap versus control conditions. (**E** and **F**) Auxin response reporter *DR5:VENUS* shows higher fluorescence signal in epidermis of root tips exposed to air-gap versus control and recovery conditions. (**G** and **H**) ABA treatments phenocopy *DR5:VENUS* response during xerobranching. Scale bar, 100 µm. *$P \leq 0.05$; **$P \leq 0.01$; ***$P \leq 0.001$; ns, nonsignificant (Student's *t* test).

The auxin reporter DII-VENUS also revealed higher auxin abundance in root tips during exposure to a xerobranching stimulus (figs. S27 and S28). The effect of a xerobranching stimulus on *DR5:VENUS* and DII-VENUS can be mimicked by exogenous application of ABA to roots (Fig. 4, G and H, and fig. S29). ABA-mediated PD gating during a xerobranching response blocks radial inward auxin movement and lateral root induction. Consistent with this model, switching off ABA signaling in the *abi1-1* mutant (which ensured that PD remained constitutively open) blocked any change in DII-VENUS auxin response after a xerobranching stimulus (fig. S30). Suppression of lateral root initiation in roots exposed to a xerobranching stimulus was visualized by using the *DR5:LUC* reporter, which normally demarks groups of lateral root stem cells in the basal meristem (or oscillation zone) that go on to form new branches in control roots, but these *DR5:LUC* oscillations were blocked in roots exposed to a xerobranching stimulus (fig. S31). Hence, the xerobranching response blocks radially inward symplastic auxin movement that is required for lateral root induction.

Root auxin distribution was originally thought to be exclusively determined by the combined activities of AUX1/LAX, ABCB, and PIN auxin influx and efflux carriers (*27*). To determine the impact of xerobranching on carrier-mediated auxin transport, reporter lines for key auxin influx (*pAUX1:AUX1-YFP*) or efflux (*pPIN2:PIN2-GFP*) carriers expressed in the root elongation zone were analyzed (fig. S32). No spatial changes were detected in AUX1-YFP or PIN2-GFP expression in the outermost root tissues after a xerobranching stimulus, consistent with the observed elevated auxin response (Fig. 4, E and F, and fig. S27) being the result of gating of hormone movement through PD rather than through modulation of apoplastic auxin transport (fig. S32). Ectopic expression of either *AUX1* or *PIN2* in every elongation zone tissue, to create a synthetic radial apoplastic auxin pathway, successfully bypassed the PD-mediated restriction of symplastic auxin flow and led to lateral root branching in air gaps (fig. S33).

Collectively, multiple lines of evidence establish a role for ABA-mediated PD gating of radial symplastic auxin flow to regulate xerobranching. Roots appear to sense water availability by comobilizing water and hormones through PD. If water, ABA, and auxin moved through substrate-specific carriers (aquaporins, ABCG, and PINs), their comobilization would be broken. Instead, because PD are large intercellular pores that are nonselective, radial hydraulic fluxes comobilize hormones either inward (such as auxin) or outward (such as ABA) when water is available or not, respectively. Thus, auxin and ABA can be considered as hydrosignals when comobilized through PD with water.

Our study has revealed that xerobranching is a widely conserved, ABA-dependent root adaptive response to localized loss of contact with soil water in eudicot and monocot species. We also report the molecular and cellular mechanisms that enable plant roots to block lateral root formation after experiencing a xerobranching stimulus (see schematic in Fig. 5). Under optimal moisture conditions,

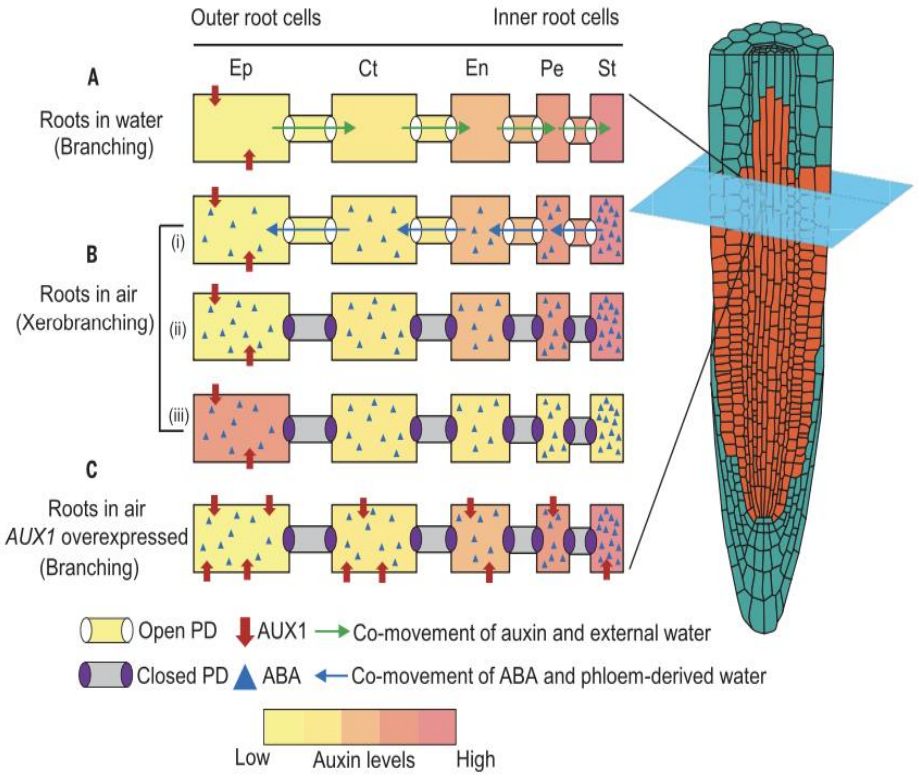


**Fig. 5. Dynamic hormone redistribution determines root branching or xerobranching response to external water availability.** Schematics illustrate cellular auxin, ABA, and water fluxes in root basal meristem (highlighted cell files in transverse root section) exposed to water or air. (**A**) Under normal moisture conditions, roots cotransport water and auxin radially inward through PD, which delivers the key hormone signal (auxin) to pericycle cells, where lateral root initiation is triggered. (**B**) Xerobranching stimulus triggers rise in ABA levels in inner root tissues (stele), which suppresses root branching. In the transient absence of external water, phloem-derived water comobilizes ABA from inner (stele) to outer root cells (epidermis) through PD (i). ABA induces closure of PD through *PDLP*s and *CALs* (ii) disrupting symplastic radial movement of auxin to pericycle (iii). (**C**) Ectopic expression of auxin carriers such as AUX1 in all elongation zone tissue creates a synthetic radial apoplastic auxin pathway, which bypasses the disrupted symplastic auxin flow and thus causes root branching in air gap. Ct, cortex; En, endodermis; Ep, epidermis; Pe, pericycle; St, stele.

roots cotransport auxin and water inward between root basal meristem tissues through PD and thus provide a symplastic pathway to radially mobilize this key hormone signal with hydraulic fluxes from epidermal to pericycle cells, where auxin triggers lateral root initiation. However, when the external source of water is transiently unavailable, root tips rely on an internal (phloem) source of water to continue growing (*15*) and couple its outward radial flow with movement of the hormone ABA. This key water stress signal reduces PD aperture, disrupting radial movement of the branching signal auxin to lateral root "stem cells" in the pericycle. Restoring an external water source (during the recovery phase) rapidly reduces ABA levels in the outermost root tissues (>3 hours) and thus restores open PD and symplastic auxin transport. Once reconnected with an external water source, the abundance and distribution of these signals reset in root-tip tissues to pre-xerobranching-stimulus levels. These dynamic regulatory events—coupling changes in hydraulic fluxes with hormone redistribution, which we term hydrosignaling—enable plant roots to calibrate spatial root branching responses in heterogeneous soil environments, which are the norm rather than the exception. Climate change is likely to exacerbate water scarcity (*9*, *10*); thus, that water in soils will be even more heterogeneously distributed in the future than at present is highly likely. Insight into the molecular and cellular mechanisms through which roots acclimate under these conditions may improve the climate resilience of future crops.

## REFERENCES AND NOTES


1. B. Muller *et al.*, *Trends Plant Sci.* **24**, 810–825 (2019).
2. J. P. Lynch, *Plant Physiol.* **156**, 1041–1049 (2011).
3. H. Motte, T. Beeckman, *J. Exp. Bot.* **70**, 785–793 (2019).
4. E. C. Morris *et al.*, *Curr. Biol.* **27**, R919–R930 (2017).
5. A. Zhan, H. Schneider, J. P. Lynch, *Plant Physiol.* **168**, 1603–1615 (2015).
6. R. Karlova, D. Boer, S. Hayes, C. Testerink, *Plant Physiol.* **187**, 1057–1070 (2021).
7. B. Orman-Ligeza *et al.*, *Curr. Biol.* **28**, 3165–3173.e5 (2018).
8. Y. Bao *et al.*, *Proc. Natl. Acad. Sci. U.S.A.* **111**, 9319–9324 (2014).
9. D. B. Lobell, S. M. Gourdji, *Plant Physiol.* **160**, 1686–1697 (2012).
10. Y. Grusson, I. Wesström, E. Svedberg, A. Joel, *Agric. Water Manage.* **249**, 106766 (2021).
11. A. J. Thompson *et al.*, *Plant Cell Environ.* **27**, 459–471 (2004).
12. I. B. Taylor, R. S. T. Linforth, R. J. Al-Naieb, W. R. Bowman, B. A. Marples, *Plant Cell Environ.* **11**, 739–745 (1988).
13. B. C. Tan, S. H. Schwartz, J. A. D. Zeevaart, D. R. McCarty, *Proc. Natl. Acad. Sci. U.S.A.* **94**, 12235–12240 (1997).
14. T. Kuromori, E. Sugimoto, K. Shinozaki, *Plant Physiol.* **164**, 1587–1592 (2014).
15. B. S. Wiegers, A. Y. Cheer, W. K. Silk, *Plant Physiol.* **150**, 2092–2103 (2009).
16. V. Couvreur *et al.*, *Plant Physiol.* **178**, 1689–1703 (2018).
17. F. C. Pascut *et al.*, *Nat. Commun.* **12**, 4682 (2021).
18. J. Rowe *et al.*, bioRxiv 2022.10.19.512731 [Preprint] (2022).
19. T. J. Ross-Elliott *et al.*, *elife* **6**, e24125 (2017).
20. I. De Smet *et al.*, *Development* **134**, 681–690 (2007).
21. M. A. Moreno-Risueno *et al.*, *Science* **329**, 1306–1311 (2010).
22. K. Prado *et al.*, *Plant Cell* **25**, 1029–1039 (2013).
23. Y. Benitez-Alfonso, *Plant Cell Physiol.* **60**, 713–714 (2019).
24. C. L. Thomas, E. M. Bayer, C. Ritzenthaler, L. Fernandez-Calvino, A. J. Maule, *PLOS Biol.* **6**, e7 (2008).
25. B. Xie, X. Wang, M. Zhu, Z. Zhang, Z. Hong, *Plant J.* **65**, 1–14 (2011).

26. S. Tylewicz *et al.*, *Science* **360**, 212–215 (2018).
27. J. Petrášek, J. Friml, *Development* **136**, 2675–2688 (2009).

**ACKNOWLEDGMENTS**

We thank P. L. Rodriguez (CSIC-UPV, Spain) for sharing *pyr/pyl1124589*, *pyr/pyl1124578*, and *pyr/pyl112458* mutants; H. Fujii (University of Turku, Finland) for sharing *snrk2.2/3/6*, *snrk2.1/4/5/7/8/9/10*, and *snrk2.1/3/4/5/6/7/8/9/10* mutants; and R. Miao (Fujian Agriculture and Forest University, China) for sharing *hab1-1abi1-2pp2ca*, *hab1-1abi1-2abi2-2*, and *Qabi2-2* mutants. We thank L. Kalmbach, Y. Helariutta (SLCU, UK), and N. Geldner (University of Lausanne, Switzerland) for sharing *pSUC2:GFP* seeds. We also thank Z. Gong and Y. Wang (China Agricultural University) for kindly sharing *abi1-1* (Col-0) seeds. We acknowledge C. Luschnig (University of Natural Resources and Life Sciences – BOKU, Vienna) and J. Friml (IST, Austria) for sharing *eir1-4/PIN2:PIN2-GFP* and *eir1-4/35S:PIN2-GFP* lines. We thank F. Augstein and A. Carlsbecker (Uppsala University, Sweden) for providing *UAS:abi1-1* and driver lines. We thank F. Chaumont (Louvain-la-Neuve, Belgium) and A. Schäffner (Helmholtz Zentrum München, Germany) for sharing the aquaporin mutant. **Funding:** This study was supported by a European Molecular Biology Organization Long-Term Fellowship (ALTF 1140-2019 to P.M.); European Union's Horizon 2020 research and innovation program, Marie Skłodowska-Curie, XEROBRANCHING (891262 to P.M.); Biotechnology and Biological Sciences Research Council Discovery Fellowship (BB/V00557X/1 to B.K.P.); the Biotechnology and Biological Sciences Research Council (BB/T001437/1 to M.J.B. and A.S.; BB/V003534/1 to M.J.B., A.S., and J.B.; BB/W008874/1 to M.J.B. and C.J.S.; BB/W015080/1 to M.J.B.; and BB/P018572/1 to A.M.J.); European Research Council grant FUTUREROOTS (294729 to M.J.B.); European Research Council, SUMOrice (grant no. 310235 to A.S.); Fonds de la Recherche Scientifique – FNRS (to V.C.); the Swedish Research Council (no. 2020-03522 to R.P.B.); European Research Council, RobustHormoneTrans (757683 to E.S.); the NSF Plant Genome Research Program (IOS-1444448 to R.E.S.); the Gatsby Charitable Foundation (to A.M.J. and J.R.); European Research Council grant INTERCELLAR (725459 to C.F.); and the Biotechnology and Biological Research Council Institute Strategic Programme, Plant Health (BBS/E/J/000PR9796 to C.F.).

**Author contributions:** Conceptualization: P.M. and M.J.B. Methodology: P.M., B.K.P., V.C., J.R., and H.D.G. Investigation: P.M., B.K.P., D.M., J.B., N.L., V.C., J.R., M.A., H.D.G., E.M., C.J.S., and R.S. Funding acquisition: P.M. and M.J.B. Supervision: M.J.B. Writing – original draft: M.J.B. and P.M. Writing – review & editing: P.M., B.K.P., D.M., J.B., N.L., V.C., J.R., M.A., H.D.G., E.M., C.J.S., R.S., S.J.M., C.F., T.B., R.P.B., E.S., A.M.J., I.C.D., R.E.S., A.S., X.D., and M.J.B. **Competing interests:** The authors declare no competing interests. **Data and materials availability:** No restrictions are placed on materials, such as materials transfer agreements. All data are available in the main text or the supplementary materials. 

**SUPPLEMENTARY MATERIALS**

science.org/doi/10.1126/science.add3771
Materials and Methods
Figs. S1 to S33
Tables S1 and S2
References (*28*–*59*)
MDAR Reproducibility Checklist

View/request a protocol for this paper from *Bio-protocol*.

Submitted 8 June 2022; accepted 24 October 2022
10.1126/science.add3771

## Summarizing of Arabidopsis amiRNA as target after PCR sequencing

| AmiRNA ID | TAIR ID | AmiRNA Sequence | NASC Code | SALK Name | Poolname | Family | Other target in PHANTOM Library |
|---|---|---|---|---|---|---|---|
| 1466 | AT5G03260.1 | TCCATCTGCCCAATCGTTCTG | N662726 | SALK_063746C | TRP | Laccase11 | AT1G18140 |
| | | | | | | | AT3G09220 |
| 833 | AT5G58910.2 | TCCATCTGCCCAATCGTTCTG | N668406 | SALK_064093C | TRP | Laccase16 | AT1G18140 |
| | | | | | | | AT3G09220 |
| 790 | AT5G46370.1 | TCATCGATTATATACGGTCTC | N666829 | SALK_096547C | TRP | Ca2+activated outward rectifying K+ channel2 | AT4G18160 |
| 784 | AT3G47960.1 | TGATGAAAACTGTCCTGCCAA | N923939 | SALK_090694.2 | TRP | Major facilitator superfamily protein | AT3G45660 |
| 693 | AT1G43470.1 | TCTAAAGGCATTAAGCACCCA | N69760 | SALK_142497 | TRP | mechanosensitive channel of small conductance-like 4 | AT1G78610 |
| 499 T3 -1 | AT1G42470.1 | TAGATATTGCTCAAAGGACAT | N654977 | SALK_004590C | TRP | Patched family protein | AT4G38350 |
| 633 -1 | AT5G46050.1 | TAAGCATTGAGAGCGTGACAT | N664402 | SALK_003119C | TRP | ARABIDOPSIS THALIANA PEPTIDE TRANSPORTER 3 | AT2G40460 |
| 1112 -1 | AT5G53130.1 | TGTCTACCGGATCACCTTCT | N547404 | SALK_047404 | TRP | ATCNGC1, CNGC1, , CYCLIC NUCLEOTIDE-GATED CHANNEL 1 | AT5G57940 |
| 523 -1 | AT4G09160.1 | TGTAGACATTGTAACAGACAG | N656113 | SALK_003134C | TRP | SEC14 cytosolic factor family protein / phosphoglyceride transfer family protein | AT1G30690 |
| | | | | | | | AT1G72160 |
| 524 | AT1G76800.1 | TTAACCGCTGGTGACTTCCAT | N657639 | SALK_060224C | TRP | ATVTL2, VACUOLAR IRON TRANSPORTER-LIKE 2, VTL2 | AT3G43630 |
| 2077 | AT1G51460.1 | TAAGCACTGTCCAATCGACTA | N662346 | SALK_046735C | TRP | ABC-2 type transporter family protein | AT1G51500 |
| | | | | | | | AT3G21090 |
| 478 | AT5G40840.5 | TATGCCAATGGATACAGACGT | N672286 | SALK_021337C | TRP | Rad21/Rec8-like family protein | AT4G39830 |
| | | | | | | | AT5G01190 |
| 2690 | AT5G01190.2 | TATGCCAATGGATACAGACGT | N678167 | SALK_017722C | TRP | Laccase10 | AT4G39830 |
| 1227 | AT1G66760.2 | TTTTGCCACCCTGTGCCTCAC | N581560 | SALK_081560 | TRP | MATE efflux family protein;(source:Araport11) | AT1G66780 |
| 1458 | AT5G49890.1 | TAGTATGAACCATAGGCCCT | N680169 | SALK_115644C | TRP | ATCLC-C, CHLORIDE CHANNEL C, CLC-C | AT5G33280 |
| 1484 | AT5G33280.1 | TAGTATGAACCATAGGCCCT | N686466 | SALK_087699C | TRP | ATCLC-C, CHLORIDE CHANNEL C, CLC-C | AT5G49890 |
| 2522 | AT3G47960.1 | TGATGAAAACTGTCCTGCCAA | N660899 | SALK_058919C | TRP | Major facilitator superfamily protein | AT5G46050 |
| 469 | AT5G01180.1 | TGATTTTGAAGTTAGGCCCC | N654100 | SALK_022619C | TRP | peptide transporter 5 | AT3G45690 |
| 2645 | AT3G45690.1 | TGATTTTGAAGTTAGGCCCC | N605411 | SALK_105411 | TRP | Major facilitator superfamily protein | AT5G01180 |
| 2078 | AT1G66760.2 | TTTTGCCACCCTGTGCCTCAC | N599800 | SALK_099800 | TRP | MATE efflux family protein | AT1G66780 |
| 729 | AT5G12860.1 | TAACCAGGTGAGTGGGTCCCG | N652687 | SALK_152687 | TRP | DICARBOXYLATE TRANSPORTER 1, DIT1 | AT5G64280 |
| 459 | AT5G57090.1 | TATCACACTCGCTGGCGGCG | N664960 | SALK_144447C | TRP | AGR, AGR1, ATPIN2, EIR1+B7 , MM31, , PIN2, WAV | AT1G23080 |
| | | | | | | | AT1G70940 |
| 451 | AT1G53470.1 | TCTAAAGGCATTAAGCACCCA | N685271 | SALK_013552C | TRP | mechanosensitive channel of small conductance-like 4 | AT1G78610 |

# 8 REFERENCES

**Abas, L., Benjamins, R., Malenica, N., Paciorek, T. T., Wiřniewska, J., Moulinier-Anzola, J. C., Sieberer, T., Friml, J., & Luschnig, C. (2006).** Intracellular trafficking and proteolysis of the Arabidopsis auxin-efflux facilitator PIN2 are involved in root gravitropism. *Nature Cell Biology*, *8*(3), 249–256.

**Ahuja, I., de Vos, R. C. H., Bones, A. M., & Hall, R. D. (2010).** Plant molecular stress responses face climate change. In *Trends in Plant Science* 15, (12), 664–674.

**Allen, C. D., & Breshears, D. D. (1998).** Drought-induced shift of a forest- woodland ecotone: Rapid landscape response to climate variation. In *Ecology* (95).

**Anderson, B. A. (2013)**. A value-driven mechanism of attentional selection. *Journal of Vision*, *13*(3).

**Anfang, M., & Shani, E. (2021).** Transport mechanisms of plant hormones. In *Current Opinion in Plant Biology* (Vol. 63).

**Babé, A., Lavigne, T., Séverin, J. P., Nagel, K. A., Walter, A., Chaumont, F., Batoko, H., Beeckman, T., & Draye, X. (2012).** Repression of early lateral root initiation events by transient water deficit in barley and maize. *Philosophical Transactions of the Royal Society B: Biological Sciences*.

**Bao, Y., Aggarwal, P., Robbins, N. E., Sturrock, C. J., Thompson, M. C., Tan, H. Q., Tham, C., Duan, L., Rodriguez, P. L., Vernoux, T., Mooney, S. J., Bennett, M. J., & Dinneny, J. R. (2014).** Plant roots use a patterning mechanism to position lateral root branches toward available water. *Proceedings of the National Academy of Sciences of the United States of America*, *111*(25), 9319-9324.

**Basu, D., Shoots, J. M., & Haswell, E. S. (2020).** Interactions between the N- And C-termini of the mechanosensitive ion channel AtMSL10 are consistent with a three-step mechanism for activation. *Journal of Experimental Botany*, *71*(14), 4020–4032.

**Benfey, P. N., & Scheres, B. (2022).** *Primary Root development*. *10* (22)813-815

**Benitez-Alfonso, Y. (2019).** The Role of Abscisic Acid in the Regulation of Plasmodesmata and Symplastic Intercellular Transport. In *Plant and Cell Physiology 60* (4), 713–714. Oxford University Press.

**Benková, E., Michniewicz, M., Sauer, M., Teichmann, T., Seifertová, D., Jü Rgens, G., & Friml, J. (2003).** Local, Efflux-Dependent Auxin Gradients as a Common Module for Plant Organ Formation growing shoots or roots bearing a secondary meristem at the tip. Aerial organs such as leaves and secondary shoots, including flowers, originate from primordia on. In *Cell*, *115*.

**Bennett, M., et al (2018.).** *Hydrotropism: growing with the flow*. *Journal of Experimental Botany*, 69 (11), 2759–2771 .

**Borpatragohain, P., Rose, T. J., & King, G. J. (2016).** Fire and brimstone: Molecular interactions between sulfur and glucosinolate biosynthesis in model and crop brassicaceae. In *Frontiers in Plant Science.(7).*

**Boursiac, Y., Léran, S., Corratgé-Faillie, C., Gojon, A., Krouk, G., & Lacombe, B. (2013).** ABA transport and transporters. In *Trends in Plant Science. 18* (6), 325–333.

**Boursiac, Y., Pradal, C., Bauget, F., Lucas, M., Delivorias, S., Godin, C., & Maurel, C. (2022).** Phenotyping and modeling of root hydraulic architecture reveal critical determinants of axial water transport. *Plant Physiology*, *190*(2), 1289–1306.

**Briggs, G. C., Osmont, K. S., Shindo, C., Sibout, R., & Hardtke, C. S. (2006).** Unequal genetic redundancies in Arabidopsis - a neglected phenomenon? In *Trends in Plant Science. 11,* (10) , 492–498.

**Brown, D. P. (2008).** Efficient functional clustering of protein sequences using the Dirichlet process. *Bioinformatics*, *24*(16), 1765–1771.

**Burla, B., Pfrunder, S., Nagy, R., Francisco, R. M., Lee, Y., & Martinoia, E. (2013).** Vacuolar transport of abscisic acid glucosyl ester is mediated by ATP- binding cassette and proton-antiport mechanisms in Arabidopsis. *Plant Physiology*, *163*(3), 1446–1458.

**Busk, P. K., & Pagès, M. (1998).** Regulation of abscisic acid-induced transcription. In *Plant Molecular Biology* (*37*).

**Cai Tan, B., Schwartz, S. H., Zeevaart, J. A. D., & Mccarty, D. R. (1997).** *Genetic control of abscisic acid biosynthesis in maize* (*94*).

**Casanova-Sáez, R., Mateo-Bonmatí, E., & Ljung, K. (2021).** Auxin metabolism in plants. *Cold Spring Harbor Perspectives in Medicine*, *11*(3), 1–23.

**Cassab, G. I., Eapen, D., & Campos, M. E. (2013).** Root hydrotropism: An update. *American Journal of Botany*, *100*(1), 14–24.

**Cattivelli, L., Rizza, F., Badeck, F. W., Mazzucotelli, E., Mastrangelo, A. M., Francia, E., Marè, C., Tondelli, A., & Stanca, A. M. (2008).** Drought tolerance improvement in crop plants: An integrated view from breeding to genomics. In *Field Crops Research.105* (1-2), 1–14.

**Cerri, C. E. P., Sparovek, G., Martial Bernoux, ;, Easterling, W. E., Melillo, J. M., Carlos, ;, & Cerri, C. (2007).** Tropical agriculture and global warming TROPICAL AGRICULTURE AND GLOBAL WARMING: IMPACTS AND MITIGATION OPTIONS AGRICULTURA TROPICAL E AQUECIMENTO GLOBAL: IMPACTOS E OPÇÕES DE MITIGAÇÃO. In *Sci. Agric* ( 1).

**Chen, J., Hu, Y., Hao, P., Zhang, Y., Roth, O., Njo, M. F., Sterck, L., Hu, Y., Zhao, Y., Geisler, M., Shani, E., Beeckman, T., & Vanneste, S. (2020).** *ABCB-mediated auxin transport in outer root tissues regulates lateral root 1 spacing in Arabidopsis 2*.

**Chen, S., & Gong, B. (2021).** Response and adaptation of agriculture to climate change: Evidence from China. *Journal of Development Economics*, *148*.

**Condit, R., Hubbell, S. P., & Foster, R. B. (1995).** Mortality rates of 205 neotropical tree and shrub species and the impact of a severe drought. *Ecological Monographs*, *65*(4), 419–

**Corlett, R. (2016)**. 'Plant diversity in a changing world: Status, trends, and conservation needs.', *Oxford Bibliographies Online Datasets* [Preprint].

**Cotterman, T. (2017).** *Enhanced Techniques to Plan Rural Electrical Networks Using the Reference Electrification Model*.

**COUTTS, M. P., & NICOLL, B. C. (1993).** Orientation of the lateral roots of trees: II. Hydrotropic and gravitropic responses of lateral roots of Sitka spruce grown in air at different humidities. *New Phytologist*, *124*(2), 277–281.

**Couvreur, V., Faget, M., Lobet, G., Javaux, M., Chaumont, F., & Draye, X. (2018).** Going with the flow: Multiscale insights into the composite nature of water transport in roots. *Plant Physiology*, *178*(4), 1689–1703.

**Cutler, S. R., Rodriguez, P. L., Finkelstein, R. R., & Abrams, S. R. (2010).** Abscisic acid: Emergence of a core signaling network. *Annual Review of Plant Biology*, *61*, 651–679.

**Damodaran, M., Amelink, A., Feroldi, F., Lochocki, B., Davidoiu, V., & de Boer, J. F. (2019).** In vivo subdiffuse scanning laser oximetry of the human retina. *Journal of Biomedical Optics*, *24*(09), 1.

**Davies, S. J., McGeoch, M. A., & Clusella-Trullas, S. (2015).** Plasticity of thermal tolerance and metabolism but not water loss in an invasive reed frog. *Comparative Biochemistry and Physiology -Part A : Molecular and Integrative Physiology*, *189*, 11–20.

**Davies, W. 1, & Zhang, L. (1991).** ROOT SIGNALS AND THE REGULATION OF GROWTH AND DEVELOPMENT OF PLANTS IN DRYING SOIL. In *Annu. Rev. Plant Physiol. Plant Mol. Bioi (42).*

**Davies, W. J., & Bennett, M. J. (2015).** Achieving more crop per drop. In *Nature Plants (1).* Palgrave Macmillan Ltd.

**de Smet, I., Tetsumura, T., de Rybel, B., dit Frey, N. F., Laplaze, L., Casimiro, I., Swarup, R., Naudts, M., Vanneste, S., Audenaert, D., Inzé, D., Bennett, M. J., & Beeckman, T. (2007).** Auxin-dependent regulation of lateral root positioning in the basal meristem of Arabidopsis. *Development*, *134*(4), 681– 690.

**Dietrich, D. (2018).** Hydrotropism: How roots search for water. In *Journal of Experimental Botany*. *69*(11), 2759–2771.

**Dietrich, D., Pang, L., Kobayashi, A., Fozard, J. A., Boudolf, V., Bhosale, R., Antoni, R., Nguyen, T., Hiratsuka, S., Fujii, N., Miyazawa, Y., Bae, T. W., Wells, D. M., Owen, M. R., Band, L. R., Dyson, R. J., Jensen, O. E., King, J. R., Tracy, S. R., ... Bennett, M. J. (2017).** Root hydrotropism is controlled via a cortex-specific growth mechanism. *Nature Plants*, *3*.

**Eapen, D., Barroso, M. L., Ponce, G., Campos, M. E., & Cassab, G. I. (2005)**. Hydrotropism: Root growth responses to water. In *Trends in Plant Science*.

**Enright, A. J., Dongen, S. van, & Ouzounis, C. A. (2002).** An efficient algorithm for large-scale detection of protein families. In *Nucleic Acids Research.30* (7).

**Fernando, V. C. D., & Schroeder, D. F. (2016).** Role of ABA in Arabidopsis Salt, Drought, and Desiccation Tolerance. In *Abiotic and Biotic Stress in Plants - Recent Advances and Future Perspectives*.

**Finkelstein, R. (2013).** 'Abscisic acid synthesis and response', *The Arabidopsis Book*, 11

**Fujita, Y., Nakashima, K., Yoshida, T., Katagiri, T., Kidokoro, S., Kanamori, N., Umezawa, T., Fujita, M., Maruyama, K., Ishiyama, K., Kobayashi, M., Nakasone, S., Yamada, K., Ito, T., Shinozaki, K., & Yamaguchi-Shinozaki, K. (2009).** Three SnRK2 protein kinases are the main positive regulators of abscisic acid signaling in response to water stress in arabidopsis. *Plant and Cell Physiology*, *50*(12), 2123–2132.

**Galvan-Ampudia, C. S., Julkowska, M. M., Darwish, E., Gandullo, J., Korver, R. A., Brunoud, G., Haring, M. A., Munnik, T., Vernoux, T., & Testerink, C. (2013).** Halotropism is a response of plant roots to avoid a saline environment. *Current Biology*, *23*(20), 2044–2050.

**Gao, Y., Zhang, Y., Zhang, D., Dai, X., Estelle, M., & Zhao, Y. (2014).** *Auxin binding protein 1 (ABP1) is not required for either auxin signaling or Arabidopsis development*. *PNAS. 112* (7) 2275-2280.

**Geldner, N., Anders, N., Wolters, H., Keicher, J., Kornberger, W., Muller, P., Delbarre, A., Ueda, T., Nakano, A., & Jü Rgens, G. (2003**). The Arabidopsis GNOM ARF-GEF Mediates Endosomal Recycling, Auxin Transport, and Auxin-Dependent Plant Growth. In *Cell. 24;112*(2),219-30 .

**Giri, J., Bhosale, R., Huang, G., Pandey, B. K., Parker, H., Zappala, S., Yang, J., Dievart, A., Bureau, C., Ljung, K., Price, A., Rose, T., Larrieu, A., Mairhofer, S., Sturrock, C. J., White, P., Dupuy, L., Hawkesford, M., Perin, C., ... Bennett, M. J. (2018).** Rice auxin influx carrier OsAUX1 facilitates root hair elongation in response to low external phosphate. *Nature Communications*, *9*(1).

**Gitlin, A. R., Sthultz, §christopher M, Bowker, M. A., Stumpf, S., Paxton, K. L., Kennedy, K., Mu, A., Noz˜, Bailey, J. K., & Whitham, T. G. (2006).** *Mortality Gradients within and among Dominant Plant Populations as Barometers of Ecosystem Change During Extreme Drought*.

**Gonzalez-Guzman, M., Rodriguez, L., Lorenzo-Orts, L., Pons, C., Sarrion-Perdigones, A., Fernandez, M. A., Peirats-Llobet, M., Forment, J., Moreno-Alvero, M., Cutler, S. R., Albert, A., Granell, A., & Rodriguez, P. L. (2014).** Tomato PYR/PYL/RCAR abscisic acid receptors show high expression in root, differential sensitivity to the abscisic acid agonist quinabactin, and the capability to enhance plant drought resistance. *Journal of Experimental Botany*, *65*(15), 4451–4464.

**Gorgues, L., Li, X., Maurel, C., Martinière, A., & Nacry, P. (2022).** Root osmotic sensing from local perception to systemic responses. *Stress Biology*, *2*(1).

**Grusson, Y., Wesström, I., Svedberg, E., & Joel, A. (2021).** Influence of climate change on water partitioning in agricultural watersheds: Examples from Sweden. *Agricultural Water Management*, *249*.

**Haswell, E. S., Peyronnet, R., Barbier-Brygoo, H., Meyerowitz, E. M., & Frachisse, J. M. (2008).** Two MscS Homologs Provide Mechanosensitive Channel Activities in the Arabidopsis Root. *Current Biology*, *18*(10), 730–734.

**Hauser, F., Chen, W., Deinlein, U., Chang, K., Ossowski, S., Fitz, J., Hannon, G. J., & Schroeder, J. I. (2013).** A genomic-scale artificial MicroRNA library as a tool to investigate the functionally redundant gene space in arabidopsis. *Plant Cell*, *25*(8), 2848–2863.

**Hayashi, K. I., Neve, J., Hirose, M., Kuboki, A., Shimada, Y., Kepinski, S., & Nozaki, H. (2012).** Rational design of an auxin antagonist of the SCF TIR1 auxin receptor complex. *ACS Chemical Biology*, *7*(3), 590–598.

**Hertel, T. W., Burke, M. B., & Lobell, D. B. (2010).** The poverty implications of climate-induced crop yield changes by 2030. *Global Environmental Change*, *20*(4), 577–585.

**Hochholdinger, F., & Tuberosa, R. (2009).** Genetic and genomic dissection of maize root development and architecture. In *Current Opinion in Plant Biology.12*( 2), 172–177.

**Hu, Q. et al., 2021**. GhWRKY1-like, a WRKY transcription factor, mediates drought tolerance in Arabidopsis via modulating ABA biosynthesis. *BMC Plant Biology*, 21(1).

**Ishimaru, Y., Oikawa, T., Suzuki, T., Takeishi, S., Matsuura, H., Takahashi, K., Hamamoto, S., Uozumi, N., Shimizu, T., Seo, M., Ohta, H., & Ueda, M. (2017).** GTR1 is a jasmonic acid and jasmonoyl-L-isoleucine transporter in Arabidopsis thaliana. *Bioscience, Biotechnology and Biochemistry*, *81*(2), 249– 255.

**Kafri, R., Springer, M., & Pilpel, Y. (2009).** Genetic Redundancy: New Tricks for Old Genes. In *Cell* 136 Issue 3, pp. 389–392). Elsevier B.V.

**Kang, J., Hwang, J. U., Lee, M., Kim, Y. Y., Assmann, S. M., Martinoia, E., & Lee, Y. (2010).** PDR-type ABC transporter mediates cellular uptake of the phytohormone abscisic acid. *Proceedings of the National Academy of Sciences of the United States of America*, *107*(5), 2355–2360.

**Kang, J., Yim, S., Choi, H., Kim, A., Lee, K. P., Lopez-Molina, L., Martinoia, E., & Lee, Y. (2015).** Abscisic acid transporters cooperate to control seed germination. *Nature Communications*, *6*.

**Karim, S., Holmström, K. O., Mandal, A., Dahl, P., Hohmann, S., Brader, G., Palva, E. T., & Pirhonen, M. (2007).** AtPTR3, a wound-induced peptide transporter needed for defence against virulent bacterial pathogens in Arabidopsis. *Planta*, *225*(6), 1431–1445.

**Karim, S., Lundh, D., Holmström, K. O., Mandal, A., & Pirhonen, M. (2005).** Structural and functional characterization of AtPTR3, a stress-induced peptide transporter of Arabidopsis. *Journal of Molecular Modeling*, *11*(3), 226–236.

**Karlova, R., Boer, D., Hayes, S., & Testerink, C. (2021).** Root plasticity under 125 abiotic stress. *Plant Physiology*, *187*(3), 1057–1070.

**Kim, H., Lee, K., Hwang, H., Bhatnagar, N., Kim, D. Y., Yoon, I. S., Byun, M. O., Kim, S. T., Jung, K. H., & Kim, B. G. (2014).** Overexpression of PYL5 in rice enhances drought tolerance, inhibits growth, and modulates gene expression. *Journal of Experimental Botany*, *65*(2), 453–464.

**Kiss, J. Z. (2007).** Where's the water? Hydrotropism in plants. *Proceedings of the National Academy of Sciences*, *104*(11), 4247–4248.

**Kobayashi, A., Takahashi, A., Kakimoto, Y., Miyazawa, Y., Fujii, N., Higashitani, A., & Takahashi, H. (2007).** A gene essential for hydrotropism in roots. *Proceedings of the National Academy of Sciences*.

**Krouk, G., Lacombe, B., Bielach, A., Perrine-Walker, F., Malinska, K., Mounier, E., Hoyerova, K., Tillard, P., Leon, S., Ljung, K., Zazimalova, E., Benkova, E., Nacry, P., & Gojon, A. (2010)**. Nitrate-regulated auxin transport by NRT1.1 defines a mechanism for nutrient sensing in plants. *Developmental Cell*, *18*(6), 927–937.

**Kuromori, T., Miyaji, T., Yabuuchi, H., Shimizu, H., Sugimoto, E., Kamiya, A., Moriyama, Y., & Shinozaki, K. (2010).** ABC transporter AtABCG25 is involved in abscisic acid transport and responses. *Proceedings of the National Academy of Sciences of the United States of America*, *107*(5), 2361–2366.

**Kuromori, T., Seo, M., & Shinozaki, K. (2018).** ABA Transport and Plant Water Stress Responses. In *Trends in Plant Science* (Vol. 23, Issue 6, pp. 513– 522). Elsevier Ltd.

**Kuromori, T., Sugimoto, E., & Shinozaki, K. (2014).** Intertissue signal transfer of abscisic acid from vascular cells to guard cells. *Plant Physiology*, *164*(4), 1587–1592.

**Lavenus, J., Goh, T., Roberts, I., Guyomarc'h, S., Lucas, M., de Smet, I., Fukaki, H., Beeckman, T., Bennett, M., & Laplaze, L. (2013).** Lateral root development in Arabidopsis: Fifty shades of auxin. In *Trends in Plant Science. 18*, (8), 450–458. Elsevier Ltd.

**Léran, S., Noguero, M., Corratgé-Faillie, C., Boursiac, Y., Brachet, C., & Lacombe, B. (2020).** Functional Characterization of the Arabidopsis Abscisic Acid Transporters NPF4.5 and NPF4.6 in Xenopus Oocytes. *Frontiers in Plant Science*, *11*.

**Léran, S., Varala, K., Boyer, J. C., Chiurazzi, M., Crawford, N., Daniel- Vedele, F., David, L., Dickstein, R., Fernandez, E., Forde, B., Gassmann, W., Geiger, D., Gojon, A., Gong, J. M., Halkier, B. A., Harris, J. M., Hedrich, R., Limami, A. M., Rentsch, D., Lacombe, B. (2014).** A unified nomenclature of nitrate transporter 1/peptide transporter family members in plants. In *Trends in Plant Science .19* (1), 5–9.

**Li, L., He, Z., Pandey, G. K., Tsuchiya, T., & Luan, S. (2002).** Functional cloning and characterization of a plant efflux carrier for multidrug and heavy metal detoxification. *Journal of Biological Chemistry*, *277*(7), 5360–5368.

**Lobell, D. B., & Gourdji, S. M. (2012).** The influence of climate change on global crop productivity. *Plant Physiology*, *160*(4), 1686–1697.

**Lu, G., Gao, C., Zheng, X., & Han, B. (2009).** Identification of OsbZIP72 as a positive regulator of ABA response and drought tolerance in rice. *Planta*, *229*(3), 605–615.

**Lumba, S., Toh, S., Handfield, L. F., Swan, M., Liu, R., Youn, J. Y., Cutler, S. R., Subramaniam, R., Provart, N., Moses, A., Desveaux, D., & McCourt, P. (2014).** A mesoscale abscisic acid hormone interactome reveals a dynamic signaling landscape in arabidopsis. *Developmental Cell*, *29*(3), 360–372.

**Luo, P., Shen, Y., Jin, S., Huang, S., Cheng, X., Wang, Z., Li, P., Zhao, J., Bao, M., & Ning, G. (2016).** Overexpression of Rosa rugosa anthocyanidin reductase enhances tobacco tolerance to abiotic stress through increased ROS scavenging and modulation of ABA signaling. *Plant Science*, *245*, 35–49.

**Lynch, J. (2016).** Root Architecture and Plant Productivity. *Plant Physiology*, *109*(1), 7–13.

**Lynch, J. P. (2011).** Root phenes for enhanced soil exploration and phosphorus acquisition: Tools for future crops. *Plant Physiology*, *156*(3), 1041–1049.

**Lynch, J. P. (2013).** Steep, cheap and deep: An ideotype to optimize water and N acquisition by maize root systems. In *Annals of Botany 112*, (2), 347–357.

**Maksaev, G., & Haswell, E. S. (2012).** MscS-Like10 is a stretch-activated ion channel from Arabidopsis thaliana with a preference for anions. *Proceedings of the National Academy of Sciences of the United States of America*, *109*(46), 19015–19020.

**Marchant, A., Bhalerao, R., Casimiro, I., Eklöf, J., Casero, P. J., Bennett, M., & Sandberg, G. (2002).** AUX1 promotes lateral root formation by facilitating indole-3-acetic acid distribution between sink and source tissues in the Arabidopsis seedling. *Plant Cell*, *14*(3), 589–597.

**Martínez-Ballesta, M. D. C., Muries, B., Moreno, D. Á., Dominguez-Perles, R., García-Viguera, C., & Carvajal, M. (2014).** Involvement of a glucosinolate (sinigrin) in the regulation of water transport in Brassica oleracea grown under salt stress. *Physiologia Plantarum*, *150*(2), 145–160.

**Martínez-Ballesta, M., Moreno-Fernández, D. A., Castejón, D., Ochando, C., Morandini, P. A., & Carvajal, M. (2015).** The impact of the absence of aliphatic glucosinolates on water transport under salt stress in Arabidopsis thaliana. *Frontiers in Plant Science*, *6*(JULY).

**Mehra, P., Pandey, B. K., Melebari, D., Banda, J., Leftley, N., Couvreur, V., Rowe, J., Anfang, M., de Gernier, H., Morris, E., Sturrock, C. J., Mooney, S. J., Swarup, R., Faulkner, C., Beeckman, T., Bhalerao, R. P., Shani, E., Jones, A. M., Dodd, I. C., ... Bennett, M. J. (2022).** *Hydraulic flux-responsive hormone redistribution determines root branching*. *Science. 37*, 762-768.

**Mehrotra, R., Bhalothia, P., Bansal, P., Basantani, M. K., Bharti, V., & Mehrotra, S. (2014).** Abscisic acid and abiotic stress tolerance - Different tiers of regulation. *Journal of Plant Physiology*, *171*(7), 486–496.

**Merilo, E., Yarmolinsky, D., Jalakas, P., Parik, H., Tulva, I., Rasulov, B., Kilk, K., & Kollist, H. (2018).** Stomatal VPD response: There is more to the story than ABA. *Plant Physiology*, *176*(1), 851–864.

**Miyazawa, Y., Ito, Y., Moriwaki, T., Kobayashi, A., Fujii, N., & Takahashi, H. (2009).** A molecular mechanism unique to hydrotropism in roots. In *Plant Science* (Vol. 177, Issue 4, pp. 297–301).

**Miyazawa, Y., Takahashi, A., Kobayashi, A., Kaneyasu, T., Fujii, N., & Takahashi, H. (2009).** GNOM-mediated vesicular trafficking plays an essential role in hydrotropism of Arabidopsis roots. *Plant Physiology*, *149*(2), 835–840.

**Mizuno, H., Kobayashi, A., Fujii, N., Yamashita, M., & Takahashi, H. (2002).** Hydrotropic Response and Expression Pattern of Auxin-Inducible Gene, CS-IAA1, in the Primary Roots of Clinorotated Cucumber Seedlings. In *Plant Cell Physiol* (Vol. 43, Issue 7).

**Monshausen, G. B., & Gilroy, S. (2009).** The exploring root - root growth responses to local environmenttal conditions. In *Current Opinion in Plant Biology* (Vol. 12, Issue 6, pp. 766–772).

**Moritz, C., & Agudo, R. (2013).** The future of species under climate change: Resilience or decline? In *Science* (Vol. 341, Issue 6145, pp. 504–508). American Association for the Advancement of Science.

**Moriwaki, T., Miyazawa, Y., Kobayashi, A., & Takahashi, H. (2013).** Molecular mechanisms of hydrotropism in seedling roots of Arabidopsis Thaliana (Brassicaceae). *American Journal of Botany*.

**Morohashi, K., Okamoto, M., Yamazaki, C., Fujii, N., Miyazawa, Y., Kamada, M., Kasahara, H., Osada, I., Shimazu, T., Fusejima, Y., Higashibata, A., Yamazaki, T., Ishioka, N., Kobayashi, A., & Takahashi, H. (2017).** Gravitropism interferes with hydrotropism via counteracting auxin dynamics in cucumber roots: clinorotation and spaceflight experiments. *New Phytologist*, *215*(4), 1476–1489.

**Morris, E. C., Griffiths, M., Golebiowska, A., Mairhofer, S., Burr-Hersey, J., Goh, T., von Wangenheim, D., Atkinson, B., Sturrock, C. J., Lynch, J. P., Vissenberg, K., Ritz, K., Wells, D. M., Mooney, S. J., & Bennett, M. J. (2017).** Shaping 3D Root System Architecture. In *Current Biology*. *27*(17), 919–930. Cell Press.

**Mravec, J., Skůpa, P., Bailly, A., Hoyerová, K., Křeček, P., Bielach, A., Petrášek, J., Zhang, J., Gaykova, V., Stierhof, Y. D., Dobrev, P. I., Schwarzerová, K., Rolčík, J., Seifertová, D., Luschnig, C., Benková, E., Zažímalová, E., Geisler, M., & Friml, J. (2009).** Subcellular homeostasis of phytohormone auxin is mediated by the ER-localized PIN5 transporter. *Nature*, *459*(7250), 1136–1140.

**Muller, B., Guédon, Y., Passot, S., Lobet, G., Nacry, P., Pagès, L., Wissuwa, M., & Draye, X. (2019).** Lateral Roots: Random Diversity in Adversity. In *Trends in Plant Science* (Vol. 24, Issue 9, pp. 810–825). Elsevier Ltd.

**Mustilli, A. C., Merlot, S., Vavasseur, A., Fenzi, F., & Giraudat, J. (2002).** Arabidopsis OST1 protein kinase mediates the regulation of stomatal aperture by abscisic acid and acts upstream of reactive oxygen species production. *Plant Cell*, *14*(12), 3089–3099.

**Nakajima, Y., Nara, Y., Kobayashi, A., Sugita, T., Miyazawa, Y., Fujii, N., & Takahashi, H. (2017).** Auxin transport and response requirements for root hydrotropism differ between plant species. *Journal of Experimental Botany*, *68*(13), 3441–3456.

**Nguyen, C. T., Agorio, A., Jossier, M., Depré, S., Thomine, S., & Filleur, S. (2016).** Characterization of the chloride channel-like, AtCLCg, involved in chloride tolerance in arabidopsis thaliana. *Plant and Cell Physiology*, *57*(4), 764– 775.

**Nibau, C., Gibbs, D. J., & Coates, J. C. (2008).** Branching out in new directions: The control of root architecture by lateral root formation. In *New Phytologist 179* ( 3), 595–614.

**Nishimura, N., Sarkeshik, A., Nito, K., Park, S. Y., Wang, A., Carvalho, P. C., Lee, S., Caddell, D. F., Cutler, S. R., Chory, J., Yates, J. R., & Schroeder, J. I. (2010).** PYR/PYL/RCAR family members are major in-vivo ABI1 protein phosphatase 2C-interacting proteins in Arabidopsis. *Plant Journal*, *61*(2), 290– 299.

**Noh, B., Murphy, A. S., & Spalding, E. P. (2001).** Multidrug Resistance –like Genes of Arabidopsis Required for Auxin Transport and Auxin-Mediated Development . *The Plant Cell*, *13*(11), 2441–2454.

**Nour-Eldin, H. H., Andersen, T. G., Burow, M., Madsen, S. R., Jørgensen, M. E., Olsen, C. E., Dreyer, I., Hedrich, R., Geiger, D., & Halkier, B. A. (2012).** NRT/PTR transporters are essential for translocation of glucosinolate defence compounds to seeds. *Nature*, *488*(7412), 531–534.

**Oono, Y., Ooura, C., Rahman, A., Aspuria, E. T., Hayashi, K. I., Tanaka, A., & Uchimiya, H. (2003).** p-Chlorophenoxyisobutyric Acid Impairs Auxin Response in Arabidopsis Root. *Plant Physiology*, *133*(3), 1135–1147.

**Orellana, S., Yañez, M., Espinoza, A., Verdugo, I., González, E., Ruiz-Lara, S., & Casaretto, J. A. (2010).** The transcription factor SlAREB1 confers drought, salt stress tolerance and regulates biotic and abiotic stress-related genes in tomato. *Plant, Cell and Environment*, *33*(12), 2191–2208.

**Orman-Ligeza, B., Morris, E. C., Parizot, B., Lavigne, T., Babé, A., Ligeza, A., Klein, S., Sturrock, C., Xuan, W., Novák, O., Ljung, K., Fernandez, M. A., Rodriguez, P. L., Dodd, I. C., de Smet, I., Chaumont, F., Batoko, H., Périlleux, C., Lynch, J. P., ... Draye, X. (2018).** The Xerobranching Response Represses Lateral Root Formation When Roots Are Not in Contact with Water. *Current Biology*, *28*(19), 3165-3173.e5.

**Orosa-Puente, B., Leftley, N., von Wangenheim, D., Banda, J., Srivastava, A. K., Hill, K., Truskina, J., Bhosale, R., Morris, E., Srivastava, M., Kümpers, B., Goh, T., Fukaki, H., M Vermeer, J. E., Vernoux, T., Dinneny, J. R., French, A. P., Bishopp, A., Sadanandom, A., & Bennett, M. J. (2018).** *Root branching toward water involves posttranslational modification of transcription factor ARF7*. *Science. 362*(6421), 1407-1410.

**Ossowski, S., Schwab, R., & Weigel, D. (2008).** Gene silencing in plants using artificial microRNAs and other small RNAs. In *Plant Journal .53,* (4), 674–690.

**Panikashvili, D., Shi, J. X., Schreiber, L., & Aharoni, A. (2011).** The Arabidopsis ABCG13 transporter is required for flower cuticle secretion and patterning of the petal epidermis. *New Phytologist*, *190*(1), 113–124.

**Park, J., Lee, Y., Martinoia, E., & Geisler, M. (2017).** Plant hormone transporters: What we know and what we would like to know. In *BMC Biology .15,* (1). BioMed Central Ltd.

**Pascut, F. C., Couvreur, V., Dietrich, D., Leftley, N., Reyt, G., Boursiac, Y., Calvo-Polanco, M., Casimiro, I., Maurel, C., Salt, D. E., Draye, X., Wells, D. M., Bennett, M. J., & Webb, K. F. (2021).** Non-invasive hydrodynamic imaging in plant roots at cellular resolution. *Nature Communications*, *12*(1).

**Pawela, A., Banasiak, J., Biała, W., Martinoia, E., & Jasiński, M. (2019).** MtABCG20 is an ABA exporter influencing root morphology and seed germination of Medicago truncatula. *Plant Journal*, *98*(3), 511–523.

**Péret, B., de Rybel, B., Casimiro, I., Benková, E., Swarup, R., Laplaze, L., Beeckman, T., & Bennett, M. J. (2009).** Arabidopsis lateral root development: an emerging story. In *Trends in Plant Science* (Vol. 14, Issue 7, pp. 399–408).

**Petrášek, J., & Friml, J. (2009).** Auxin transport routes in plant development. *Development*, *136*(16), 2675–2688.

**Prado, K., Boursiac, Y., Tournaire-Roux, C., Monneuse, J. M., Postaire, O., da Ines, O., Schäffne, A. R., Hem, S., Santoni, V., & Maurel, C. (2013).** Regulation of Arabidopsis leaf hydraulics involves light-dependent phosphorylation of aquaporins in veins. *Plant Cell*, *25*(3), 1029–1039.

**Qin, P., Zhang, G., Hu, B., Wu, J., Chen, W., Ren, Z., Liu, Y., Xie, J., Yuan, H., Tu, B., Ma, B., Wang, Y., Ye, L., Li, L., Xiang, C., & Li, S. (2021).** *Leaf- derived ABA regulates rice seed development via a transporter-mediated and temperature-sensitive mechanism*.*Science 7*(3).

**Raghavendra, A. S., Gonugunta, V. K., Christmann, A., & Grill, E. (2010).** ABA perception and signalling. In *Trends in Plant Science* .15(7), 395–401.

**Raza, A., Razzaq, A., Mehmood, S. S., Zou, X., Zhang, X., Lv, Y., & Xu, J. (2019).** Impact of climate change on crops adaptation and strategies to tackle its outcome: A review. In *Plants. 8,* (2).

**Reichelt, M., Brown, P. D., Schneider, B., Oldham, N. J., Stauber, E., Tokuhisa, J., Kliebenstein, D. J., Mitchell-Olds, T., & Gershenzon, J. (2001)** *Benzoic acid glucosinolate esters and other glucosinolates from Arabidopsis thaliana*.

**Ross-Elliott, T. J., Jensen, K. H., Haaning, K. S., Wager, B. M., Knoblauch, J., Howell, A. H., Mullendore, D. L., Monteith, A. G., Paultre, D., Yan, D., Otero, S., Bourdon, M., Sager, R., Lee, J.-Y., Helariutta, Y., Knoblauch, M., & Oparka, K. J. (2017).** *Phloem unloading in Arabidopsis roots is convective and regulated by the phloem-pole pericycle.ELife.*

**Rowe, J., Grangé-Guermente, M., Exposito-Rodriguez, M., Lenz, M., Shetty, K., Cutler, S. R., & Jones, A. M. (2022).** *Next-generation ABACUS biosensors reveal cellular ABA dynamics driving root growth at low aerial humidity*. *bioRxiv.*

**Růžička, K., Strader, L. C., Bailly, A., Yang, H., Blakeslee, J., Łangowski, Ł., Nejedlá, E., Fujita, H., Itoh, H., Syono, K., Hejátko, J., Gray, W. M., Martinoia, E., Geisler, M., Bartel, B., Murphy, A. S., & Friml, J. (2010).** Arabidopsis PIS1 encodes the ABCG37 transporter of auxinic compounds including the auxin precursor indole-3-butyric acid. *Proceedings of the National Academy of Sciences of the United States of America*, *107*(23), 10749–10753.

**Saab, I. N., Sharp, R. E., Pritchard2, J., & Voetberg, G. S. (1990).** Increased Endogenous Abscisic Acid Maintains Primary Root Growth and Inhibits Shoot Growth of Maize Seedlings at Low Water Potentials1. In *Plant Physiol* (93).

**Saito, H., Oikawa, T., Hamamoto, S., Ishimaru, Y., Kanamori-Sato, M., Sasaki-Sekimoto, Y., Utsumi, T., Chen, J., Kanno, Y., Masuda, S., Kamiya, Y., Seo, M., Uozumi, N., Ueda, M., & Ohta, H. (2015).** The jasmonate- responsive GTR1 transporter is required for gibberellin-mediated stamen development in Arabidopsis. *Nature Communications*, *6*.

**Schwab, R., Ossowski, S., Riester, M., Warthmann, N., & Weigel, D. (2006).** Highly specific gene silencing by artificial microRNAs in Arabidopsis. *Plant Cell*, *18*(5), 1121–1133.

**Seo, M. and Koshiba, T. (2002) .‘**Complex regulation of ABA biosynthesis in plants’, Trends in *Plant Science, 7*(1), 41–4.

**Seo, P. J., & Park, C. M. (2009).** Auxin homeostasis during lateral root development under drought condition. *Plant Signaling and Behavior*, *4*(10), 1002–1004.

**Shkolnik, D., & Fromm, H. (2016).** The Cholodny-Went theory does not explain hydrotropism. In *Plant Science* (Vol. 252, pp. 400–403). Elsevier Ireland Ltd.

**Shohat, H., Illouz-Eliaz, N., Kanno, Y., Seo, M., & Weiss, D. (2020).** The tomato della protein procera promotes abscisic acid responses in guard cells by upregulating an abscisic acid transporter. *Plant Physiology*, *184*(1), 518–528.

**Sivamani, E., Bahieldin, A., Wraith, J. M., Al-Niemi, T., Dyer, W. E., David Ho, T.-H., & Qu, R. (2000).** *Improved biomass productivity and water use efficiency under water deficit conditions in transgenic wheat constitutively expressing the barley HVA1 gene*. *Plant Science. 155*(1),1-9.

**Smith, S., & de Smet, I. (2012).** Root system architecture: Insights from Arabidopsis and cereal crops. *Philosophical Transactions of the Royal Society B: Biological Sciences*, *367*(1595), 1441–1452.

**Spollen, W. G., Lenoble, M. E., Samuels, T. D., Bernstein, N., & Sharp, R. E. (2000).** *Abscisic Acid Accumulation Maintains Maize Primary Root Elongation at Low Water Potentials by Restricting Ethylene Production 1*. Plant Physiology. *122*( 3), , 967–976.

**Su, S. H., Gibbs, N. M., Jancewicz, A. L., & Masson, P. H. (2017).** Molecular Mechanisms of Root Gravitropism. In *Current Biology*.27(17), R964–R972. Cell Press.

**Swarup, R., Friml, J., Marchant, A., Ljung, K., Sandberg, G., Palme, K., & Bennett, M. (2001).** Localization of the auxin permease AUX1 suggests two functionally distinct hormone transport pathways operate in the Arabidopsis root apex. *Genes and Development*, *15*(20), 2648–2653.

**Takahashi, F., Hanada, K., Kondo, T., & Shinozaki, K. (2019).** Hormone-like peptides and small coding genes in plant stress signaling and development. In *Current Opinion in Plant Biology* (Vol. 51, pp. 88–95). Elsevier Ltd.

**Takahashi, H. (1997).** Hydrotropism: the Current State of Our Knowledge. In *Journal of Plant Research by The Botanical Society of Japan* (Vol. 110).

**Takahashi, N., Goto, N., Okada, K., & Takahashi, H. (2002).** Hydrotropism in abscisic acid, wavy, and gravitropic mutants of Arabidopsis thaliana. *Planta*. *216*(2*).*

**Tang, N., Zhang, H., Li, X., Xiao, J., & Xiong, L. (2012).** Constitutive activation of transcription factor OsbZIP46 improves drought tolerance in rice. *Plant Physiology*, *158*(4), 1755–1768.

**Taniguchi, Y. Y., Taniguchi, M., Tsuge, T., Oka, A., & Aoyama, T. (2010).**

Involvement of Arabidopsis thaliana phospholipase Dζ2 in root hydrotropism through the suppression of root gravitropism. *Planta*, *231*(2), 491–497.

**Teale, W. D., Paponov, I. A., & Palme, K. (2006).** Auxin in action: Signalling, transport and the control of plant growth and development. In *Nature Reviews Molecular Cell Biology* (Vol. 7, Issue 11, pp. 847–859). **Xie, B., Wang, X., Zhu, M., Zhang, Z., & Hong, Z. (2011).** CalS7 encodes a callose synthase responsible for callose deposition in the phloem. *Plant Journal*, *65*(1), 1–14.

**Thompson, A. J., Jackson, A. C., Symonds, R. C., Mulholland, B. J., Dadswell, A. R., Blake, P. S., Burbidge, A., & Taylor, I. B. (2000).** Ectopic expression of a tomato 9-cis-epoxycarotenoid dioxygenase gene causes over- production of abscisic acid. *Plant Journal*, *23*(3), 363–374.

**Tian, X., Wang, Z., Li, X., Lv, T., Liu, H., Wang, L., Niu, H., & Bu, Q. (2015).**Characterization and Functional Analysis of Pyrabactin Resistance-Like Abscisic Acid Receptor Family in Rice. *Rice*, *8*(1).

**Ubeda-Tomás, S., Beemster, G. T. S., & Bennett, M. J. (2012).** Hormonal regulation of root growth: Integrating local activities into global behaviour. In *Trends in Plant Science.* 17(6),326–331).

**Uga, Y., Sugimoto, K., Ogawa, S., Rane, J., Ishitani, M., Hara, N., Kitomi, Y., Inukai, Y., Ono, K., Kanno, N., Inoue, H., Takehisa, H., Motoyama, R., Nagamura, Y., Wu, J., Matsumoto, T., Takai, T., Okuno, K., & Yano, M. (2013).** Control of root system architecture by DEEPER ROOTING 1 increases rice yield under drought conditions. *Nature Genetics*, *45*(9), 1097–1102.

**Verstraeten, I., Schotte, S., & Geelen, D. (2014).** Hypocotyl adventitious root organogenesis differs from lateral root development. In *Frontiers in Plant Science*.5 (SEP), Frontiers Media S.A.

**Verslues, P.E., Bray, E.A., 2006.** Role of abscisic acid (ABA) and Arabidopsis thaliana ABA-insensitive loci in low water potential-induced ABA and proline accumulation. *Journal of Experimental Botany*, 201–212. 10.

**Voesenek, L. A. C. J., & Bailey-Serres, J. (2015).** Flood adaptive traits and processes: An overview. In *New Phytologist.206* (1), 57–73.

**Waadt, R., Seller, C. A., Hsu, P. K., Takahashi, Y., Munemasa, S., & Schroeder, J. I. (2022).** Plant hormone regulation of abiotic stress responses. In

**Xie, Q., Essemine, J., Pang, X., Chen, H., Jin, J., & Cai, W. (2021**). Abscisic Acid Regulates the Root Growth Trajectory by Reducing Auxin Transporter PIN2 Protein

Levels in Arabidopsis thaliana. *Frontiers in Plant Science*, *12*. *Nature Reviews Molecular Cell Biology*. Nature Research.

**Wan, Y., Jasik, J., Wang, L., Hao, H., Volkmann, D., Menzel, D., Mancuso, S., Baluška, F., & Lin, J. (2012).** The signal transducer NPH3 integrates the phototropin1 photosensor with PIN2-based polar auxin transport in Arabidopsis root phototropism. *Plant Cell*, *24*(2), 551–565.

**Wang, Y., Beaith, M., Chalifoux, M., Ying, J., Uchacz, T., Sarvas, C., Griffiths, R., Kuzma, M., Wan, J., & Huang, Y. (2009).** Shoot-specific down- regulation of protein farnesyltransferase (α-subunit) for yield protection against drought in Canola. *Molecular Plant*, *2*(1), 191–200.

**War, A. R., Paulraj, M. G., Ahmad, T., Buhroo, A. A., Hussain, B., Ignacimuthu, S., & Sharma, H. C. (2012).** Mechanisms of plant defense against insect herbivores. In *Plant Signaling and Behavior*.7( 10). Landes Bioscience.

**Wasilewska, A., Vlad, F., Sirichandra, C., Redko, Y., Jammes, F., Valon, C., Frei Dit Frey, N., & Leung, J. (2008).** An update on abscisic acid signaling in plants and more ⋯. In *Molecular Plant*. 1,(2), 198–217). Oxford University Press.

**Watanabe, S., Takahashi, N., Kanno, Y., Suzuki, H., Aoi, Y., Takeda- Kamiya, N., Toyooka, K., Kasahara, H., Hayashi, K.-I., Umeda, M., & Seo, M (2013).** (*The Arabidopsis NRT1/PTR FAMILY protein NPF7.3/ NRT1.5 is an indole-3-butyric acid transporter involved in root gravitropism. Sci USA.117*(49), 31500-31509.

**Wiegers, B. S., Cheer, A. Y., & Silk, W. K. (2009).** Modeling the hydraulics of root growth in three dimensions with phloem water sources. *Plant Physiology*, *150*(4), 2092–2103.

**Xu, Z. Y., Lee, K. H., Dong, T., Jeong, J. C., Jin, J. B., Kanno, Y., Kim, D. H., Kim, S. Y., Seo, M., Bressan, R. A., Yun, D. J., & Hwang, I. (2012).** A vacuolar β-Glucosidase homolog that possesses glucose-conjugated abscisic acid hydrolyzing activity plays an important role in osmotic stress responses in Arabidopsis. *Plant Cell*, *24*(5), 2184–2199.

**Yao, L., Cheng, X., Gu, Z., Huang, W., Li, S., Wang, L., Wang, Y. F., Xu, P., Ma, H., & Ge, X. (2018).** The AWPM-19 family protein OsPM1 mediates abscisic acid influx and drought response in rice. *Plant Cell*, *30*(6), 1258–1276.

**Zazímalová, E., Murphy, A. S., Yang, H., Hoyerová, K., & Hosek, P. (2010).** Auxin transporters--why so many? In *Cold Spring Harbor perspectives in biology.2* (3).

**Zhan, A., Schneider, H., & Lynch, J. P. (2015).** Reduced lateral root branching density improves drought tolerance in maize. *Plant Physiology*, *168*(4), 1603– 1615.

**Zhang, H., Zhu, H., Pan, Y., Yu, Y., Luan, S., & Li, L. (2014).** A DTX/MATE- type transporter facilitates abscisic acid efflux and modulates ABA sensitivity and drought tolerance in Arabidopsis. *Molecular Plant*, *7*(10), 1522–1532.

**Zhang, L., Zhao, Y., Liang, H., Li, X., Gallagher, K. L., & Wu, S. (2020).** Gateway-compatible vectors for functional analysis of proteins in cell type specific manner. *Plant Methods*, *16*(1).

**Zhang, Y., Nasser, V., Pisanty, O., Omary, M., Wulff, N., di Donato, M., Tal, I., Hauser, F., Hao, P., Roth, O., Fromm, H., Schroeder, J. I., Geisler, M., Nour-Eldin, H. H., & Shani, E. (2018).** A transportome-scale amiRNA-based screen identifies redundant roles of Arabidopsis ABCB6 and ABCB20 in auxin transport. *Nature Communications*, *9*(1).

**Zhao, Y. (2012).** Auxin biosynthesis: A simple two-step pathway converts tryptophan to indole-3-Acetic acid in plants. *Molecular Plant*, *5*(2), 334–338.

**Zhijin, Z., Haiwen, Z., Ruidan, Q., Xue-Chen, W., & Rongfeng, H. (2009**). Transcriptional regulation of the ethylene response factor leerf2 in the expression of ethylene biosynthesis genes controls ethylene production in tomato and tobacco. *Plant Physiology*, *150*(1), 365–377.

**Zhu, J. K. (2002).** Salt and drought stress signal transduction in plants. In *Annual Review of Plant Biology.7*(53),247–273.

**Zolman, B. K., Silva, I. D., & Bartel, B. (2001).** The Arabidopsis pxa1 mutant is defective in an ATP-binding cassette transporter-like protein required for peroxisomal fatty acid β-oxidation. *Plant Physiology*, *127*(3), 1266–1278.